

Protease Distribution in J774 Macrophages

by

JACLYN McDOWALL

BSc, BScHons (*cum laude*) (KwaZulu-Natal)

Submitted in fulfillment of the academic requirements for the degree of Master
of Science

in the School of Biochemistry, Genetics, Microbiology and Plant Pathology

University of KwaZulu-Natal

Pietermaritzburg

April 2007

PREFACE

The experimental work described in this dissertation was carried out in the Department of Biochemistry, School of Biochemistry, Genetics, Microbiology and Plant Pathology, University of KwaZulu-Natal, Pietermaritzburg from January 2005 to June 2006, under the supervision of Dr Edith Elliott.

These studies represent original work by the author and have not been submitted in any other form to another university. Where use was made of the work of others, it has been duly acknowledged in the text.

Jaelyn McDowall
April 2007

Dr Edith Elliott
April 2007

ABSTRACT

Cathepsin, matrix metalloproteinase (MMP) enzyme and tissue inhibitor of MMP (TIMP) distribution in J774 mouse macrophages has not been comprehensively studied. The distribution and vesicle regulation, trafficking and release of these is important, possibly suggesting drug targets for the therapeutic regulation of inflammatory disease and phagosomal killing of pathogenic organisms in J774 and other macrophages. Percentage immunofluorescence and ultrastructural enzyme and inhibitor distribution, together with LysoTracker (acidity) and lysosome-associated membrane proteins (LAMPs) colocalisation (both indicating late endosome or “lysosomal” association), western blot estimates of percentage processed- and unprocessed intracellular and secreted enzyme and inhibitor, and vesicle size was used to assign enzyme and inhibitor to “classical” vesicle types. Antibodies against TIMP-1 and TIMP-2 were raised and all antibodies characterised for this purpose.

Together these were used to assign cathepsins H, S, D, B and L to possible secretory vesicles (± 20 nm, non-acidic, LAMPs-negative, containing precursor enzymes) and identify at least 6 other endosome-“lysosome-like” vesicles. Cathepsin H appears to be present in classical early endosomes (± 100 nm, non-acidic, LAMPs-negative) and cathepsin S in late endosomes (± 50 nm, acidic, LAMPs-positive) and possibly “lysosomal” (“hybrid” or digestive organelles) (± 150 - 200 nm, acidic, LAMPs-positive). Both cathepsins H and S, however, seem only reliable markers if used together with additional markers. Cathepsin D appears mainly associated with “lysosomal” (“hybrid” or digestive organelles) (± 150 - 200 nm, acidic, LAMPs-positive), possibly consisting of further subpopulations which requires further investigation e.g. labelling for LAMP-1 and LAMP-2 and cathepsin D. Cathepsins B and L may occur in late endosomes and/or hybrid organelles and “secretory lysosomes” containing cathepsins B, D and L may also exist (± 30 - 50 nm, acidic, LAMPs-positive).

The distribution of MMP-9, TIMP-1 and -2 in vesicles (non-acidic, LAMP-2-negative) that appear novel and distinct from late endosome-“lysosome” vesicles were also demonstrated. In LPS-stimulated cells, the identity of the large (± 450 nm), possible recycling endosomes (Rab11-positive, LAMPs-negative), containing colocalised MMP-9 and TIMP-1, needs investigation i.e., requires further verification with triple labelling and EM. Possible cell membrane and recycling endosome localisation of TIMP-2 needs confirmation with labelling of non-permeabilised cells and labelling for MT1-MMP and proMMP-2, respectively.

ACKNOWLEDGEMENTS

I would like to express my appreciation and thanks to the following people for their contribution to this dissertation:

My supervisor, Dr Edith Elliott, for her constant support, encouragement, enthusiasm and expertise during both the experimental work and the writing up of this dissertation. Many thanks for arranging the various informative microscopy workshops and for encouraging me to present my work at conferences.

Prof. Clive Dennison, for teaching me the do's and don'ts of scientific writing and for introducing me to 'styles', thus making the construction of the 'Table of Contents' so simple.

Prof. Dean Goldring and Prof. Theresa Coetzer, for both showing an interest in my work, for offering advice and for letting me borrow reagents or equipment, when I was in dire straits.

The Staff of the Centre for Electron Microscopy. Tony Bruton, for allowing me to work in his excellent facility. Vijay Bandu, for all his help on the TEM and practical advice. Priscilla Donnelly and Belinda White, for offering advice and making sure that the correct camera was always in place on the fluorescent microscope.

The University of KwaZulu-Natal and the National Research Foundation (NRF), for bursaries and scholarships throughout my entire academic career.

Jennifer and Robyn, for obtaining quotations and understanding the urgency of ordering the various reagents.

Charmaine, for taking care of all admin matters.

Celia Snyman, many, many thanks! Firstly, for teaching me the art of cutting ultrathin sections and eagerness to share your vast knowledge and experience of all aspects of microscopy. Secondly, for all our informative and beneficial brainstorming sessions - "informal lab meetings" and conversations on life in general. For your efforts to keep the lab neat and tidy and lastly, for being a great listener and wonderful friend.

Jessica, for letting me borrow equipment when I was desperate, for organising and preparing the third year pracs - making my job as demonstrator a great deal easier, and also for our little chats!

Amanda, for your infinite computer knowledge and helping me solve my computer problems, as well as your very interesting conversations.

My colleagues in Lab 43, for making day to day life in the lab enjoyable.

Fellow postgraduates in Labs 39 and 40, for being interested in my work and always ready to listen and offer advice.

Nicholas, for all your love, support and perseverance throughout my University career and for understanding when my work kept me away longer than I would have liked.

My parents and Darren, for all your love, support and encouragement throughout both my schooling and University careers.

TABLE OF CONTENTS

PREFACE	i
ABSTRACT	ii
ACKNOWLEDGEMENTS	iii
LIST OF FIGURES	x
LIST OF TABLES	xiv
LIST OF ABBREVIATIONS AND SYMBOLS	xvi
CHAPTER 1	1
INTRODUCTION	1
1.1 Macrophages.....	1
1.2 Phagocytosis	2
1.2.1 Receptors involved in phagocytosis	3
1.2.1.1 Fc-receptor-mediated phagocytosis.....	3
1.2.1.2 Complement-receptor-mediated phagocytosis	4
1.2.2 The phagosome and phagosome maturation.....	4
1.3 Microbicidal killing mechanisms	6
1.4 Content of the macrophage.....	9
1.4.1 Cathepsins.....	14
1.4.1.1 Macrophage cathepsins.....	18
1.4.2. Matrix metalloproteinases and tissue inhibitors of matrix metalloproteinases .	21
1.4.2.1 Macrophage MMPs and TIMPs	27
1.5 Objectives of the current study.....	29
CHAPTER 2	32
GENERAL MATERIALS AND METHODS	32
2.1 Reagents	32
2.2 Cell culture	33
2.2.1 Reagents.....	33
2.2.2 Procedure	34
2.3 SDS-PAGE.....	34
2.3.1 Laemmli system.....	35
2.3.1.1 Reagents.....	36

2.3.1.2	Procedure	37
2.4	Staining of protein in SDS-PAGE gels	38
2.4.1	Coomassie brilliant blue staining	38
2.4.1.1	Reagents.....	39
2.4.1.2	Procedure	39
2.4.2	Imidazole-SDS-zinc reversible staining	39
2.4.2.1	Reagents.....	40
2.4.2.2	Procedure	40
2.5	Zymography	40
2.5.1	Reagents.....	41
2.5.2	Procedure	42
2.6	Western blotting	42
2.6.1	Chromogenic blots.....	43
2.6.2	'Tank' buffer system.....	44
2.6.2.1	Reagents.....	44
2.6.2.2	Procedure	46
2.6.3	'Semi-dry blotting' system	47
2.6.3.1	Reagents.....	47
2.6.3.2	Procedure	47
2.7	Electron microscopy and immunogold labelling.....	48
2.7.1	Fixation and embedding of J774 cells in LR White resin	51
2.7.1.1	Reagents.....	51
2.7.1.2	Procedure	52
2.7.2	Glass knife production and preparation of grids.....	52
2.7.3	Immunolabelling protocol	52
2.7.3.1	Reagents.....	52
2.7.3.2	Procedure	53
2.8	Fluorescent microscopy and immunolabelling.....	54
2.8.1	Immunolabelling protocol	55
2.8.1.1	Reagents.....	55
2.8.1.2	Procedure	56

REFERENCES.....184

PUBLICATIONS213

LIST OF FIGURES

Figure 1.1	Schematic diagram showing the killing mechanisms used by J774 macrophages to control <i>Mycobacterium smegmatis</i> infection.....	8
Figure 1.2	Factors responsible for the regulation of cathepsin activity.....	17
Figure 1.3	Domain composition and important structural features of the various subtypes of MMPs.....	22
Figure 3.1	Reducing SDS-PAGE of human recombinant TIMP-1 and TIMP-2 to assess protein purity.	60
Figure 3.2	ELISA of the progress of immunisation of a chicken with human recombinant TIMP-1.	67
Figure 3.3	ELISA of the progress of immunisation of a chicken with human recombinant TIMP-2.	67
Figure 3.4	Reducing SDS-PAGE separation of J774 macrophage homogenates and supernatants.	71
Figure 3.5	Characterisation of chicken anti-TIMP-1 using J774 macrophage homogenates and supernatants.	71
Figure 3.6	Characterisation of chicken anti-TIMP-2 using J774 macrophage homogenates and supernatants.	73
Figure 3.7	Characterisation of chicken anti-TIMP-1 and anti-TIMP-2 using human recombinant TIMP-1 and TIMP-2.	73
Figure 3.8	Reducing SDS-PAGE separation of human monocyte and J774 mouse macrophage homogenates.....	76
Figure 3.9	Detection of cathepsin B in J774 macrophage and human monocyte homogenates.	78
Figure 3.10	Detection of cathepsin D in J774 macrophage and human monocyte homogenates.	78

Figure 3.11	Detection of cathepsin H in J774 macrophage and human monocyte homogenates.	79
Figure 3.12	Detection of cathepsin L in J774 macrophage and human monocyte homogenates.	80
Figure 3.13	Detection of cathepsin S in J774 macrophage and human monocyte homogenates.	81
Figure 3.14	Detection of MMP-9 in human monocyte homogenate.	82
Figure 3.15	Detection of TIMP-1 in J774 macrophage homogenate.	82
Figure 4.1	Model of the endocytic pathway.	87
Figure 4.2	Model of dense core lysosome-late endosome fusion and re-formation of lysosomes.	89
Figure 4.3	Schematic model of the four major vesicular compartments capable of fusing with the phagosome during <i>M. smegmatis</i> infection.	92
Figure 4.4	Fluorescent and protein A gold labelling of cathepsin H in J774 macrophages.	98
Figure 4.5	Fluorescent and protein A gold labelling of cathepsin S in J774 macrophages.	100
Figure 4.6	Fluorescent and protein A gold labelling of cathepsin D in J774 macrophages.	102
Figure 4.7	Fluorescent and protein A gold labelling of cathepsin B in J774 macrophages.	103
Figure 4.8	Fluorescent and protein A gold labelling of cathepsin L in J774 macrophages.	104
Figure 4.9	Fluorescent and protein A gold labelling of cathepsins S and H in J774 macrophages.	109
Figure 4.10	Fluorescent and protein A gold labelling of cathepsins D and S in J774 macrophages.	110

Figure 5.3	Localisation of MMP-9 in unstimulated and LPS-stimulated J774 macrophages.	164
Figure 5.4	Localisation of TIMP-1 or TIMP-2 in unstimulated and LPS-stimulated J774 macrophages.	165
Figure 5.5	Colocalisation of MMP-9 and TIMP-1 in unstimulated and LPS-stimulated J774 macrophages.	167
Figure 5.6	Colocalisation of TIMP-1 and TIMP-2 in unstimulated and LPS-stimulated J774 macrophages.	168
Figure 5.7	LysoTracker and labelling of LAMP-2 and MMP-9 in unstimulated J774 macrophages.	171
Figure 5.8	LysoTracker and labelling of LAMP-2 and TIMP-1 in unstimulated J774 macrophages.	172
Figure 5.9	LysoTracker and labelling of TIMP-2 in J774 macrophages.	173

Table 4.4	Summary of colocalisation, western blot data and apparent vesicular distribution of cathepsins.	118
Table 4.5	Classification of J774 macrophage endosome-lysosome vesicle populations based on pH and the presence of LAMPs.....	121
Table 4.6	Summary of colocalisation between LAMPs and cathepsins, western blot data and apparent vesicular distribution of these proteins.	134
Table 4.7	Summary of colocalisation between LysoTracker, LAMPs and cathepsins, western blot data and apparent vesicular distribution of these proteins.	145
Table 5.1	Comparison of activated murine macrophage subpopulations.	153

LIST OF ABBREVIATIONS AND SYMBOLS

ε	extinction coefficient
λ	wavelength
Φ	quantum yield
%C	monomer crosslinking concentration
%T	total monomer concentration
ABTS	2,2'-azino-di(3-ethyl)-benzthiozoline sulfonic acid
ADAM	a disintegrin and metalloprotease domain
ADAM-TS	a disintegrin and metalloprotease domain with thrombospondin type-1 domains
ALG-2	apoptosis-linked gene -2
AMAC-1	alternative macrophage activation-associated chemokine-1
APCs	antigen presenting cells
ARP3	actin-like protein 3
ATPase	adenosine triphosphatase
BCIP	5-bromo-4-chloro-3-indolyl phosphate
bFGF	basic fibroblast growth factor
BIP	binding protein
BM-40 (SPARC)	osteonectin
BPI	bactericidal/permeability increasing protein
Brij 35	polyoxyethylene (23) lauryl alcohol
BSA	bovine serum albumin
CABP1	calcium-binding protein 1
CAP 1	adenylyl cyclase-associated protein 1
CAPZ	actin capping protein
Cat	cathepsin
CBB	Coomassie brilliant blue
CD	cluster determinant/cluster of differentiation
C _{H1}	immunoglobulin heavy chain constant region 1
C _{H2}	immunoglobulin heavy chain constant region 2
COPD	chronic obstructive pulmonary disease

COPI	coat protein I
CR	complement receptor
CRAMP	cathelicidin-related antimicrobial peptide
CTGF	connective tissue growth factor
CT-PCPE	C-terminal fragment of procollagen C-terminal proteinase enhancer
CY3	cyanine3
CyCAP	cyclophilin C-associated protein
Da	dalton(s)
DAB	diaminobenzidine/3,3',4,4'-tetraaminobiphenyl
DAMP	3-(2,4-dinitroanilino)-3'-amino- <i>N</i> -methyldipropylamine
DEC-205	dendritic epidermal T cell -205
dH ₂ O	distilled water
DMEM	Dulbecco's Modified Eagle's Medium
DMF	dimethylformamide
DNP	2,4-dinitrophenol
DPPII	dipeptidyl peptidase II
DTT	dithiothreitol
ECM	extracellular matrix
ECV(s)	endosome carrier vesicle(s)
EDTA	ethylene diamine tetra acetic acid
EEA1	early endosomal antigen 1
EF-TU	elongation factor Tu
EGTA	ethylene glycol-bis(β -aminoethyl ether) <i>N,N,N,N,N'</i> - tetra acetic acid
ELISA	enzyme linked immunosorbent assay
EM	electron microscope/microscopy
ENA-78	epithelial neutrophil activating peptide
ER	endoplasmic reticulum
ERP	leucine-responsive regulatory protein
F	"free" (i.e soluble)
Fc	fragment crystallisable
Fc γ Rs	receptors binding the Fc region of the indicated Ig molecule (γ for IgG)

FCA	Freund's complete adjuvant
FCS	foetal calf serum
FIA	Freund's incomplete adjuvant
FITC	fluorescein isothiocyanate
fMLP	formylmethionyl-leucyl-phenylalanine
FSG	fish skin gelatin
g	relative centrifugal force
GAPDH	glyceraldehyde-3-phosphate dehydrogenase
GCAP39	calcium ion- and polyphosphoinositide-regulated actin capping protein
GDI	GDP-dissociation inhibitor
GFP	green fluorescent protein
GILT	IFN- γ -inducible lysosomal thiol reductase
GM-CSF	granulocyte-macrophage colony stimulating factor
GPI	glycosylphosphatidylinositol
GRB2	growth factor receptor bound protein 2
GRO	growth-related oncogene protein
GRP	glycine-rich protein
GTPase	guanosine triphosphatase
h	hour(s)
HBSS	Hank's Balanced Salts
hCAP-18	human cathelicidin protein
Hck	hematopoietic cell kinase
HEPES	<i>N</i> -2-hydroxy-piperazine- <i>N'</i> -2 ethane sulfonic acid
H ₂ O ₂	hydrogen peroxide
HRP	horseradish peroxidase
HSC	hemopoietic stem cell
HSP	heat shock protein
ICAM	intercellular adhesion molecule
IFN- γ	interferon- γ
IGF	insulin-like growth factor
IGFBP	insulin-like growth factor binding protein
IgG, IgY, IgA, IgE	immunoglobulins G, Y, A, E
Ii	invariant chain

IL	interleukin
IL-1RA	interleukin-1 receptor antagonist
iNOS	inducible NO synthase
IP-10, -20	IFN-inducible protein-10, -20
ITAMs	immunoreceptor tyrosine-based activation motifs
kDa	kilodalton(s)
l	litre(s)
LAMP(s)	lysosomal-associated membrane protein(s)
LBPs	latex bead containing phagosomes
LE	large, electron-dense, late endosome-like
LIMP II	lysosomal integral membrane protein
LPS	lipopolysaccharide
LT	large, translucent, early endosome-like
LYAAT	lysosomal amino acid transporter
LYCAM	lysozyme C, type M
Lys	lysosome-like i.e. “hybrid” organelle or digestive body
M	membrane-bound
mA	milliAmp
MAC-2	galectin-3
MCP-1	monocyte chemoattractant protein-1
M-CSF	macrophage colony-stimulating factor
MDM(s)	monocyte-derived macrophage(s)
MFG-E8	milk fat globule-epidermal growth factor 8
MHC	major histocompatibility complex
min	minute(s)
MIP-1 α	macrophage-inflammatory protein 1 α
MPO	myeloperoxidase
MMP(s)	matrix metalloproteinase(s)
MOPS	3-(<i>N</i> -morpholino)propanesulfonic acid
MPR(s)	mannose-6-phosphate receptor(s)
MPS	mononuclear phagocyte system
MPS1	mitogen-activated protein kinase
M_r	relative molecular mass
MR	mannose receptor

least three distinct FcγRs, FcγRI, FcγRII and FcγRIII in macrophages (Shibata *et al.*, 1991; Kusner *et al.*, 1999). In addition to IgG, IgA and IgE also have cognate receptors, Fcα and Fcε, respectively (May and Machesky, 2001). Binding of IgG to the FcγRs activates a wide variety of antimicrobial responses, including secretion of various antimicrobial agents, cytokine synthesis and secretion, the production of pro-inflammatory lipids such as arachidonic acid and reactive oxygen intermediates (Aderem and Underhill, 1999; Kusner *et al.*, 1999). IgG-FcγR interaction may result in phosphorylation of specific receptor tyrosine residues in immunoreceptor tyrosine-based activation motifs (ITAMs) essential for phagocytosis (Greenberg *et al.*, 1993). Tyrosine kinase-dependent activation of phospholipase D results and appears to regulate the ingestion of IgG-opsonised particles (Kusner *et al.*, 1999). The monomeric GTPase, Rho is subsequently essential for the accumulation of phosphotyrosine and of F-actin around phagocytic cups as well as for Fcγ-receptor-mediated Ca²⁺ signalling. This results in differential vesicle fusion with the phagosome (Hackam *et al.*, 1997).

1.2.1.2 Complement-receptor-mediated phagocytosis

Unlike Fc-receptor-mediated phagocytosis, complement receptor-mediated phagocytosis involves minimal membrane disturbance. Complement-opsonised particles appear to “sink” into the phagocyte and internalisation does not normally result in an inflammatory response or respiratory burst (May and Machesky, 2001). Following complement activation C3b containing a thioester group, can covalently bind to hydroxyl or amino groups on the microbial surface. The deposited C3b acts as an opsonin and is recognised by complement receptor (CR)1 (CD35), CR4 (CD11c/CD18), and, after its conversion to iC3b, by CR3 (CD11b/CD18) (May and Machesky, 2001; Ross and Auger, 2002). Phagocytosis of iC3b particles occurs only if the macrophage has been activated, for example, by cytokines. Activation causes a conformational change in the receptor, resulting in the clustering of receptors (necessary for the binding), allowing transduction of the phagocytic signal and the subsequent uptake of the foreign particle (Allen and Aderem, 1996; May and Machesky, 2001).

1.2.2 The phagosome and phagosome maturation

Despite the considerable membrane expanse that is internalised during phagocytosis, no net loss of surface membrane has been detected suggesting that exocytosis of membranes occurs in conjunction with phagocytosis (Hackam *et al.*, 2001). Fission of vesicles from the

macrophages are unable to produce significant amounts of reactive oxygen intermediates in the phagosome, as they appear to lack the large pool of NADPH-oxidase components found in neutrophils (Johansson *et al.*, 1995).

In addition to oxygen-dependent mechanisms, macrophages are also equipped with oxygen-independent killing mechanisms. Many vesicle-associated proteins have been shown to have antimicrobial activity. These include lysozyme, elastase, collagenases, lipases, sulfatases, phosphatases, defensins, polysaccharides, cathepsins and deoxyribonucleases (Heale and Speert, 2002; Selsted and Ouellette, 1995; Ross and Auger, 2002). These substances are delivered to the phagosome as the various compartments of the endocytic pathway fuse sequentially with the phagosome during the process of phagosomal maturation (Vieira *et al.*, 2002; Henry *et al.*, 2004).

Some years ago cathepsins B and D, released into the phagosome, were shown to possess bactericidal properties, including the ability to effect lysis of lysozyme-resistant *Staphylococcus aureus* and rendering *Acinetobacter* 199A sensitive to lysozyme (Thorne *et al.*, 1976). Despite this, until recently (Anes *et al.*, 2006; Del Cerro-Vadillo *et al.*, 2006), a direct role for macrophage proteases in controlling bacterial infection had not been established and it was thought that the proteases mainly performed protein turnover functions in the phagosome (Heale and Speert, 2002; Rosenberger *et al.*, 2004). Murine macrophages have been shown to use a combination of proteases and cationic peptides to limit the growth of intracellular bacterial pathogens (Rosenberger *et al.*, 2004). Multiplication of *Salmonella typhimurium* inside infected murine splenic and liver macrophages has also been shown to be controlled using increased levels of reactive oxygen intermediates, increased expression of the murine cathelicidin-related antimicrobial peptide (CRAMP), activated by an intracellular macrophage elastase-like serine proteases (Rosenberger *et al.*, 2004). This study demonstrated the importance of antimicrobial peptides in the destruction of macrophage bacterial pathogens and, that independent killing mechanisms in macrophages, reactive oxygen species as well as intracellular proteases, cooperate and complement each other in impairing bacterial growth.

A recent study has also identified cathepsin D as an important non-oxidative bactericidal agent effective against *Listeria monocytogenes* infection in both macrophages and fibroblasts (Del Cerro-Vadillo *et al.*, 2006). Acid sphingomyelinase was shown to produce ceramide, a

Protein	Remark	Protein	Remark
NDK B	Nucleotide diphosphatase kinase B.	NSF	Vesicular-fusion protein. N-ethylmaleimide-sensitive factor.
ORP150	Oxygen regulated protein.	Palmitoyl-protein thioesterase	Removes thioester-like fatty acyl groups from modified cysteine residues in proteins or peptides during lysosomal degradation.
PDI (ER-59)	Protein disulfide isomerase.	PDI-(ER-60)	Involved in MHC class I assembly.
PGAM-B	Phosphoglycerate mutase, brain form.	Prohibitin	Present in lipid rafts.
Rab2	Vesicular traffic. Associated with an intermediate compartment between the ER and Golgi apparatus.	Rab3c	Protein transport and vesicular traffic.
Rab5c	Regulates early endocytic/phagocytic trafficking.	Rab7	Regulates late endocytic /phagocytic trafficking.
Rab10	Vesicular traffic and neurotransmitter release.	Rab11b	Involved in membrane recycling.
Rab14	Vesicular traffic and neurotransmitter release.	RAP1B	Involved in initiation of oxidative burst in neutrophils.
RHO GDI α	RHO GDP-dissociation inhibitor 1.	RSP4	40S ribosomal protein SA. Cytoplasmic.
SNAP- α	Soluble NSF attachment protein.	SNAP- γ	Required to prepare intracellular membranes for fusion.
Stomatin	Found in lipid rafts, exposed on the cytoplasmic surface of the membrane.	Syntenin	Localised in early endocytic compartments.
TCP-1 α	T-complex protein 1. Molecular chaperone. Known to play a role, <i>in vitro</i> , in the folding of actin and tubulin. Cytoplasmic.	TCBP-49	Taipoxin-associated calcium binding protein 49.
Thioreductase peroxidase 2	Cytoplasmic.	TCP-1 β	T-complex protein 1. Molecular chaperone. Known to play a role, <i>in vitro</i> , in the folding of actin and tubulin. Cytoplasmic.
TMP21	Transmembrane protein. Vesicular protein trafficking. Type I membrane protein. Present in Golgi cisternae.	Ti-225 (ubiquitin C)	Similar to human ubiquitin.
Trimeric G $\alpha 2$	Guanine nucleotide-binding protein. G(I)/G(S)/G(T). Adenylate cyclase-inhibiting Ga protein. Regulatory G-proteins of signalling cascades.	TRAIL	TNF-related apoptosis inducing ligand.
Tropomyosin 5	Cytoskeletal type.	Trimeric G β 1	Guanine nucleotide-binding protein. G(I)/G(S)/G(T). Adenylate cyclase-inhibiting Ga protein. Regulatory G-proteins of signalling cascades.
UDPGT	UDP-glucuronosyltransferase. ER protein	Tubulin α -6	Microtubule protein.

Table 1.6 indicates the fairly wide pH optimum, of most cathepsins. This suggests that the cathepsins may occur in different vesicular compartments along the endocytic pathway, where the pH for maximal activity exists or may be regulated by pH fluctuation. In order for cathepsins to play a role in the three killing phases in J774 macrophages (Figure 1.1) (Anes *et al.*, 2006), and the accompanying changing pH of the maturing phagosome, suggest that cathepsins B, H, S and L may be located in different vesicle populations that may fuse with the phagosome during the first killing phase (mild pH) and subsequently recycle out of the phagosome, or, as they are active at lower pH, fuse with the phagosome prior to the second and third killing phases (low pH) (Figure 1.1).

Table 1.5 Properties and distribution of cathepsins.

Cathepsin	Endopeptidase		Exopeptidase		Tissue expression
		Carboxypeptidase	Amino	peptidase	
B	+	+			Widespread
L	+				Widespread
S	+				APCs
H	+		+		Widespread
K	+				Osteoclasts, Bronchial epithelium
F	+				Macrophages Widespread?
V	+				Thymic epithelium
W	Unknown	Unknown		Unknown	CD8 ⁺ T cells Natural killer cells
C				+	Leukocytes Macrophages
O	Unknown	Unknown		Unknown	Widespread
Z		+			Widespread
D	+				Widespread
E	+				Restricted
G	+				Neutrophils Monocytes

Abbreviation: APCs, antigen presenting cells. (Modified from Riese and Chapman, 2000; Wolters and Chapman, 2000; Turk *et al.*, 2001).

Aspartic proteases are different from cysteine or serine proteases in that an activated water molecule, as opposed to an amino acid side chain is the nucleophile that attacks the substrate peptide bond. Cathepsins D and E are aspartic endopeptidases (Table 1.5), and are bi-lobed molecules with the active site situated between the two lobes (James, 2004). The aspartate residues making up the catalytic dyad bind to, and activate, the catalytic water molecule. Catalysis requires a third residue in addition to the two aspartate residues. One of the lobes has an extra β hairpin loop known as the 'flap' that caps the active site. This loop carries Tyr137 and Thr139 which are important residues for specificity. The secreted peptidase

cathepsin D, has four disulfide bonds, whereas, the proform of cathepsin E is a disulfide linked dimer (James, 2004). Table 1.6 reflects the operating pH and pI of most of the cathepsins and cathepsins D and E appear to have a more limited, acidic operating pH range in comparison to that of the cathepsins belonging to the cysteine protease family. This suggests that the active forms of these two proteases are likely to be located in the most acidic vesicular compartments, which probably fuse with the phagosome during the second killing phase mentioned in Section 1.3 (Figure 1.1).

Table 1.6 **Endoproteases found within compartments of the endocytic pathway.**

Name	Catalytic group	Operating pH*	pI
Cathepsin B	Cys	5-6.5	5.4
Cathepsin H	Cys	5.0-6.5	7.1
Cathepsin L	Cys	4.5-6.0	5.8-6.1
Cathepsin N	Cys	3.5	6.2
Cathepsin S	Cys	5.0-7.5	6.3-6.9
Cathepsin T	Cys	6.9	?
Cathepsin K	Cys	6.0-6.5	?
Cathepsin D	Asp	2.8-5.0	5.5-6.5
Cathepsin E	Asp	3-3.5	4.1-4.44
Cathepsin G	Ser	7.5	10

* 'Operating pH' is the pH at which the enzyme is stable, this need not be the optimal pH. (Modified from Pillay *et al.*, 2002).

The serine proteases consist of a two-domain structure, with one open-ended, β -barrel in each domain, and the active site situated between the domains. Cathepsin G, the main protease in this class, has a catalytic triad consisting of His, Asp and Ser and is unusual as it lacks the highly conserved 191-220 disulfide region present in other serine proteases (Table 1.5) (Salvesen, 2004). Despite cathepsin G playing a significant role in neutrophil microbial killing, it only appears to be present in small quantities in monocytes and is virtually absent from macrophages (Kargi *et al.*, 1990).

Cathepsins are synthesised as inactive, preproenzymes. The prepeptide is removed during passage to the ER resulting in the formation of the proform of the enzyme. The propeptide assists in the proper folding, stability and correct targeting of the enzyme and blocks the active site cleft, thus keeping the protein inactive until activity is required (Chapman *et al.*, 1997). Crystallography has shown that the propieces of cathepsins B, L and K occupy the active site cleft and are positioned in the opposite orientation to that of the natural substrates and are, therefore, not digested (Riese and Chapman, 2000). Activation of the enzyme may occur by proteolytic cleavage of the N-terminal propeptide by either intermolecular

autocatalysis or by other proteases (Chapman *et al.*, 1997; Turk *et al.*, 1997; Turk *et al.*, 2001). The activation process is dependent on low pH and the concentration of glycosaminoglycans present, suggesting that active cathepsins are likely to occur in acidic vesicles (Turk *et al.*, 2001; Bühling *et al.*, 2004). Normally, the activity of proteases with limited proteolytic ability is controlled by simply balancing the amount of active enzyme with an equivalent amount of active inhibitor. The regulation of lysosomal protease activity is, however, a more complicated process and is controlled in a number of different ways, which are summarised in Figure 1.2.

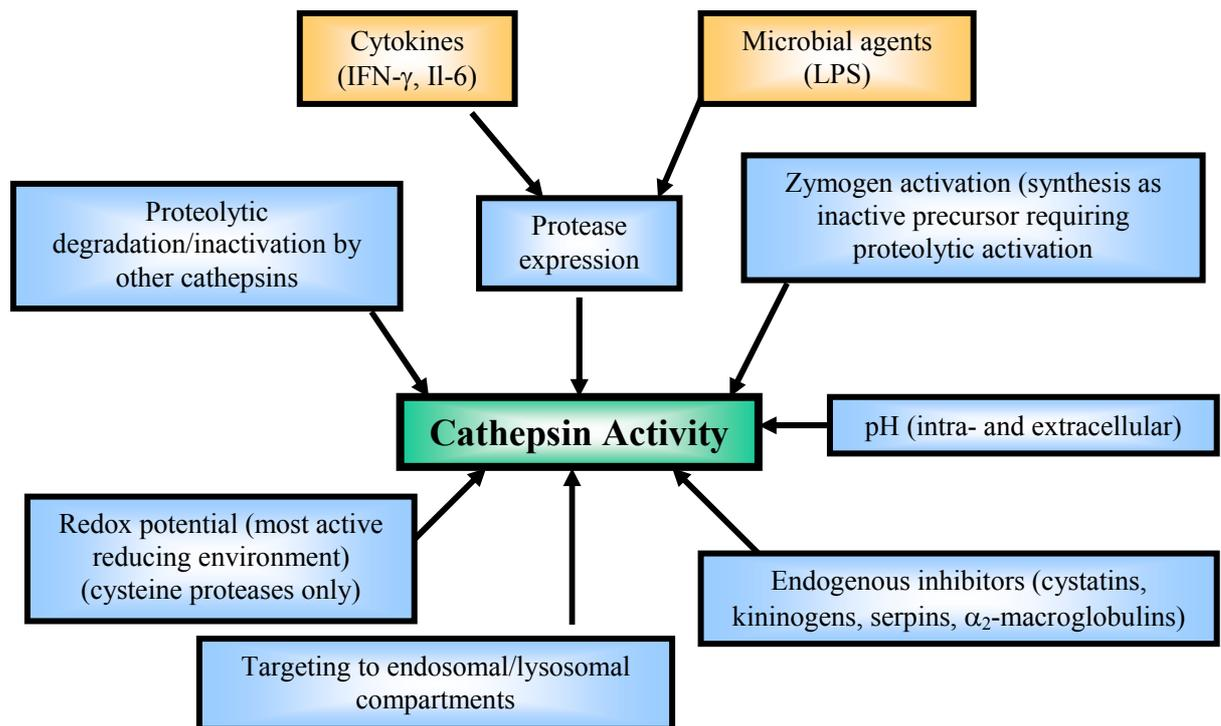


Figure 1.2 Factors responsible for the regulation of cathepsin activity.

Certain cathepsins have widespread expression throughout the body, whereas, the expression of others is limited to particular cell types. Cytokines and microbial agents can stimulate macrophages, resulting in enhanced cathepsin expression. Cathepsins are synthesised as inactive precursors, which undergo proteolytic activation to produce the mature, active enzyme which can be inactivated or degraded by other cathepsins when necessary. Cathepsins function optimally at acidic pH and are generally unstable and weakly active at neutral pH. The active site cysteine residue is easily oxidised; therefore, the enzymes are most active in reducing compartments. They possess glycosylation sites and residues allowing for binding to MPRs and the subsequent transport to endosomes and lysosomes. A number of endogenous cathepsin inhibitors are present in cells to control both intra- and extracellularly expressed cathepsins (Chapman *et al.*, 1997; Turk *et al.* 2001; Bühling *et al.*, 2004).

Cathepsins, were originally considered to be ubiquitously expressed, ‘‘housekeeping’’ proteins responsible for the degradation of unnecessary, abnormal or endocytosed proteins. This view has changed, however, since the discovery of distinct expression patterns for cathepsins and the use of gene knockouts, showing that cathepsins have specific, individual functions which are vital for the normal functioning of many biological processes (Wolters

and Chapman, 2000; Turk *et al.*, 2001; Bühling *et al.*, 2004). Cathepsins are involved in antigen processing (Shi *et al.*, 1999), normal bone and ECM remodelling (Chapman *et al.*, 1997; Turk *et al.*, 2000; Wolters and Chapman, 2000) and apoptosis (Leist and Jäättelä, 2001; Salvesen, 2001; Roberg *et al.*, 2002), for example. Cathepsins are also associated with various pathological conditions such as rheumatoid arthritis (Schurigt *et al.*, 2005), osteoarthritis, osteoporosis, neurological disorders (Goto *et al.*, 1987), chronic obstructive pulmonary lung disease including asthma, emphysema, idiopathic pulmonary fibrosis (Takahashi *et al.*, 1993; Chapman and Shi, 2000; Wolters and Chapman, 2000) and cancer (Turk *et al.*, 2000) as well as with inherited genetic diseases such as pycnodysostosis, a disease characterised by osteosclerosis, short stature, acro-osteolysis of the distal phalanges, bone fragility, clavicular dysplasia and skull deformities with delayed suture closure (Gelb *et al.*, 1996) and Papillon-Lefèvre syndrome, a disorder characterised by palmo-plantar hyperkeratosis and severe early onset periodontitis, resulting in the loss of the primary and secondary dentitions (Hart *et al.*, 1999; Toomes *et al.*, 1999).

1.4.1.1 Macrophage cathepsins

As mentioned cathepsins A, B, D, H, L, S and Z have been identified in J774 macrophage phagosomes (Garin *et al.*, 2001) and isolated vesicles (Claus *et al.*, 1998). Diment and Stahl (1985) first identified a cathepsin D-like protease in rabbit alveolar macrophages and later identified this as a (possibly early endosome-) membrane-associated form of cathepsin D, processed to an active form while still attached to the endosomal membrane (Diment *et al.* 1988). Both cathepsins B and D have been associated with inflammation and alveolar macrophages of smokers have larger vesicles containing more cathepsin D compared to those of non-smokers (Chang *et al.*, 1989). As cathepsin D is capable of degrading a number of proteins, it is possibly responsible for the structural damage of the lungs associated with cigarette smoking. Increased levels of active cathepsin D and B have also been identified in peritoneal macrophages stimulated *in vivo* with mineral oil and thioglycollate (Lesser *et al.*, 1985) and with inflammation of the peritoneal cavity, inflammation also correlating with an increase in the size and number of cytoplasmic vesicles containing cathepsin D and B. *In vitro* studies indicate that macrophages are capable of secreting cathepsin B between the macrophage and ECM, suggesting a role for cathepsin B in the degradation of the ECM (Mørland and Pedersen, 1979) and cathepsins B and D also play degradative roles within the phagosome (Mørland and Pedersen, 1979).

In vitro labelling of macrophages with [³⁵S] methionine and immunoprecipitation with anti-cathepsin L antibodies have indicated that macrophages also synthesise cathepsin L. This is synthesised as a 43 kDa precursor and processed into a 25 kDa mature form through a 34 kDa intermediate (Reilly *et al.*, 1989). Claus *et al.* (1998) suggested that both cathepsins B and L may be located in a specialised secretory lysosome or vesicle, as both were secreted upon addition of either chloroquine or bafilomycin A1. Whereas, cathepsin H, α -galactosidase and β -hexosaminidase were not. This is possibly an important fact which should be borne in mind when interpreting vesicle colocalisations.

Cathepsin L was initially considered to be the only elastolytic cysteine protease present in human alveolar macrophages (Mason *et al.*, 1986; Reilly *et al.*, 1989; Shi *et al.*, 1992). Macrophages of smokers, however, were shown to have greater intracellular, elastolytic activity than non-smokers, but both had equivalent cathepsin L activities. This suggested the contribution of at least one additional protease (Reilly *et al.*, 1991). One such protease was subsequently identified as cathepsin S (Shi *et al.*, 1992; Reddy *et al.*, 1995). Both cathepsins S and L are now known to be differentially expressed in antigen presenting cells (APCs), however, and appear to be mainly involved in degradation of the invariant chain (Ii) and regulation MHC class II presentation (Shi *et al.*, 1999; Hsieh *et al.*, 2002; Beers *et al.*, 2003). Cathepsin S has also been found to be mainly associated with the late endosome where such processing may take place (Claus *et al.*, 1998).

Cathepsin K, on the other hand, discovered in rabbit osteoclasts (Chapman *et al.*, 1997), human monocyte-derived macrophages (MDMs) (Punturieri *et al.*, 2000) and alveolar macrophages (Shi *et al.*, 1995) has subsequently been shown to have the greatest elastolytic potential of all mammalian elastases (Chapman *et al.*, 1997; Punturieri *et al.*, 2000). It appears to be up-regulated in inflamed areas, with cigarette smokers having twice the amount of mRNA and more protein than non-smokers (Chapman *et al.*, 1997). By using MDMs, cultured under conditions in which the differentiated cells show a tissue-destructive phenotype similar to that seen in chronic inflammatory sites *in vivo*, Punturieri *et al.* (2000) showed that MDMs secrete both processed and inactive cathepsin K along with cathepsins L and S. Up-regulated expression of vacuolar-type H⁺-ATPase components for pumping protons out of the cell, simultaneously allows the development of an acidic pericellular

compartment in macrophages has not yet been identified as the vesicular compartments and the MMP protease complement of vesicles remains virtually unknown. TIMP-1 is able to complex and inhibit both proMMP-9 and MMP-9 itself (Triebel *et al.*, 1995; Goetzl *et al.*, 1996; Price *et al.*, 2000), and complex formation shields the carboxyl-terminus of MMP-9 from MMP-3 thus preventing MMP-3 from activating MMP-9 (Goetzl *et al.*, 1996). Price *et al.* (2000) demonstrated that, in neutrophils, TIMP-1 is found in distinct vesicles, largely separate from the neutrophil MMPs proMMP-8 and proMMP-9. Differential release of TIMP-1 and proMMPs may play a role in controlling the extent of extracellular MMP activity. Differential secretion is extremely important as it may provide a drug target for controlling many pathological conditions, especially inflammatory disease. This is currently under investigation in the neutrophil.

Vesicle localisation and regulation is also unknown in macrophages as vesicle characterisation has not been performed to date but is potentially important and more so as Osiewicz *et al.* (1999), showed that mice deficient for TIMP-1 appear to be more resistant to *Pseudomonas aeruginosa* infections, indirectly suggesting that active MMPs are required for immunity. Differential regulation of TIMP-1 and MMPs may, therefore, contribute to immunity by regulation of processing or degradation of cytokines, MMP activity being very important in cytokine processing (Folgueras *et al.*, 2004) (Table 1.8). Even though this seemed to be a neutrophil-dependent phenomenon, macrophages may also require active MMPs for fighting bacterial infection and it would thus be useful to know whether the various TIMPs, MMPs and cathepsins are located in a particular vesicle types and whether fusion with the phagosome and release of these vesicles is separately and differentially regulated under specific stimulation. An initial step to establishing which combinations of proteins are present in the macrophage vesicles and whether there are indeed different vesicle populations is required and will assist in future studies of the various macrophage processes, such as antigen presentation and the killing of organisms in the phagosome which seem highly complex (Figure 1.1) (Anes *et al.*, 2006).

1.5 Objectives of the current study

At the commencement of this study, the vesicular distribution of cathepsins B, D, H, S and L as well as MMP-9, TIMP-1 and TIMP-2 in J774 macrophages was virtually unknown as few studies have focused on establishing their vesicle distribution. The major aim of this study was to establish the distribution of the above cathepsins, MMPs and TIMPs in the hope of

identifying marker enzymes for different vesicle populations. Antibodies to cathepsins B, D, H, S and L and to MMP-9, TIMP-1 and TIMP-2 raised against antigens from other species were available in our laboratory. For studies on TIMP-1 and TIMP-2, however, it was decided to raise additional antibodies against recombinant human forms of the proteins, as TIMP-1 and -2 are highly conserved blood proteins and hence most antibodies react weakly at best. All antibodies needed to be characterised for species cross-reactivity with the mouse antigens and to be optimised (Chapter 3). These antibodies were subsequently used in immuno-EM and fluorescent microscopy studies of J774 cells, the cells most characterised to date (Claus *et al.*, 1998; Jahraus *et al.*, 1998).

As cathepsins H and S had previously been identified by activity assays as possible markers for early and late endosomes, respectively (Claus *et al.*, 1998; Jahraus *et al.*, 1998), colocalisation studies were performed to determine whether cathepsins B, D and L occurred in such vesicular compartments (Chapter 4). As macrophages are known to have highly active and fairly complex endosome-lysosome systems (Rabinowitz *et al.*, 1992; Astarie-Dequeker *et al.*, 2002), additional markers were used to verify the presence of the cathepsins in classically defined endosome-lysosome systems i.e. low pH compartments, labelling for lysosomal-associated membrane proteins (LAMPs). Colocalisations between the cathepsins and LysoTracker (acidic compartment) (Via *et al.*, 1998) and LAMPs and proposed vesicle subpopulations were compared with those identified by Anes *et al.* (2006) (Chapter 4) and markers such as cathepsins S, H and D evaluated as markers for the early endosome (non-acidic, LAMPs-negative), late endosome (acidic, LAMPs-positive) and lysosome (most acidic, LAMPs-positive), respectively. Emerging evidence seems to indicate that the final killing of specific pathogens is brought about by the fusion of specific digestive enzymes (proteases) with the phagosome. Knowledge of the complement of proteases in specific vesicles and regulation of their release is potentially important as such information may allow therapeutic strategies to be developed. Knowledge of the distribution of proteases in specific vesicle populations may also reveal new marker enzymes for specific types.

The distribution of MMP-9 and MMP inhibitors (TIMPs) in J774 macrophages was considered next (Chapter 5). It was suspected that, as MMPs and their inhibitors are usually secreted and seem largely to function extracellularly (Campbell *et al.*, 1991), they would be located in vesicles belonging to the secretory pathway (non-acidic, LAMPs-negative) as opposed to the endosome-lysosome vesicle system (acidic, LAMPs-positive). Thus, it was

CHAPTER 2

GENERAL MATERIALS AND METHODS

The common biochemical techniques that were employed in this study are described here. Specialised techniques will be described in the relevant chapters.

2.1 Reagents

Dulbecco's modified Eagle's medium (DMEM), Hanks' balanced salts (HBSS), glutamine, trypsin-ethylenediaminetetra-acetic acid (EDTA), sodium bicarbonate, bisacrylamide (*N,N'*-methylene-bisacrylamide), Coomassie blue R-250, goat anti-rabbit IgG (whole molecule) alkaline phosphatase conjugate, rabbit anti-chicken IgG (whole molecule) alkaline phosphatase conjugate, donkey anti-sheep IgG (whole molecule) alkaline phosphatase conjugate, goat anti-mouse IgG (whole molecule) alkaline phosphatase conjugate, rabbit anti-chicken IgG (whole molecule) fluorescein isothiocyanate (FITC) conjugate, donkey anti-sheep IgG (whole molecule) FITC conjugate, goat anti-rabbit IgG (whole molecule) FITC conjugate, goat anti-rat IgG (whole molecule) FITC conjugate, goat anti-rabbit IgG (whole molecule) tetramethyl rhodamine isothiocyanate (TRITC) conjugate, piperazine-*N,N'*-bis(2-ethanesulfonic acid) (PIPES), *N*-2-hydroxy-piperazine-*N'*-2 ethane sulfonic acid (HEPES), ethylene glycol-bis(β -aminoethyl ether) *N,N,N,N,N'*-tetra acetic acid (EGTA), polyoxyethylene (23) lauryl alcohol (Brij 35 solution), diaminobenzidine/3,3',4,4'-tetraaminobiphenyl (DAB), Freund's complete and Freund's incomplete adjuvants (FCA and FIA), citric acid, bovine serum albumin (BSA), saponin, gelatin (porcine skin) and fish skin gelatin (FSG) were from Sigma (St. Louis, Missouri). Acrylamide, ammonium persulfate, sodium chloride, sodium hydroxide, potassium chloride, Na₂HPO₄, Na₂HPO₄.H₂O, sodium azide, glycine, paraformaldehyde (PFA), glutaraldehyde (25% solution), polyoxyethylene (9-10) *p-t*-octyl phenol (Triton X-100) and EDTA disodium salt, hydrochloric acid, CaCl₂.2H₂O, 2,2'-azino-di(3-ethyl)-benzthiozoline sulfonic acid (ABTS) and H₂O₂ 35% (v/v) were from BDH (Poole, England). Sodium dodecyl sulfate (SDS) was from Boehringer Mannheim (Mannheim, Germany) and 2-amino-2-(hydroxymethyl)-1,3-propandiol (Tris) was from MP Biomedicals (Eschwege, Germany). Methanol, glacial acetic acid, KH₂PO₄ and MgCl₂.6H₂O were from Saarchem (Wadeville, South Africa). Glycerol was from AR-Associated Chem. Enterprises (Glenvista, South Africa). Mercaptoethanol and amido black were from Merck Schuchardt OHG (Munich, Germany). Serva blue G was

which has a higher pH and decreased pore size the glycine becomes anionic. The glycinate ions now move faster than the proteins, with their mobility approaching that of the chloride ions, resulting in the proteins being left behind the chloride and glycinate ions to separate in a constant voltage gradient. The proteins are separated by the sieving effect of the gel according to their M_r 's.

2.3.1.1 Reagents

Acrylamide/bisacrylamide monomer stock solution [30% (m/v) acrylamide, 2.7% (m/v) bisacrylamide]. Acrylamide monomer (58.4 g) and *N, N'*-methylenebisacrylamide (1.6 g) were dissolved and made up to 200 ml with dH_2O . The solution was filtered through Whatman No. 1 filter paper and stored in an amber bottle at $4^\circ C$.

4 x Separating gel buffer [1.5 M Tris-HCl buffer, pH 8.8]. Tris (36.3 g) was dissolved in dH_2O (~ 180 ml), adjusted to pH 8.8 with HCl and made up to 200 ml. The buffer was filtered through Whatman No. 1 filter paper and stored at $4^\circ C$.

4 x Stacking gel buffer [500 mM Tris-HCl, buffer pH 6.8]. Tris (12 g) was dissolved in dH_2O (~ 180 ml), adjusted to pH 6.8 with HCl and made up to 200 ml. The buffer was filtered through Whatman No. 1 filter paper and stored at $4^\circ C$.

SDS stock solution [10% (m/v) in dH_2O]. SDS (10 g) was dissolved in dH_2O , with gentle heating and made up to 100 ml. The solution was stored at room temperature (RT).

Ammonium persulfate initiator solution [10% (w/v) in dH_2O]. Ammonium persulfate (0.1 g) was dissolved in dH_2O (1 ml) just before use. The solution was kept at $4^\circ C$ for up to 1 week.

Tank buffer [25 mM Tris-HCl and 192 mM glycine-HCl buffer, 0.1% (m/v) SDS, pH 8.3]. Tris (3 g) and glycine (14.4 g) were dissolved in dH_2O and made up to 1 l. Prior to use SDS stock solution (2.5 ml) was added to 250 ml.

2.5.2 Procedure

The procedure for SDS-PAGE was modified from that described (Section 2.3.1.2) in that 0.1% gelatin was incorporated into the separating gel to allow for the detection of proteinases (Heussen and Dowdle, 1980). Stock gelatin solution (1.5 ml) was added to 4 x separating gel buffer (2.25 ml) and the rest of the solution for casting a 12.5% gel (Table 2.1) and by pouring the gel as quickly as possible. Gels were allowed to set for 1 h. Samples were prepared in non-reducing treatment buffer (Section 2.3.1.1) and the electrophoresis carried out as described (Section 2.3.1.2).

After electrophoresis the gel was briefly rinsed in dH₂O and renatured in unbuffered renaturation solution (50 ml) (3 x 30 min, RT) with agitation. The gel was subsequently placed in a clean plastic container with pre-warmed digestion buffer (250 ml) and the digestion allowed to proceed for 18 h at 37°C for MMPs. After this time, the gel was washed with dH₂O (3 x 1 min), stained for 1 h in Amido black staining solution, destained in several changes of destaining solution and stored at 4°C until photographed. Gels were photographed using a VersaDoc 4000 Imager (BioRad, California, USA) and analysed using Quantity One software.

2.6 Western blotting

Many techniques have been utilised for the detection of specific proteins following SDS-PAGE, however, the most widely used is western blotting with antibodies directed against the proteins of interest (Bischoff *et al.*, 1998). This technique provides information about antibody specificities and the target antigen such as its molecular weight, its activation state (i.e. proform of the enzyme versus the active form), oligomeric arrangement or post-translational modification.

The choice of immobilising matrix used for protein transfer is dependent on the subsequent investigations that follow the transfer. Generally, for immunoblotting, proteins are transferred onto a nitrocellulose membrane with a pore size of 0.45 μm (Van Dam, 1994). Nitrocellulose membranes are made by allowing nitric acid-esterified cellulose, solubilised in an organic solvent mixture, to gel by the evaporation of the solvents. The pore size of the membrane depends on how the temperature and the time of the drying process are regulated (Gershoni and Palade, 1983). Nylon membranes appear to bind certain antigens more strongly than nitrocellulose. The major disadvantage of this membrane type is that blocking

is usually performed at high temperatures which may denature sensitive antigens (Van Dam, 1994). If the protein transfer is followed by protein sequencing, then polyvinylidene difluoride (PVDF) membranes are used as they are able to withstand the harsh chemicals used in the sequencing process.

The composition of the transfer buffer should be carefully considered especially if proteins are being transferred to nitrocellulose membranes. Towbin *et al.* (1979) used a transfer buffer containing methanol, which counteracted the swelling of the gel. The incorporation of methanol into transfer buffers has both advantages and disadvantages. It increases the binding capacity of the nitrocellulose membrane for proteins, however, it also decreases the pore size of the gel, removes SDS from the proteins and may lead to fixation of the proteins in the gel, so concentrations greater than 20% should be avoided (Gershoni and Palade, 1983; De Maio, 1994; Van Dam, 1994). The addition of SDS to transfer buffers increases protein transfer, however, this appears to be dependent on the nature of the proteins being transferred (Van Dam, 1994). Transfer buffers containing SDS but lacking methanol have been used successfully in protein transfer (Gershoni and Palade, 1982). As the choice of specific buffers and detergents is determined by the nature of the proteins being transferred, the buffer proposed by Towbin *et al.* (1979) was used with the incorporation of 0.01% SDS for the current study.

The unoccupied binding sites of the membrane are blocked before antibody probing. This is done by incubating the membrane in a solution of an 'inert' protein such as BSA, ovalbumin, haemoglobin or non-fat milk. Non-fat milk is not suitable for blocking when lectins or antibodies recognising carbohydrate moieties are to be used, as milk contains large amounts of sugar that may prevent binding. Non-ionic detergents such as Tween-20 may also be used as they reduce the binding of proteins to the nitrocellulose, thus reducing the background but, they should not be used at concentrations greater than 0.5% as they may remove proteins from the membrane (De Maio, 1994).

2.6.1 Chromogenic blots

The substrate products used in chromogenic blots should be insoluble, light stable and easily visible. The enzymes most frequently used for western blotting are HRP and alkaline phosphatase (Nadkarni and Linhardt, 1997). Although the most common substrates for HRP are 4-chloro-1-naphthol and DAB, tetramethylbenzidine (TMB) can also be used (Van Dam,

1994). H₂O₂ needs to be added to both 4-chloro-1-naphthol and DAB before use, whereas, TMB requires dioctylsulfosuccinate. DAB is considered to have intermediate sensitivity which can be enhanced by the use of imidazole and divalent metal ions such as cobalt. HRP catalyses the transfer of electrons from DAB, causing the DAB to become oxidised, forming an insoluble brown polymer. It is thought that the imidazole causes the formation of an additional electron transfer site in HRP, increasing its activity (Nadkarni and Linhardt, 1997). Additional metal ions improve DAB polymer formation and cause a colour change in the final product. 4-chloro-1-naphthol is less sensitive than DAB but generally produces less background. DAB and 4-chloro-1-naphthol can be combined to produce a highly sensitive detection system (Van Dam, 1994). Alkaline phosphatase hydrolyses BCIP forming an intermediate that can dimerise to produce an insoluble indigo precipitate. The reduction of NBT yields an insoluble purple formazan. The combination of BCIP and NBT with alkaline phosphatase yields a dark purple precipitate that is much more sensitive than either substrate alone. During this reaction the NBT is reduced by the two reducing equivalents produced by the dimerisation of BCIP. BCIP/NBT usually produces sharp band resolution with little background. The reaction rate of alkaline phosphatase remains constant during the reaction allowing for the relative sensitivity to be controlled. This is not possible with other enzymes.

2.6.2 ‘Tank’ buffer system

This type of apparatus is fairly simple. An electrophoretic field is generated to transfer proteins from a matrix, such as an acrylamide gel, to an immobilising matrix such as a nitrocellulose membrane. The transfer cassette containing the gel and nitrocellulose is placed in a ‘tank’ of buffer allowing for the electrophoretic protein transfer. Usually, an efficient cooling system is used in conjunction with this apparatus. Transfers can be carried out overnight as the buffer does not become depleted during the transfer.

2.6.2.1 Reagents

Transfer buffer [25 mM Tris-HCl and 192 mM glycine-HCl buffer, 20% (v/v) methanol, 0.01% (m/v) SDS, pH 8.3]. Tris (6.05 g), glycine (28.8 g) and SDS [2 ml of 10% (w/v) solution] were dissolved in 1.6 l of dH₂O. Methanol (400 ml) was added and the solution stored at –20°C without pH adjustment.

with primary antibody diluted in the antibody diluent solution (2 h, RT). Following washing in TBS II (2 x 5 min), the membrane was incubated with the appropriate enzyme conjugated secondary antibody diluted in the antibody diluent solution (1 h, RT). The membrane was subsequently washed in both TBS II (2 x 5 min) and TBS III (1 x 5 min), immersed in the appropriate substrate solution and developed in the dark until distinct bands were observed. The nitrocellulose was rinsed with dH₂O, dried between filter paper and kept in the dark until photographed with a VersaDoc 4000 Imager (BioRad, California, USA) and analysed using Quantity One software, the percentage of each processing form being visually assessed.

Towards the end of the study, PBS was used instead of the three separate TBS solutions.

2.6.3 'Semi-dry blotting' system

With the 'semi-dry blotting' system a stack of wet filter papers surrounding the gel and nitrocellulose membranes act as the buffer reservoir instead of the tank as in the 'tank' buffer system. The electrodes consist of conductive plates which produce a high-strength electrical field with higher current densities in comparison to the wire electrodes that are used in the 'tank' systems. The plate electrodes are in direct contact with the buffer soaked filter papers maximising the field strength across the gel, allowing for fast and efficient transfers. This system is less expensive than the 'tank' system as a relatively small amount of buffer is required. This small buffer volume limits the time for which the transfer can be carried out as the buffer becomes depleted. It should be noted that small proteins may pass straight through the membrane with this system and, as the voltages are limited by the lack of a cooling system, the transfer of high molecular weight proteins may be difficult (Jacobson, 1994).

2.6.3.1 Reagents

See Section 2.6.2.1.

2.6.3.2 Procedure

Following SDS-PAGE (Section 2.3.1.2) the gel was removed from the electrophoresis unit and submerged in transfer buffer. A mylar mask was prepared by cutting a rectangle 2 mm smaller than the gel on either side and placed on the anode in the base of the apparatus (Hoefer SemiPhor™ Semi-Dry Transfer Unit). Nitrocellulose membrane and six pieces of filter paper were cut slightly smaller than the gel and saturated in transfer buffer. Three

pieces of filter paper were centered in the opening of the mylar mask, with their edges slightly overlapping the cutout on all sides. The nitrocellulose was placed on the filter paper stack and the gel on top of the nitrocellulose. Three pieces of filter paper were placed on top of the gel. The transfer was performed at 26 mA for 2 h. The remainder of the procedure was carried out as previously described (Section 2.6.2.2).

2.7 Electron microscopy and immunogold labelling

The main EM techniques used in this study were transmission electron microscopy (TEM) of ultrathin resin sections and immunogold labelling (De Mey, 1987).

If fine structure immunocytochemistry is to be performed the choice of resin to be used should be carefully considered as it should possess certain characteristics. Firstly, it should easily infiltrate cells/tissues and must harden uniformly without any shrinkage or swelling. Secondly, the resin blocks should be hard but have a degree of plasticity allowing for smooth sectioning. The processes leading up to and including infiltration, polymerisation and sectioning should not prevent the demonstration of antigens by immunocytochemistry nor change the fine structure. The resin should allow for drying of sections without loss of fine structure and sections should also be resistant to radiation by the electron beam (Griffiths, 1993).

Methacrylates or ‘acrylic resins’ have several advantages over other embedding media used for EM. These include, the rapid penetration of cells/tissues (as a result of the low viscosity and the rapid diffusion of low molecular weight monomers of the resin), the resin is also relatively inexpensive and non-toxic. Disadvantages include absolute hydrophobicity and the requirement for total dehydration of the specimens in organic solvents prior to infiltration. This, together with a requirement for strong heat polymerisation (60°C for 4 days), make methacrylate resins unsuitable for immunocytochemical studies, as such treatment of tissue destroys antigenicity.

The resin chosen for the current study was LR White, a hydrophilic resin that has become increasingly popular. Its hydrophilicity makes ultrathin sections permeable to aqueous solutions (immunoreagents), eliminating the need for pre-etching of hydrophobic resin surfaces to introduce hydrophilic groups before labelling. Membrane and cytosol structures can be observed without lipid-stabilising osmium treatment as LR White does not solubilise

lipids. The only problem, however, is that membrane structures are quite difficult to stain reproducibly. As the resin is miscible with a small amount of water, however, infiltration can be performed on partially dehydrated specimens (70% dehydrated) that have greater antigenicity than fully dehydrated samples.

Besides difficulties with staining and contrast, disadvantages include instability in the electron beam, and the adverse effects of oxygen on polymerisation. Final polymerisation of resin in a resin-filled gelatin capsule impermeable to oxygen, solves this problem. Slowly increasing the intensity of the beam also allows resin stabilisation and prevents specimen damage (Griffiths, 1993; Philimonenko *et al.*, 2002). Another compromise between the preservation of antigenicity and organelle structure also needs to be made for successful immunocytochemistry. This involves the choice of fixative and fixation protocol.

Glutaraldehyde is the best choice for the preservation of tissue ultrastructure. It is extensively cross-linking, however, and can alter epitopes resulting in loss of antigenicity or prevention of access to the antigen. Formaldehyde, on the other hand, results in better preservation of antigenicity, due to lower cross-linking, but gives poorer ultrastructural preservation. Macrophage ultrastructure also seems difficult to preserve and combination fixatives with approximately 4% PFA or less and low levels of glutaraldehyde (0.5% or less) have been shown to provide an adequate balance between the retention of ultrastructure and antigenicity, however (Griffiths, 1993).

The buffers used during the fixation process are important as well. Both carbonate and cacodylate buffers have been used in the past, but both have pKa's too low for proper fixation. Phosphate buffers are also popular, but they have limited solubility in the presence of divalent cations and generally extract protein during the fixation process. The buffers introduced by Good *et al.* (1966) are considered to be good buffers for fixation and include PIPES, HEPES and MOPS. PIPES buffers in particular result in much less extraction in comparison with phosphate buffers (Griffiths, 1993). The buffer chosen for use in the current study is a combination of PIPES, HEPES, EGTA and MOPS and is described by Santama *et al.* (1998).

Sectioning of specimens requires the use of an ultramicrotome. Glass knives are produced by fracturing glass strips into squares and then right-angled triangles to produce edges that

can cut hard resin. Knives for resin sectioning have a limited lifespan as edges become blunt over time due to the fluid nature of glass. Older knives can be used for the initial trimming of the resin block, whereas ultrathin sectioning requires the use of new knives. The sections are usually collected on formvar coated grids, the formvar acting as a support for the section. Immunolabelling requires that ultrathin sections be incubated with an antibody against the antigen to be located. Subsequently, the section is incubated with another molecule that binds the antigen-antibody complex allowing for detection by the EM (Geuze *et al.*, 1981; Slot and Geuze, 1985). Protein A from *Staphylococcus aureus* binds the Fc region of antibodies in a 1:1 stoichiometric ratio. This protein can, therefore be adsorbed to electron-dense, gold colloids and used to localise a particular antigen in a cell section. Protein A has a particularly high affinity for rabbit IgG, so if the primary antibody used is not raised in rabbits, but another species with a lower protein A affinity, a linker antibody (e.g. rabbit anti-chicken IgY) should be incorporated and the protein A gold probe used to detect this antibody. The use of a linker antibody increases the labelling density as more than one rabbit IgG binds per IgY molecule (Griffiths, 1993; Slot and Geuze, 1985).

Immunocytochemistry allows for the cellular location of antigens to be determined and if it is to be performed there are several important points that need to be considered. A well characterized, high-affinity antibody against the antigen should be used. The antibody and electron dense markers should have access to all parts of the cells/tissues. The antigen being localised should possess a large amount of antigenicity after fixation and at the same time the preservation of fine-structure should be adequate (Griffiths, 1993). Control labelling experiments are essential for identifying any potential non-specific, high-affinity interactions with pre-immune sera. Controls include: incubation of the section with pre-immune IgG/IgY and detection with protein A and incubation of the section with protein A gold only. In all cases the pre-immune IgG/IgY and protein A gold probes are used at the same concentration as used in the labelling with the specific antibodies.

2.7.1 Fixation and embedding of J774 cells in LR White resin

2.7.1.1 Reagents

130 mM PIPES, 60 mM HEPES, 20 mM EGTA, 4 mM MgCl₂, pH 7.3 (2 x PHEM). PIPES (9 g), HEPES, (2.68 g), EGTA, (1.875 g) and MgCl₂.6H₂O (0.163 g) were dissolved in 180 ml of dH₂O, adjusted to pH 7.3 with NaOH and made up to 200 ml. The solution was aliquotted and stored at -20°C.

65 mM PIPES, 30 mM HEPES, 10 mM EGTA, 2 mM MgCl₂, pH 7.3 (1 x PHEM). 2 x PHEM (50 ml) was diluted with dH₂O (45 ml), adjusted to pH 7.3 if necessary and made up to 100 ml.

PFA stock solution [16% (m/v) in dH₂O]. PFA (16 g) was dissolved in dH₂O (80 ml), heated to 60°C (in a fumehood) and the solution cleared with the dropwise addition of a 1M NaOH solution. After cooling, the volume was made up to 100 ml and aliquots stored at -20°C.

8% PFA in PHEM, pH 7.3. PFA stock solution (25 ml) was added to 2x PHEM (12.5 ml), adjusted to pH 7.3 with 1 M HCl and made up to 50 ml with dH₂O. The solution was stored at -20°C until required.

8% (m/v) PFA, 0.2% (v/v) glutaraldehyde in PHEM, pH 7.3. PFA stock solution (50 ml) and glutaraldehyde [800 µl of 25% (v/v)] were added to 2 x PHEM (25 ml), made up to 90 ml with dH₂O, adjusted to pH 7.3 with 1 M HCl and made up to 100 ml. The solution was stored at -20°C until required.

20 mM Glycine in PHEM, pH 7.3. Glycine (15 mg) was dissolved in 1 x PHEM (10 ml).

10 % (m/v) Gelatin in PHEM, pH 7.3. Microbiological grade gelatin (10 g) was added to 1 x PHEM (100 ml) and dissolved by heating. The volume was made up to 100 ml (if necessary) with dH₂O and the solution chilled rapidly on ice.

2.7.1.2 Procedure

Table 2.2 Protocol for the fixation and embedding of J774 cells in LR White resin.

Fixation	Time and Temperature
Fix in 8% (m/v) PFA, 0.2% (v/v) glutaraldehyde in PHEM, pH 7.3 with equal volume of medium.	2 h, RT
Replace with 8% PFA in PHEM, scrape of monolayers, transfer to tubes, centrifuge (700 x g, 10 min), store in 8% PFA. Pellet the cells (223 x g, 2 min), remove excess fixative.	Overnight, 4°C
Quench remaining free aldehyde groups with 20 mM glycine in PHEM.	2 x 15 min, RT
Pellet the cells (223 x g, 2 min). Remove excess glycine. Infiltrate with 10% (m/v) gelatin in PHEM, pH 7.3.	2 h, 37°C
Pellet the cells (223 x g, 2 min). Remove excess glycine and chill pellet rapidly on ice.	
Place a thin layer of buffer over the gelatin-infiltrated pellet to prevent drying out and cut into small blocks (2 x 2 x 2 mm).	
Embedding	
Dehydration 25% ethanol	15 min, RT
Dehydration 50% ethanol	15 min, RT
Dehydration 70% ethanol	1 h, RT
Dehydration 90% ethanol	30 min, RT
Dehydration 100% ethanol	30 min, RT
LR White resin : ethanol (1 : 1)	30 min, RT
LR White resin : ethanol (2 : 1)	30 min, RT
LR White resin	2 x 30 min, RT
LR White resin	1 h, RT
LR White resin	Overnight, RT
Fill gelatin capsules with fresh resin, place cubes in tip of a gelatin capsule.	
Quickly close the capsule and fill completely with syringe. Allow to polymerise.	48 h, 50°C

2.7.2 Glass knife production and preparation of grids

The glass strip was cleaned with detergent and water, dried and positioned on a LKB 7800 glass knife maker modified as described by Moorewood *et al.* (1992) and fractured to produce glass knives. The knife edges were examined and those with a barely visible counter-piece width were selected for ultrathin sectioning. A section collection trough made from aluminium foil tape was attached to the knife and sealed with nail varnish to produce a watertight boat. Ultrathin resin sections (90-110 nm) were cut using an ultramicrotome and sections were collected on formvar coated, copper grids.

2.7.3 Immunolabelling protocol

2.7.3.1 Reagents

10 x PBS stock solution, pH 7.2. NaCl (8 g), KCl (0.2 g), Na₂HPO₄ (0.115 g), KH₂PO₄ (0.2 g) and NaN₃ (0.2 g) were dissolved in dH₂O (90 ml), titrated to pH 7.2 with NaOH and made up to 100 ml. The solution was autoclaved and stored at 4°C.

1 x PBS working solution, pH 7.2. PBS stock solution (1 ml) was diluted with dH₂O (9 ml).

Glutaraldehyde fixative [1% (v/v) in PBS]. Glutaraldehyde [1 ml of a 25% (v/v) stock solution] was diluted to 25 ml with PBS.

BSA-PBS [1% (m/v) in PBS]. BSA (1 g) was dissolved in PBS and made up to 100 ml.

20 mM Glycine-PBS. Glycine (0.15 g) was dissolved in PBS and made up to 100 ml.

FSG-BSA [1% (v/v) FSG, 0.8% (m/v) BSA in 20 mM glycine-PBS]. FSG [1.11 ml of a 45% (v/v) solution] and BSA (0.4 g) were dissolved in glycine-PBS in a final volume of 50 ml. The solution was centrifuged (10 000 x g, 2 h, 4°C) to remove insoluble debris and the supernatant aliquotted and stored at -20°C.

2.7.3.2 Procedure

Immunogold labelling was performed by incubating the grids on droplets of reagent on Parafilm at RT. The steps followed are shown in Table 2.3. After the final staining the grids were air dried and viewed in a Philips CW120 Biotwin TEM at 80-100 kV.

Table 2.3 Procedure for immunogold labelling of J774 cells.

Step	Solution	Volume	Incubation Time
1. Blocking	BSA in PBS	20 µl	10 min
2. Blocking and aldehyde quenching	FSG-BSA	20 µl	4 x 1 min
3. Primary antibody	Diluted in FSG-BSA	10 µl	1 h
4. Wash	FSG-BSA	20 µl	5 x 4 min
5. Linker antibody (if required)	Diluted in FSG-BSA	10 µl	1 h
6. Wash	FSG-BSA	20 µl	5 x 4 min
7. Protein-A gold probe	Diluted in FSG-BSA	10 µl	1 h
8. Wash	FSG-BSA	20 µl	5 x 4 min
9. Fixation*	Glutaraldehyde fixative	10 µl	5 min
10. Wash	dH ₂ O	100 µl	4 x 5 min
11. Staining	Uranyl acetate	Droplet	6 min
	Lead citrate	Droplet	4 min

* If double immunogold labelling is to be performed, steps 1-9 are repeated at this point.

Controls included the substitution of pre-immune antisera at the same concentration as the test.

Two problems associated with fluorescent microscopy are photobleaching and quenching (Tanke, 1998). Photobleaching or fading refers to the loss of fluorescence during high-intensity excitation and is caused by photodecomposition of the fluorochrome or by the production of heat as energy is absorbed. This destruction of the excited fluorochrome becomes the factor limiting fluorescence detectability (Tanke, 1998). Photobleaching can be reduced by increasing the detection sensitivity, allowing the excitation intensity to be reduced. Detection sensitivity can be increased by using low-light detection devices such as CCD cameras or by using objectives with high numerical apertures. Photobleaching can also be significantly reduced by using antifade reagents during mounting (Longin *et al.*, 1993; Ono *et al.*, 2001). These reagents usually contain compounds that scavenge the oxygen radicals that result from the process of fluorescence; these radicals if not removed may react with the fluorochrome producing a product with less fluorescence (Tanke, 1998).

2.8.1 Immunolabelling protocol

2.8.1.1 Reagents

PBS, pH 7.4 [8 mM Na₂HPO₄, 1.5 mM KH₂PO₄, 137 mM NaCl, 2.7 mM KCl, 1 mM CaCl₂.2H₂O and 0.5 mM MgCl₂.6H₂O, pH 7.4]. Na₂HPO₄ (1.144 g) and KH₂PO₄ (0.2 g) were first dissolved in dH₂O (200 ml). NaCl (7.999 g), KCl (0.1998 g), CaCl₂.2H₂O (0.147 g) and MgCl₂.6H₂O (0.1016 g) were added and the solution made up to 1 l with dH₂O. The solution was filtered through Whatman No. 1 filter paper and stored at 4°C.

PFA stock solution [16% (m/v) in dH₂O]. PFA (16 g) was dissolved in dH₂O (80 ml), heated to 60°C (in a fumehood) and the solution cleared with the dropwise addition of a 1M NaOH solution. After cooling, the volume was made up to 100 ml and aliquots stored at -20°C.

3.7% (m/v) PFA in PBS, pH 7.4. PFA stock solution (6.0 ml) was added to PBS, pH 7.4 (20 ml). The solution was made up just before use.

Saponin-PBS [0.1% (m/v) in PBS, pH 7.4]. Saponin (0.17 g) was dissolved in PBS (170 ml). The solution was filtered through Whatman No. 1 filter paper and was made up just before use.

BSA-PBS [1% (m/v) in PBS, pH 7.4]. BSA (0.13 g) was dissolved in PBS, pH 7.4 (13 ml). The solution was made up just before use.

BSA-Saponin-PBS [1% (m/v) in saponin-PBS, pH 7.4]. BSA (0.13 g) was dissolved in saponin-PBS, pH 7.4 (13 ml). The solution was made up just before use.

2.8.1.2 Procedure

A round, glass coverslip (12 mm diameter) was placed into each well of a 24 well plate, DMEM supplemented with 10% FCS (500 μ l/well) added and the coverslips allowed to condition overnight. J774 macrophages were cultured and trypsinized (Section 2.2.2) and resuspended in approximately 12 ml DMEM supplemented with 10% FCS. The medium from each well was removed, J774 cell suspension (500 μ l/well) added and the cells grown to approximately 70% confluency. Cells were fixed with 3.7% PFA in PBS (400 μ l/well, 10 min, RT), washed with PBS (400 μ l/well, 3 x, RT) and non-specific binding sites blocked by incubating the cells in BSA-PBS (400 μ l/well, 45 min, RT). Cells were incubated in primary antibody diluted in saponin-PBS (150 μ l/well, 1 h, RT) and washed in saponin-PBS (400 μ l/well, 6 x, RT) and blocked again with BSA-saponin-PBS (400 μ l/well, 1 h, RT). This was followed by incubation in secondary antibody diluted in saponin-PBS (150 μ l/well, 1 h, RT) and as fluorescent probes are light sensitive, the plate was wrapped in foil from this point onwards. The cells were washed in saponin-PBS (400 μ l/well, 6 x), post-fixed with 3.7% PFA (400 μ l/well, 10 min) and washed finally in saponin-PBS (400 μ l/well, 3 x). If double immunolabelling was to be performed the labelling procedure was repeated at this point. Controls included the substitution of pre-immune sera at the same level as the test and performing each labelling individually and in the opposite order (labelling for second antigen first) in repeat experiments. Coverslips was removed from the wells, dipped several times in dH₂O and air dried (RT). *SlowFade*TM(anti-fade reagent) (1 μ l) or Mowiol (4 μ l) were applied to microscope slides and the coverslips mounted and sealed with clear nail varnish. Labelling was viewed using either an Olympus epifluorescent microscope and F-View CCD camera or a Zeiss 510 Meta confocal microscope and images analysed using ImageJ software. Images of colocalisation using colour (i.e. red and green images merged to form yellow) are highly influenced by display settings and intensity, and, therefore, colocalisation based on colour analysis alone is problematic and can lead to incorrect conclusions. Grey scale images (i.e. black and white) on the other hand, are not affected by display settings and

should be assessed when visually judging the following colocalisation images, as the yellow colour (indicating the degree of colocalisation in the composite image) varies depending on settings and printer type. The percentage colocalisation was determined manually by counting the number of vesicles in an average of at least 3 representative cells and reporting average vesicle colocalisation as a percentage.

3.5.2 Procedure

Wells of microtitre plates were coated with human recombinant antigen [150 μ l/well, 1 μ g/ml in PBS, 16 h, RT], blocked with BSA-PBS (200 μ l/well, 1 h, 37°C) and washed with Tween-PBS (3 x). Egg yolk extracts were diluted with two volumes of phosphate buffer and used as the primary antibody [100 μ l/well, 1:20 (v/v) in BSA-PBS and serially diluted twofold thereafter to 1: 10 240 (v/v), 1 h, 37°C]. Excess antibody was washed out with Tween-PBS (3 x) and a suitable dilution of rabbit anti-chicken IgY-HRP conjugate in BSA-PBS was added (120 μ l/well, 30 min, 37°C). Excess antibody was washed out with Tween-PBS (3 x). The substrate solution was added and incubated in the dark for optimal colour development (150 μ l/well, 10-20 min, RT) and the enzyme reaction stopped by the addition of NaN₃ [50 μ l/well, 0.1% (m/v) in citrate-phosphate buffer]. Absorbances were read at 405 nm in a Bio-Tek EL312 Microplate Bio-kinetics reader. For the controls, either the blocking solution, primary antibody or secondary antibody was omitted to assess the efficiency of the blocking or the specificities of the primary/secondary antibodies. Titration curves were constructed by plotting -log IgY dilution versus absorbance to assess the immune response and determine which eggs should be selected for IgY isolation.

Selected egg yolks were separated from the egg whites, carefully washed in a stream of water, the yolk sacs punctured and the yolk volume measured. Two volumes of phosphate buffer were added and mixed gently by inversion after sealing the measuring cylinder with Parafilm. Crushed PEG 6 kDa was added [3.5% (m/v)] and dissolved by stirring. The precipitated vitellin fraction (containing lipoproteins) was pelleted by centrifugation (4420 x g, 30 min, RT) and the contaminating lipids removed by filtering the supernatant fluid through cottonwool placed in the neck of a funnel. PEG [8.5% (m/v)] was added to the clear filtrate to bring the final volume to 12% (m/v). The solution was mixed, centrifuged (12 000 x g, 10 min, RT) and the pellet dissolved in phosphate buffer, in a volume equal to that of the initial egg yolk volume. PEG was added [12% (m/v)], mixed and the solution centrifuged (12 000 x g, 10 min, RT). The supernatant fluid was discarded and the IgY pellet dissolved in phosphate buffer equal to 1/6th of the original egg yolk volume. A 1:50 dilution of IgY in phosphate buffer was prepared and the IgY in the undiluted solution was calculated using the IgY extinction coefficient ($E_{280nm}^{1mg/ml} = 1.25$) and the equation [IgY] = [(A₂₈₀/1.25) x 50] (mg/ml) (Goldring and Coetzer, 2003).

Early studies suggested that only the proforms of certain cathepsins are secreted by monocytes/macrophages (Portnoy *et al.*, 1986; Reilly *et al.*, 1989). Both thioglycolate-elicited mouse peritoneal macrophages and J774 mouse macrophages secrete a 36 kDa form of procathepsin L (Portnoy *et al.*, 1986), whereas, human alveolar macrophages secrete a 43 kDa precursor form (Reilly *et al.*, 1989). Monocytes allowed to mature under specific culture conditions form MDMs with a highly proteolytic phenotype. These cells secrete the proforms of cathepsin B (45 kDa), cathepsin L (43 kDa), cathepsin S (37 kDa) as well as the mature, single chain forms of cathepsin B (31 kDa), cathepsin L (34 kDa) and cathepsin S (25 kDa) (Reddy *et al.*, 1995). Both the pro- and mature forms of cathepsins K and L appear to be secreted within 5 and 3 culture days, respectively, whereas, the proforms of cathepsin B and S were detected after 3 culture days, with mature forms being detected after 5 days for cathepsins B and L and 12 days for cathepsin S (Punturieri *et al.*, 2000). The variation in secretion between the types of cathepsin as well as between the different forms suggests that these proteins are packaged and secreted from different intracellular compartments. Although both forms of cathepsin L were secreted, cathepsin L was preferentially secreted as mature enzyme (Punturieri *et al.*, 2000). Active cathepsin H has been identified in both mouse macrophages (Muno *et al.*, 1990; Claus *et al.*, 1998) and human monocytes (Greiner *et al.*, 2003). Fully differentiated peripheral blood monocytes show more cathepsin H activity than immature monocytes (Greiner *et al.*, 2003). MDMs are also capable of secreting both pro- and mature forms of cathepsin D, with the proform being secreted in the first 5 days of culture (Punturieri *et al.*, 2000).

Before immunolocalisation studies on these antigens in macrophages were carried out the cross-reactivity of chicken anti-human liver cathepsin B (Elliott, 1993), chicken anti-porcine cathepsin D (Fortgens *et al.*, 1997; Elliott *et al.*, 1995), chicken anti-cathepsin S (Morrison, L., unpublished), rabbit anti-cathepsin H (Coetzer, 1992), rabbit anti-cathepsin L (Pike, 1990), chicken anti-human MMP-9 (Price *et al.*, 2000) and chicken anti-human TIMP-1 (Clulow, M., unpublished) with mouse antigens was checked. Sheep anti-human TIMP-2 serum supplied by Dr Linda Troeberg (Imperial College, London) was previously checked for cross-reactivity with mouse antigens and was, therefore, not repeated.

3.7.1 Reagents

Antibodies were kind gifts from current or former members of our research group in the Department of Biochemistry, University of KwaZulu-Natal, Pietermaritzburg. Chicken anti-human liver cathepsin B was from Dr E. Elliott, chicken anti-porcine cathepsin D was from Dr P. Fortgens, chicken anti-cathepsin S was from Miss L. Morrison, rabbit anti-cathepsin H was from Prof T. H. T. Coetzer, rabbit anti-cathepsin L was from Dr R. Pike, chicken anti-human MMP-9 was from Dr B. Price and chicken anti-human TIMP-1 was from Miss M. Clulow.

Pre-immune sera were not from the same animals used to raise the antibodies but were from pooled samples.

Reagents for the culture of J774 cells, SDS-PAGE, CBB staining and western blotting were prepared according to Sections 2.2.1, 2.3.1.1, 2.4.1.1 and 2.6.2.1, respectively.

10 x PBS. Na₂HPO₄ (2.6 g), NaH₂PO₄·H₂O (0.36 g) and NaCl (16.4 g) were dissolved in a final volume of 200 ml dd.H₂O without pH adjustment. The solution was autoclaved (121°C, 15 min) and stored in aliquots at -20°C.

Percoll [63% (v/v) in PBS]. 63 parts 100% Percoll (density 1.13 g/ml) were diluted with 7 parts 10 x PBS and 30 parts 1 x PBS just before use, and kept on ice.

Percoll [72% (v/v) in PBS]. 72 parts 100% Percoll (density 1.13 g/ml) were diluted with 8 parts 10 x PBS and 20 parts 1 x PBS just before use, and kept on ice.

3.7.2 Procedure

Preparation of crude monocyte homogenates

Venous blood was drawn from a healthy, non-smoking volunteer into a centrifuge tube containing citrate-phosphate-dextrose anticoagulant (7 ml) to a final volume of 50 ml. Percoll [63% (v/v)] (15 ml) was added to a sterile 50 ml conical centrifuge tube and carefully underlaid with Percoll [72% (v/v)] (15 ml), taking care not to disturb the discontinuous gradient with air bubbles. Anticoagulated whole blood (15 ml) was slowly layered on top of the pre-cooled Percoll gradient and centrifuged (500 x g, 30 min, RT). The plasma and mononuclear cell layer (from which the monocytes were obtained) were removed, aspirated, the cells resuspended in physiological saline (~1–5 ml) and stored at -20°C (Boyum, 1976).

When required, blood monocytes were thawed and centrifuged (17 203 x g, 12 min, RT). The pellet was sonicated (30 min, RT) and for SDS-PAGE was combined with equal volumes of reducing treatment buffer and boiled for 90 s. A sample of human plasma was similarly treated and used as the control.

Crude serum-containing J774 macrophage homogenates were initially frozen in medium before preparation in reducing treatment buffer for SDS-PAGE analysis (Section 3.6.2). SDS-PAGE and CBB staining were performed according to Sections 2.3.1.2 and 2.4.1.2. Serum-containing J774 homogenates (12 µl) and supernatants (10 µl), human monocyte homogenate (5 µl) and plasma (10 µl) were separated on 12.5% Laemmli gels (Section 2.3.1.2), transferred to nitrocellulose and probed with chicken anti-human liver cathepsin B [20 µg/ml or 35 µg/ml], chicken anti-cathepsin D [20 µg/ml or 40 µg/ml], rabbit anti-cathepsin H [10 µg/ml or 20 µg/ml], rabbit anti-cathepsin L [5 µg/ml or 10 µg/ml], chicken anti-cathepsin S [10 µg/ml or 20 µg/ml], chicken anti-MMP-9 [30 µg/ml], chicken anti-human TIMP-1 [10 µg/ml], rabbit anti-chicken IgG-alkaline phosphatase [1:100 000], goat anti-rabbit IgG-alkaline phosphatase [1: 30 000] according to Section 2.6.2.2.

3.7.3 Results

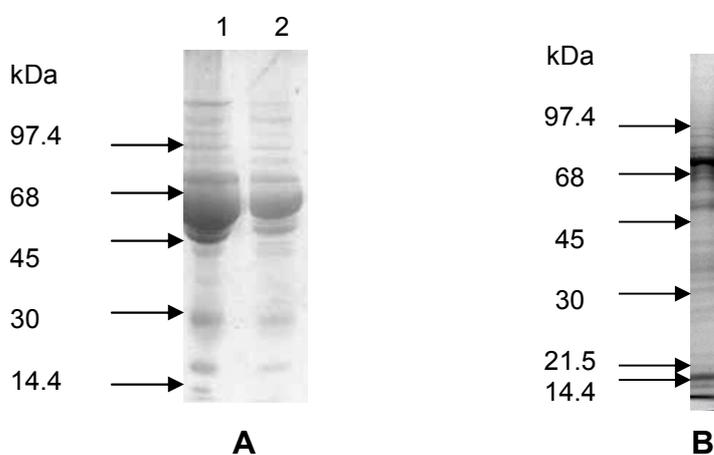


Figure 3.8 Reducing SDS-PAGE separation of human monocyte and J774 mouse macrophage homogenates.
A, human plasma (lane 1, 2 µl), human monocyte homogenate (lane 2, 2 µl) and B, serum-free J774 homogenate prepared immediately in reducing treatment buffer (15 µl), diluted [1:1] with reducing treatment buffer, combined with bromophenol blue [5 µl, 0.1% (m/v) in dH₂O] and separated on a 12.5% (v/v) Laemmli gel. A and B, stained with CBB.

Reducing SDS-PAGE showed a number of bands present in the serum-free J774 homogenate (Figure 3.8, B) which are not found in the human plasma and monocyte homogenate (Figure 3.8, A, lanes 1 and 2, respectively). Certain bands in the human monocyte homogenate

(Figure 3.8, A, lane 2) may be due to the presence of plasma in the monocyte homogenate (Figure 3.8, A, lane 1).

The antibodies to cathepsins B, D, H, L and S targeted only bands of the anticipated molecular weights in crude monocyte and J774 cell homogenates. Bands of approximately 39 kDa in the J774 mouse macrophage homogenate (Figure 3.9, A, lane 4) and 44 kDa in the human monocyte homogenate (Figure 3.9, B, lane 4) identified with the IgY anti-human liver cathepsin B antibody seem to correspond to the 40 kDa molecular weight of glycosylated human procathepsin B (Chan *et al.*, 1986) with variations in targeted bands possibly representing differences in glycosylation patterns. A 20 kDa band in the J774 homogenate (Figure 3.9, A, lane 4) may correspond to the 22 kDa heavy chain of human cathepsin B (Kirschke *et al.*, 1998) and a band of approximately 31 kDa in the homogenate of human monocytes (Figure 3.9, B, lane 4) may correspond to the single chain of human cathepsin B (25 kDa) (Kirschke *et al.*, 1998). No detectable secreted cathepsin B was observed in the J774 supernatant (Figure 3.9, A, lane 3), however, the 44 kDa proform of cathepsin B appeared to be detected in the human plasma (Figure 3.9, B, lane 3). Assuming that the IgY anti-human liver cathepsin B antibody detects both pro- and mature forms to the same extent and from the intensity of the targeted bands it appears that antibody detected equivalent amounts of both pro- (approximately 50%) and mature (approximately 50%) cathepsin B in J774 macrophages (Figure 3.9, A, lane 4).

The 56 and 16 kDa bands in the J774 homogenate (Figure 3.10, A, lane 4) and 58 and 15 kDa bands in the human plasma (Figure 3.10, B, lane 3) revealed with the chicken anti-cathepsin D antibody appear to correspond to the 53 kDa precursor and 15 kDa light chain of cathepsin D previously observed in rabbit alveolar macrophages (Diment *et al.*, 1988). In the J774 homogenate (Figure 3.10, A, lane 4), cathepsin D appears predominantly (approximately 80%) as a light chain as opposed to the precursor form in the monocyte homogenate (Figure 3.10, B, lane 4). This could indicate that the light chain contains most of the antigenic epitopes or that the heavy chain (35 kDa) has been degraded (Takahashi and Tang, 1983; Campaine *et al.*, 1995).

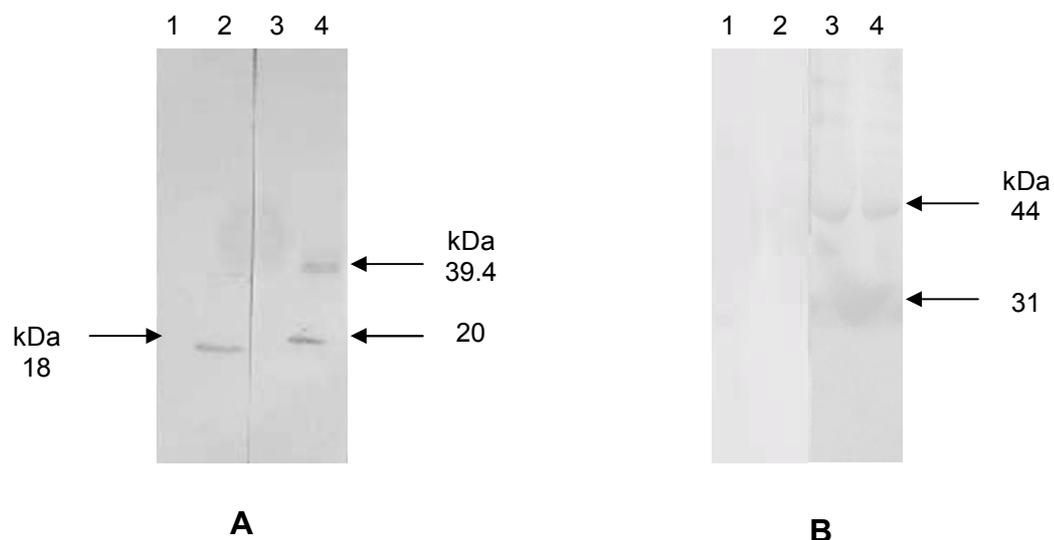


Figure 3.9 Detection of cathepsin B in J774 macrophage and human monocyte homogenates. A, serum-containing J774 homogenate (lanes 2 and 4, 12 μ l) and supernatant (lanes 1 and 3, 10 μ l) and B, human monocyte homogenate (lanes 2 and 4, 5 μ l), human plasma (lanes 1 and 3, 10 μ l) were probed with chicken pre-immune IgY [20 μ g/ml (A, lanes 1 and 2) or 35 μ g/ml (B, lanes 1 and 2)], chicken anti-human liver cathepsin B [20 μ g/ml (A, lanes 3 and 4) or 35 μ g/ml (B, lanes 3 and 4)], detected with rabbit anti-chicken IgG (whole molecule)-alkaline phosphatase [1:100 000 (A and B)] and developed in alkaline phosphatase substrate buffer after separation on a 12.5% (v/v) Laemmli gel and blotting on to nitrocellulose.

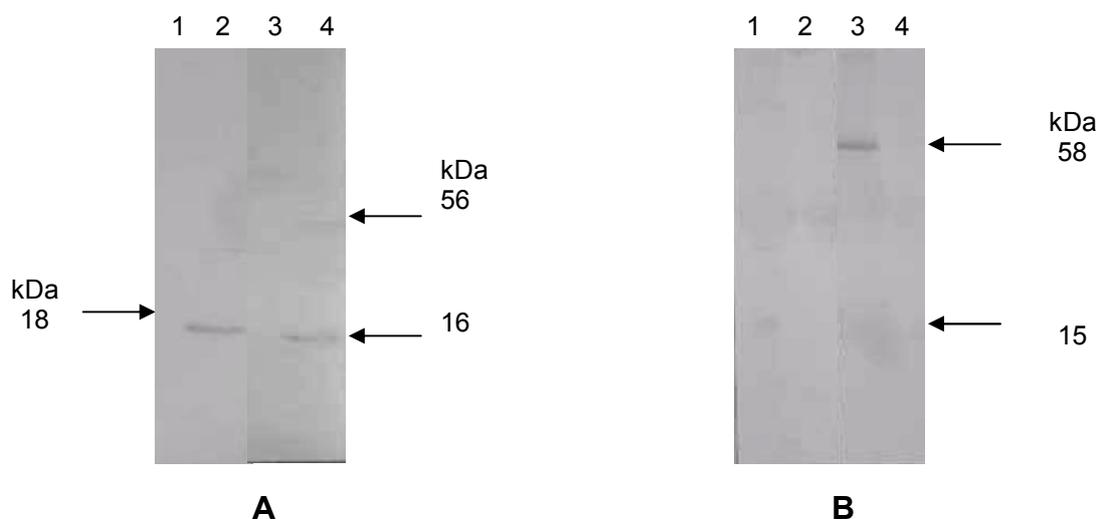


Figure 3.10 Detection of cathepsin D in J774 macrophage and human monocyte homogenates. A, serum-containing J774 homogenate (lanes 2 and 4, 12 μ l) and supernatant (lanes 1 and 3, 10 μ l) and B, human monocyte homogenate (lanes 2 and 4, 5 μ l), human plasma (lanes 1 and 3, 10 μ l) were probed with chicken pre-immune IgY [20 μ g/ml (A, lanes 1 and 2) or 40 μ g/ml (B, Lanes 1 and 2)], chicken anti-cathepsin D [20 μ g/ml (A, lanes 3 and 4) or 40 μ g/ml (B, lanes 3 and 4)], detected with rabbit anti-chicken IgG (whole molecule)-alkaline phosphatase [1:100 000 (A and B)] and developed using alkaline phosphatase substrate buffer after separation on a 12.5% (v/v) Laemmli gel and blotting on to nitrocellulose.

When the J774 and human monocyte homogenates as well as human plasma were probed with rabbit anti-cathepsin H antibodies, bands of approximately 36 kDa (Figure 3.11, A, lane 3) and 37 kDa (Figure 3.11, B, lanes 3 and 4), respectively, were seen. These are approximately the molecular weight reported for human procathepsin H (41 kDa) (Kirschke

et al., 1998). An 18 kDa (Figure 3.11, A, lane 3), close to the molecular weight (21 kDa) of the heavy chain reported for cathepsin H (Portnoy *et al.*, 1986) was also observed in the J774 homogenate. Assuming that the rabbit anti-cathepsin H antibody detects both pro- and mature cathepsin H equally, there appears to be approximately 50% pro- and approximately 50% mature cathepsin H in J774 macrophages. The light chain band (5 kDa) (Kirschke *et al.*, 1998) seems to have run off the lower edge of the blot (Figure 3.11, A, lane 3).

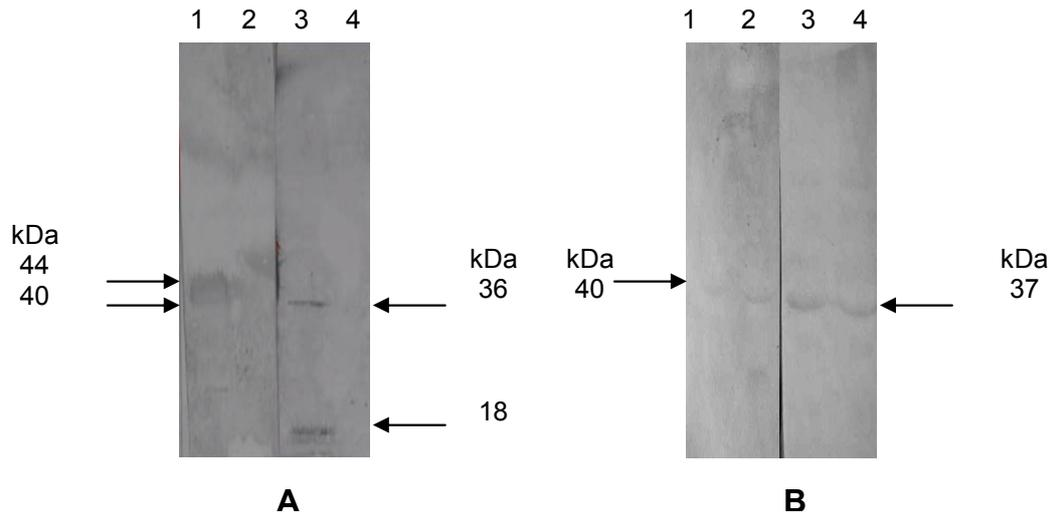


Figure 3.11 **Detection of cathepsin H in J774 macrophage and human monocyte homogenates.**

A, serum-containing J774 homogenate (lanes 1 and 3, 10 μ l) and supernatant (lanes 2 and 4, 12 μ l) and B, human monocyte homogenate (lanes 2 and 4, 5 μ l), human plasma (lanes 1 and 3, 10 μ l) were probed with rabbit pre-immune IgG [10 μ g/ml (A, lanes 1 and 2) or 20 μ g/ml (B, lanes 1 and 2)], rabbit anti-cathepsin H [10 μ g/ml (A, lanes 3 and 4) or 20 μ g/ml (B, lanes 3 and 4)], detected with goat anti-rabbit IgG (whole molecule)-alkaline phosphatase [1:30 000 (A and B)] and developed in alkaline phosphatase substrate buffer after separation on a 12.5% (v/v) Laemmli gel and blotting on to nitrocellulose.

The various forms of cathepsin L have molecular weights similar to those of cathepsin H (Kirschke *et al.*, 1998). Bands of approximately 37 kDa in the J774 homogenate (Figure 3.12, A, lane 3) and in the human plasma and monocyte homogenate (Figure 3.12, B, lanes 3 and 4) correspond to the reported molecular weight of procathepsin L (Kirschke *et al.*, 1998). The 66 kDa bands observed in the human plasma and monocyte homogenate (Figure 3.12, B, lanes 3 and 4) may represent a dimeric form of cathepsin L. Detectable active cathepsin L (28 kDa) does not appear to be present in monocyte homogenate (Figure 3.12, B), however, a band of approximately 19 kDa in the J774 homogenate (Figure 3.12, A, lane 3) may correspond to the heavy chain of cathepsin L. From the blot it appears that equivalent amounts of pro- (approximately 50%) and mature (approximately 50%) cathepsin L are present in the J774 homogenate (Figure 3.12, A, lane 3).

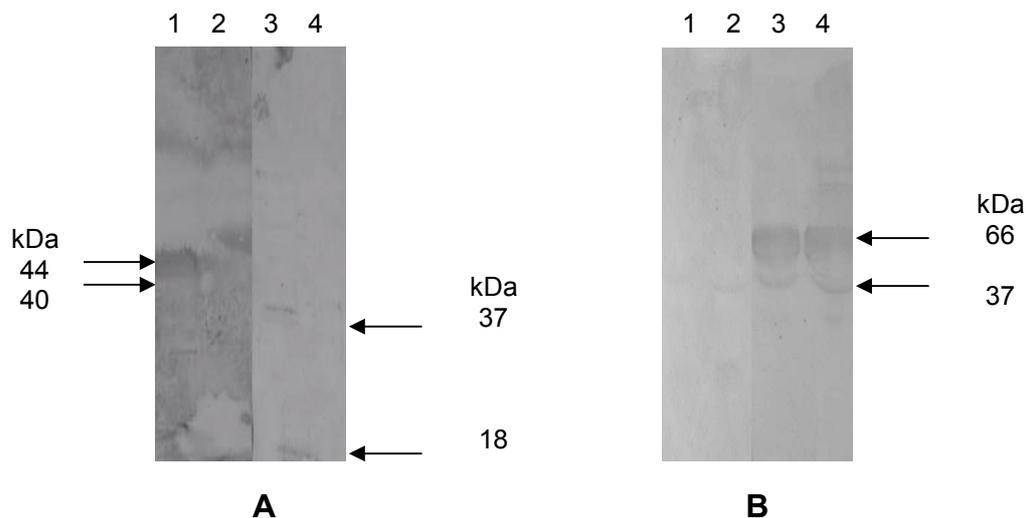


Figure 3.12 **Detection of cathepsin L in J774 macrophage and human monocyte homogenates.**

A, serum-containing J774 homogenate (lanes 1 and 3, 10 μ l) and supernatant (lanes 2 and 4, 12 μ l) and B, human monocyte homogenate (lanes 2 and 4, 5 μ l), human plasma (lanes 1 and 3, 10 μ l) were probed with rabbit pre-immune IgG [5 μ g/ml (A, lanes 1 and 2) or 10 μ g/ml (B, lanes 1 and 2)], rabbit anti-cathepsin L [5 μ g/ml (A, lanes 3 and 4) or 10 μ g/ml (B, lanes 3 and 4)], detected with goat anti-rabbit IgG (whole molecule)-alkaline phosphatase [1:30 000 (A and B)] and developed in alkaline phosphatase substrate buffer after separation on a 12.5% (v/v) Laemmli gel and blotting on to nitrocellulose.

Two bands of cathepsin S of approximately 39 kDa and 25 kDa corresponding possibly to pro- (37 kDa) and mature cathepsin S (24 kDa) were observed in the monocyte homogenate (Figure 3.13, B, lanes 3 and 4), whereas, a 34 kDa band (Figure 3.13, A, lane 3), possibly corresponding to procathepsin S was detected in the J774 homogenate (Kirschke *et al.*, 1998) and no detectable mature cathepsin S was seen in the J774 homogenate, this is in agreement with Punturieri *et al.* (2000) only detected significant amounts of mature cathepsin S in MDM lysates after 12 days of culture. It is, therefore, possible that only undetectable amounts of mature cathepsin S were present as cells were not cultured for 12 days.

A summary of the percentage of precursor to mature cathepsin present in J774 homogenates is given in Table 3.3.

Table 3.3 **Summary of western blot data showing percentage occurrence of the precursor and mature forms of cathepsins H, S, D, B and L in J774 macrophages.**

	Precursor form (%)	Mature form (%)
Cat H	50	50
Cat S	90	10
Cat D	20	80
Cat B	50	50
Cat L	50	50

Abbreviation: Cat, cathepsin.

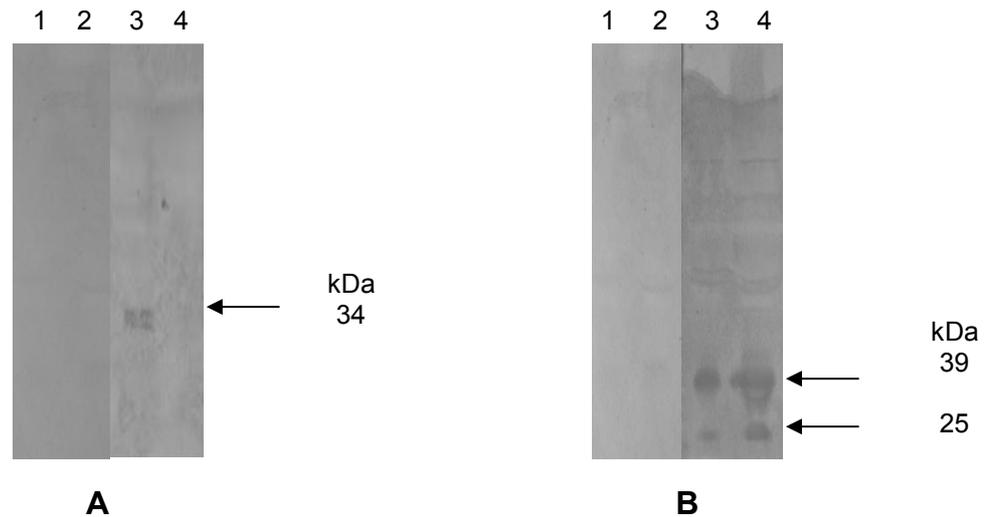


Figure 3.13 **Detection of cathepsin S in J774 macrophage and human monocyte homogenates.**

A, serum-containing J774 homogenate (lanes 1 and 3, 10 μ l) and supernatant (lanes 2 and 4, 12 μ l) and B, human monocyte homogenate (lanes 2 and 4, 5 μ l), human plasma (lanes 1 and 3, 10 μ l) were probed with chicken pre-immune IgY [10 μ g/ml (A, lanes 1 and 2) or 20 μ g/ml (B, lanes 1 and 2)], chicken anti-cathepsin S [10 μ g/ml (A, lanes 3 and 4) or 20 μ g/ml (B, lanes 3 and 4)], detected with rabbit anti-chicken IgG (whole molecule)-alkaline phosphatase [1:100 000 (A and B)] and developed alkaline phosphatase substrate buffer after separation on a 12.5% (v/v) Laemmli gel and blotting on to nitrocellulose.

The antibodies against MMP-9 and TIMP-1 appeared to target antigens of the anticipated molecular weight. The chicken anti-MMP-9 antibody detected bands of approximately 121, 70 and 65 kDa (Figure 3.14, lanes 3 and 4) in the monocyte homogenate. The high molecular weight form could be a heterodimer of MMP-9 (Goldman *et al.*, 2003), however, a 120 kDa complex of MMP-9 bound to neutrophil gelatinase-B associated lipocalin (NGAL) has been identified under reducing SDS-PAGE conditions in neutrophils (Owen *et al.*, 2003). NGAL or an NGAL equivalent does not seem to be present in macrophages, at least not according to phagosomal analyses (Table 1.4) but PDI does (Garin *et al.*, 2001). Macrophage PDI involved in disulfide crosslinking, may be responsible for the high M_r complexes seen in TIMPs, though glycosylation has been reported to be a major contributor (Hasegawa *et al.*, 2003). The 70 and 65 kDa bands are probably processed active forms of MMP-9 as bands of 74 and 65 kDa have been reported (Woessner and Nagase, 2002). Interestingly, the chicken anti-MMP-9 did not detect either pro- or mature MMP-9 in the J774 homogenate (results not shown). It is known, however, that mouse macrophages appear to have less MMP-9 than human macrophages (Filippov *et al.*, 2003), therefore, the levels of MMP-9 in the J774 cells may have been below the detection limit. The chicken anti-human TIMP-1 antibody detected a band of approximately 22 kDa in the J774 homogenate which may correspond to a 20.6 kDa unglycosylated form of TIMP-1 (Figure 3.15) (Woessner and Nagase, 2002).

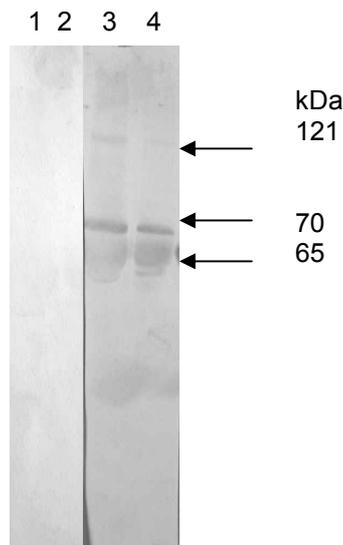


Figure 3.14 **Detection of MMP-9 in human monocyte homogenate.**

Human monocyte homogenate (lanes 1 and 3, 5 μ l), human plasma (lanes 2 and 4, 10 μ l) were probed with chicken pre-immune IgY [30 μ g/ml (lanes 1 and 2)], chicken anti-MMP-9 [30 μ g/ml (lanes 3 and 4)], detected with rabbit anti-chicken IgG (whole molecule)-alkaline phosphatase [1:100 000] and developed in alkaline phosphatase substrate buffer after separation on a 12.5% (v/v) Laemmli gel and blotting on to nitrocellulose.

The pooled pre-immune preparations, however, used at the same level showed non-specific bands at 44 and 40 kDa in the J774 homogenate using the rabbit pre-immune (Figure 3.11, A, lane 1 and Figure 3.12, A, lane 1) and 18 kDa using the chicken pre-immune (Figure 3.9, A, lane 2 and Figure 3.10, A, lane 2), respectively. The 18 kDa band was not seen in the pre-immune IgY preparation from chickens used to make anti-TIMP-1 and anti-TIMP-2 antibodies (Figures 3.5, B and 3.6, B) used at similar levels on similar homogenates and may, therefore, just represent background antibodies present at low levels in this particular pre-immune IgY preparation.

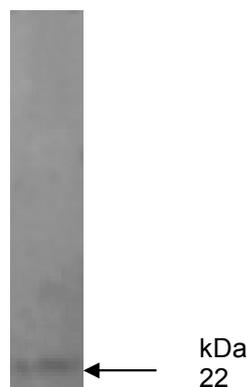


Figure 3.15 **Detection of TIMP-1 in J774 macrophage homogenate.**

Serum-containing J774 macrophage homogenate were separated on a 12.5% Laemmli gel, blotted on to nitrocellulose, probed with chicken anti-human TIMP-1 [10 μ g/ml] detected with rabbit anti-chicken IgG (whole molecule)-alkaline phosphatase [1:100 000] and developed using BCIP, 0.015% (m/v), NBT, 0.03% (m/v) in alkaline phosphatase substrate buffer.

3.8 Discussion

High molecular weight forms of TIMPs (56, 62, 66, 56, 70 and polymeric forms 28-120 kDa) have been targeted in many studies and their presence has been ignored (Nagayama *et al.*, 1984; Cawston *et al.*, 1986; Drouin *et al.*, 1988; Sorsa *et al.*, 1994; De Lorenzo *et al.*, 2000; Price *et al.*, 2000). Various antibody preparations have also shown variable recognition for different antigenic regions in TIMP-1 (Holten-Andersen *et al.*, 2002). As the newly produced antibodies against TIMP-1 and -2 do not detect reported and recognised forms of TIMP-1 and -2, these antibodies will not be used in this study and rather a chicken anti-TIMP-1 antibody previously made against human TIMP-1 (Clulow, M., unpublished) and a sheep anti-recombinant human TIMP-2 (Dr Linda Troeberg, Imperial College, London) targeting the correct molecular weights will be used. To verify that the high molecular weight bands are TIMP-1 and TIMP-2 western ligand blots (Price *et al.*, 2000) and sequencing may be performed to verify the identification of such bands.

The current western blotting of J774 mouse macrophages showed pro- (39 and 44 kDa) and a smaller processed form (20 kDa) of cathepsin B. Greiner *et al.* (2003), however, reported only a 32 kDa form of cathepsin B in human monocytes and it is possible that only the precursor is present as the lower band may actually be the same molecular weight as the non-specific band detected by the pre-immune IgY. Western blotting also showed only the proform of cathepsin L in human monocyte homogenates, whereas, both pro- and mature forms were present in J774 macrophages. Only the proform of cathepsin S was seen in J774 homogenates, though both pro- and mature forms were present in human monocytes. If cathepsin S occurs only in its precursor form and is considered a marker for the late endosome (Jahraus *et al.*, 1998), the presence of an immature form would be most unanticipated, as cathepsins are usually processed in the acidic environment of the late endosome (Kirschke *et al.*, 1998).

Whereas both the pro- and mature forms of cathepsins B and H were detected in the J774 and human monocyte homogenates, only mature cathepsin D was detected in J774 cells. For immunolabelling studies this could have important consequences. Polyclonal antibody preparations recognise all forms of cathepsins and if different vesicle populations contain either pro- or mature cathepsins, it would be impossible to distinguish these different populations using such antibodies. As cathepsin D is mainly known as a marker for the acidic digestive body i.e. the lysosome and/or possibly the late endosome, where cathepsin D should be in its active form in both cases, and as J774 cells seem to contain almost

exclusively mature cathepsin D, the cathepsin D antibody could form one of the most reliable markers. Cathepsin B and H antibodies, for example, would be labelling both precursor and mature forms of the enzyme, here demonstrated to be present in the J774 cell, and hence acidic (containing mature enzyme) and non-acidic secretory vesicles (containing immature enzyme) could not be distinguished. This would complicate the use of these antigens as marker antigens for distinguishing various endocytic populations without the use of additional markers or probes for e.g. pH. Where only a mature or immature form of the enzyme is present, as apparently the case with cathepsin D (mature form), polyclonal antibodies are more useful, as they could be used reliably without additional probes.

From these blots, assuming equal recognition of all bands, it is interesting to note the differences in cathepsin content between human monocyte/macrophages and J774 cells. It would seem, that J774 mouse macrophages and human blood monocytes contain equal amounts of pro- and mature cathepsin B, blood monocytes have more pro- than mature cathepsin D, whereas, J774 macrophages appear to be the reverse. Similarly, cathepsins H and L appear to have equal amounts of both pro- and mature in J774 macrophages, while monocytes have only the proform. The blood monocytes have equal amounts of pro- and mature cathepsin S, but J774 macrophages have only procathepsin S.

The specificity and cross-reactivity of cathepsin, MMP-9 and TIMP-1 antibodies with mouse antigens seems to have been established and, therefore, were used in immunolabelling studies. The most important findings, besides the establishment of the variable suitability of the available antibodies for immunolabelling studies, seems to be that there do appear to be differences between the molecular weight and ratio of forms of cathepsin (precursor and mature) in J774 macrophages and human blood monocytes, verifying previous statements about the phenotypic differences between monocyte/macrophages from different species.

CHAPTER 4

J774 MOUSE MACROPHAGE VESICLE POPULATIONS

4.1 Introduction

Neutrophils (PMNs) and mononuclear phagocytes, or their activated counterparts, macrophages, are considered first and second line defence phagocytes of the innate immune system, respectively (van Oss, 1986; Garin *et al.*, 2001; Ross and Auger, 2002). Both differentiate from a single myeloblast precursor that expresses key enzymes, such as cathepsins B and D, MPO and elastase (Tapper, 1996).

Upon promyeloblast differentiation and progression to the promyelocyte, myelocyte and finally to the PMN, cathepsin G and MPO continue to be expressed but cathepsin B and D expression ceases. Mature myelocytes or PMNs, therefore, contain cathepsin G and MPO but little cathepsin B or D. Upon synthesis, PMN expressed proteins are packaged into large granules via a non-sorting process known as “targeting by timing”, particular proteins expressed at a specific time being packaged into granules of specific morphology (Tapper, 1996; Gullberg *et al.*, 1997; Borregaard and Cowland, 1997; Faurschou and Borregaard, 2003).

On the other hand, during differentiation of the promonoblast, to give rise to promonocytes, monocytes and finally macrophages, expression of cathepsins B and D persists but the expression of elastase and MPO is terminated (Tapper, 1996; Gullberg *et al.*, 1997; Borregaard and Cowland, 1997; Faurschou and Borregaard, 2003). Monocytes and their activated macrophage counterparts, therefore, contain cathepsin B and D but little elastase or MPO (Campbell *et al.*, 1989; Ross and Auger, 2002). As promonocytes differentiate to monocytes, distinctive granule populations seem to be lost and smaller vesicular- and endosome-lysosome type populations seem to predominate. Many more cathepsins are also expressed (Schmid *et al.*, 2002; Rivera-Marrero *et al.*, 2004). These enzymes have been described in various cell types as having a distinctive trafficking and processing pattern. This involves precursor trafficking from the Golgi to the late endosome via the MPR for activation and subsequent targeting to “lysosomal” storage organelles (Chapman *et al.*, 1997). This is unlike the “targeting by timing” of proteases seen in the PMN which utilises

no sorting mechanism (Borregaard and Cowland, 1997; Faurschou and Borregaard, 2003). The markers associated with this trafficking and other markers and properties associated with the endosome-lysosome-like system of most cell types (Clague, 1998; Pillay *et al.*, 2002) may, therefore, potentially be useful in describing the organelles present in the macrophage (Claus *et al.*, 1998; Anes *et al.*, 2006). It is now beginning to become evident that many of the classical markers for organelles previously designated “lysosomal” due to the presence of LAMPs, acidity or mature lysosomal enzymes and the lack of the 215 kDa MPR, may require re-evaluation as subpopulations within these previous groupings have been identified (Anes *et al.*, 2006). For this reason, effort will be made to highlight these possibly oversimplified classifications by indicating such as “classical” assignments in the explanations given below.

In classical descriptions of endosome-lysosome systems (Figure 4.1), small particles, solutes, transmembrane proteins and membrane-bound ligands are incorporated into vesicles derived from the plasma membrane (Vieira *et al.*, 2002), or, in the case of the macrophage this is most often membrane from the ER (Gagnon *et al.*, 2002). Vesicles and their cargo are classically targeted to the early or tubulovesicular, sorting endosomes which label with Rab5 and EEA1 (Ghosh *et al.*, 1994). Classically described as mildly acidic (pH of 6.3-6.5), and usually poor in proteases, these organelles have been reported to sort and recycle membrane and contain receptors such as the transferrin receptor to the plasma membrane, recycling endosomes or to the late endosome to be degraded (Pillay *et al.*, 2002; Vieira *et al.*, 2002). Generally closely associated with microtubules, recycling endosomes have been described as less acidic (pH 6.5) than lysosomes (pH <5.5) and Rab11-positive (Vieira *et al.*, 2002).

Sorting in sorting endosomes is also classically agreed to occur via either of two model systems. In the shuttle vesicle model, vesicles carrying endocytosed material and specific membrane components shuttle between pre-existing, stable early endosomes, endosome carrier vesicles (ECVs) and multivesicular bodies (MVBs) or late endosomes (Griffiths, 1996a; Clague, 1998; Pillay *et al.*, 2002). In the maturation model, on the other hand, sorting endosomes are transient organelles capable of maturing into ECVs, MVBs or late endosomes via fusion and fission events (Murphy *et al.*, 1991; Vieira *et al.*, 2002). The phagosome, into which larger particles are captured, is the only organelle that can definitively be seen to “mature”. In this case, only recently has it been revealed that there is a gradual pH change from near neutral to acidity. This is accompanied by the acquisition of lysosomal enzymes

which is in turn associated with the transient association of markers for the early endosome (Rab5), late endosome (Rab7) and finally most of the markers of the late endosome and lysosome (Desjardins *et al.*, 1994a; Desjardins *et al.*, 1995; Desjardins *et al.*, 1997; Pillay *et al.*, 2002). Since the phagosome is not a focus of the current study, however, further details of phagosome maturation will not be included here. Most of the studies on the early and late endosomes, recycling endosomes, and lysosomes, as well as the phagosome, have been considerably facilitated by the ability to distinguish organelles in the endosome-lysosome system by filling the pathway and following endocytic traffic in pulse-chase studies. This has allowed the separation, and hence identification and purification of marker receptors such as Rab5 or EEA1 and the late endosomal Rab7 marker (Meresse *et al.*, 1995) as well as the major 215 kDa MPR involved in trafficking of cathepsin enzymes (Griffiths, 1996a; Pillay *et al.*, 2002; Vieira *et al.*, 2002).

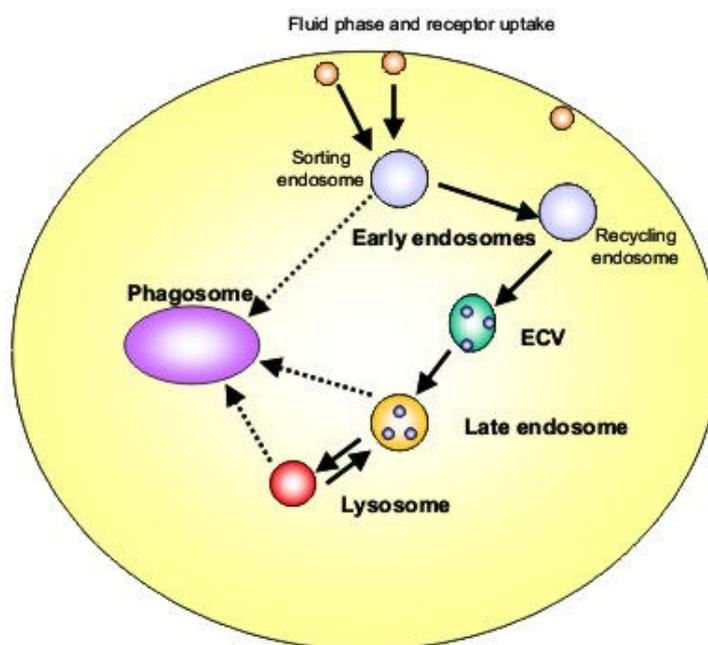


Figure 4.1 **Model of the endocytic pathway.**

Organisation of the endocytic pathway showing most important organelles, the early endosome, late endosome and lysosome. Solid arrows between compartments indicate vesicular trafficking or direct fusion. The phagosome is an additional compartment of the endocytic pathway and broken arrows indicate the compartments that interact with the phagosome and deliver proteolytic content to the phagosome, aiding in the process of phagosomal maturation (modified from Pillay *et al.*, 2002; Gruenberg and van der Goot, 2006).

Identification of the classical acidic multivesicular or multilamellar late endosomes (pH 5.5) on the other hand was considerably facilitated using two approaches. These involved following the endocytic traffic for sorting and degradation, and the distinctive trafficking and processing pattern of cathepsins. The unique trafficking of cathepsins was revealed initially by studies on lysosomal enzyme storage and secretion diseases, such as I cell and Hurler's

diseases (Kornfeld, 1986). These diseases showed the importance of ER and Golgi processing, i.e. the addition of the high mannose-6-phosphate tag to lysosomal cathepsins, and the presence of 215 kDa MPR for the correct trafficking of the cathepsins between the Golgi and the late endosome for activation (Kornfeld, 1986; Turk *et al.*, 2000; Wolters and Chapman, 2000; Barrett *et al.*, 2004). These studies also showed that deficiency in either results in secretion of procathepsins i.e. default secretion via a “secretory” pathway not to be confused with the “regulated secretory” pathway which contains late endosome-processed cathepsins (Brown *et al.*, 1986). Such a “regulated secretory” vesicle is also classically known as a “secretory lysosome” or a lysosome capable of regulated exocytosis (Griffiths, 1996b). Though later studies showed an additional 46 kDa receptor also responsible for lysosomal targeting of these proteins (Hoflack and Kornfeld, 1985; Riese and Chapman, 2000; Wolters and Chapman, 2000), studies on the 215 kDa receptor revealed the late endosome as the major sorting and processing organelle for enzymes such as the cathepsins and receptors such as the MPR and the necessity for an acid pH to perform the sorting and recycling role (Brown *et al.*, 1986).

At the acidic pH of the classical late endosome (identified due to the presence of the 215 kDa MPR) the MPR releases the MPR-bound proenzyme and weakens the interaction between the propeptide and the catalytic region. This allows activation of the cathepsins (Riese and Chapman, 2000; Turk *et al.*, 2000; Barrett *et al.*, 2004). Activated lysosomal enzymes may be subsequently trafficked to a “lysosomal” population where they are stored (Griffiths, 1996a). On the other hand, the late endosome has been described as containing 20% of the total cellular hydrolytic enzymes, at any one time, and to be the main site for protein turnover (Griffiths, 1996a; Tjelle *et al.*, 1996). It is also described to be associated with Rab7, Rab9, lysobisphosphatidic acid, MPRs and LAMPs markers (Griffiths, 1996a; Pillay *et al.*, 2002; Vieira *et al.*, 2002). Whereas LAMP-1 and LAMP-2 are reportedly located on the limiting membranes of late endosomes and lysosomes, LAMP-3 appears predominantly associated with the internal multivesicular membranes of the late endosome and the outer membranes of specialised secretory organelles (Kobayashi *et al.*, 2000). Not all late endosomes may be LAMPs-positive, however. This may be possible as lysosomal enzyme storage vesicles or “lysosomes” have been shown to fuse with the late endosomes forming a hybrid, acidic organelle only when proteolysis is required (Figure 4.2). Such a fusion may bring with it both the content and markers of the lysosomes i.e. LAMPs markers as well as proteolytic enzymes (Bright *et al.*, 1997; Luzio *et al.*, 2000), the MPRs recycle back to the

“Lysosomes”, classically the most acidic ($\text{pH} < 5.5$), small, electron-dense (dense core), MPR-negative organelles have been described as containing the bulk of activated and stored, but not necessarily active, hydrolytic enzymes (Table 4.1). The literature also often does not distinguish if the lysosome-like organelle to which reference is made is the small electron-dense organelle, previously known as a primary lysosome [as it contained no fused endocytic cargo (de Duve, 1983)] this will be called a “storage lysosome” (but may be acidic or non-acidic) (Griffiths, 1996a) from the late endosome and cathepsin D-labelling, LAMPs-positive, acidic body judged to be a “hybrid organelle” formed by fusion of the small electron-dense organelle with the late endosome also known as a “secondary lysosome” or “digestive body” (de Duve, 1983) (Table 4.1 and Figure 4.2). It is also not absolutely clear that the “hybrid organelle” is not different from the cathepsin D-labelled “digestive body” described by de Duve, (1983) (Table 4.1). This complicates reporting and interpretation of the literature. When a lack of certainty exists describing such populations, quotation marks (i.e. “lysosome”) will be used. If it is the “hybrid organelle” to which reference is made, this term will be substituted. Both the “hybrid organelles” and “digestive bodies” as well as “storage lysosomes” are usually located in the perinuclear area of the cell and label with LAMPs (Griffiths, 1996a; Pillay *et al.*, 2002) (Figure 4.2) (Table 4.1), however. Though usually perinuclear, these “lysosomes” may redistribute towards the cell edge, if the cytoplasmic pH becomes acidic (Heuser, 1989) and may be tubular, depending upon the state of polymerisation of microtubules (Swanson *et al.*, 1987; Knapp and Swanson, 1990), or may be released in response to various agonists via regulated exocytosis (Andrews, 2000).

Regulated exocytosis of lysosome-like populations (“secretory lysosomes”) may be induced by increased levels of free, intracellular Ca^{2+} , especially in cells of a haemopoietic lineage (Griffiths, 1996b; Stinchcombe and Griffiths, 1999). This seems a temperature and ATP-dependent process regulated by synaptotagmin VII (Rodríguez *et al.*, 1997; Andrews, 2000; Martinez *et al.*, 2000). Claus *et al.* (1998) identified only two functionally distinct, dense “lysosomal compartments” in J774 macrophages. One was secreted in the presence of the acidotropic drugs, chloroquine and bafilomycin A1 (and hence possibly acidic) and contained primarily cathepsins B and L as well as furin. The non-secreted compartment contained dipeptidyl peptidase II (DPPII), β -glucuronidase and β -hexosaminidase. Addition of acidotropic drugs did not affect the secretion of the latter compartment. This compartment could, therefore, be non-acidic. The morphology of “secretory lysosomes” is

also reported to be a combination of the multilamellar structures of conventional late endosomes and the dense cores of secretory granules (Blott and Griffiths, 2002) and could in fact be late endosomes and classical lysosomes. Rabinowitz *et al.* (1992) similarly described two compartments in mouse macrophages as tubular elements and small vesicles in which poorly degradable endocytic or phagocytic material accumulated. These, in fact could even be “residual bodies” of the autophagic pathway (Eskelinen *et al.*, 2002). Without additional markers morphological descriptions seem to be of limited use in distinguishing numbers of vesicles.

Early studies on human bone marrow promonocytes and blood monocytes also suggested the existence of at least two distinct vesicle populations (Nichols *et al.*, 1971; Stachura, 1989). One type was shown to contain acid phosphatase, aryl sulfatase and peroxidase. The content of the second type remained unknown (Ross and Auger, 2002). Two ultrastructurally distinct vesicle populations were subsequently described in rabbit alveolar macrophages (Cohn and Wiener, 1963). These were thought to be lysosomal or secretory but were shown, using enzyme marker assays (Peters *et al.*, 1972; Peters, 1976), to consist of three vesicle populations (Lowrie *et al.*, 1979) (Table 4.2).

Table 4.2 Identification of three vesicle types in rabbit alveolar macrophages.

Vesicle Contents	Vesicle Types		
	Type A	Type B	Type C
Lysozyme	✓	?	
N-acetyl- β -glucosaminidase		✓	
β -galactosidase		✓	
β -glucuronidase		✓	
Cathepsin D			✓
Acid phosphatase		✓	✓

✓ present in vesicle population, ? may be present. (Lowrie *et al.*, 1979).

Lysozyme was shown to be a marker for one of these populations (type A-vesicles). Cathepsin D, the major protease present in lysosomes and frequently used as a marker for lysosomes (Conner, 2004), was shown to be a marker for another (type C-vesicles). A third vesicle (type B-vesicles) was identified by the presence of *N*-acetyl- β -glucosaminidase, β -galactosidase, β -glucuronidase or by the absence of cathepsin D (Lowrie *et al.*, 1979). These possibly, respectively, represented the acidic- and two non-acidic- or slightly acidic vesicles subsequently described by Anes *et al.* (2006).

non-acidic) (Anes *et al.*, 2006) (Figure 4.3). Another population was LAMP-positive and acidic (possibly a hybrid organelle). The last was a LAMP-1-positive organelle which was largely non-acidic (only 2% colocalisation with LysoTracker) (Figure 4.3). Anes *et al.* (2006) did not seem to consider the early endosomal vesicle population (LAMP-negative, slightly acidic) which would be difficult to distinguish from the Hck/LYAAT vesicle (LAMP-negative, moderately acidic). The 5 possible populations identified could, therefore, either be largely acidic and LAMP-1-negative, largely weakly acidic and LAMP-1-negative (potential early endosomes and Hck/LYAAT vesicles), acidic and LAMP-1-positive or largely non-acidic and LAMP-1-positive (Figure 4.3). The late endosomal population was, however, defined by pulse-chase uptake of gold particles and no labelling was performed for MPRs. The possibility that one of the 5 populations described was also a late endosome, therefore, cannot be conclusively excluded.

4.2 Localisation of cathepsins in J774 macrophages using both immunogold and fluorescent labelling

It was hoped that, with the establishment of the cathepsin enzyme distribution [especially with respect to cathepsin H, as an early endosome marker, and cathepsin S, as a late endosome marker (Claus *et al.*, 1998; Jahraus *et al.*, 1998)] in relation to LysoTracker, it would be possible to identify equivalents of the V-ATPase-compartment and other populations described by Anes *et al.* (2006). LysoTracker labelling (i.e. acidity) of vesicles should also be an indicator that cathepsins should be in their activated or processed form. LAMP-1 (and possibly LAMP-2), it was hoped, would assist in identifying similar sub-populations to those identified by Anes *et al.* (2006) which classically would be associated with active enzymes (Table 4.1). The approximate percentage of pro- and mature enzyme, it was hoped, would be moderately accurately determined from western blotting (Chapter 3). It was anticipated that at least 5 populations would be revealed, either largely acidic and LAMP-1-negative, largely weakly acidic and LAMP-1-negative (early endosomes or Hck/LYAAT vesicles), acidic and LAMP-1-positive and largely non-acidic and LAMP-1-positive. An additional equivalent of the late endosomal population (acidic, LAMPs-positive) could possibly be defined by the presence of cathepsin S or cathepsin D, differentiating this body from the “hybrid organelle” or “digestive body”.

The cathepsins have a wide range of optimal operating pH's (Section 1.4.1, Table 1.6) and are thus well suited to the endosome-lysosome system where the pH ranges from less than

5.5 to 6.5 (Berg *et al.*, 1995). The distribution of proteases and differences in pH, particularly in late endosomes, where activation and inactivation of specific proteins as well as antigen processing occurs, may also be used to control proteolysis e.g. for restricted cleavage of the invariant chain and limited antigen processing for MHC class II antigen presentation (Lennon-Duménil *et al.*, 2002a).

Diment *et al.* (1988) also described a 46 kDa, partially membrane-bound endosomal form of cathepsin D, and both cathepsins D and B have been implicated in the macrophage early endosomal degradation of the A chain of the plant toxin ricin in this compartment of almost neutral pH (Blum *et al.*, 1991). Although cathepsins D and B are known to have largely acidic pH optima it has been suggested that the local conditions in early endosomes may affect the activity of particular enzymes (Pillay *et al.*, 2002). *In vitro* studies have also shown different buffer systems to have marked effects on the activity and observed pH optimum of cathepsins B and L, both cathepsins being shown to have significant activity at physiological pH in certain buffers (Dehrmann *et al.*, 1996). The membrane-bound form of cathepsin D may also have a higher pH optimum than the soluble form present in lysosomes. Cathepsin B also has both exo- and endopeptidase activity, with the endopeptidase having a higher pH optimum (Blum *et al.*, 1991; Linebaugh *et al.*, 1999). The presence of cathepsin B in a compartment with a higher pH than considered optimal for the exopeptidase activity, therefore, may favour the endopeptidase activity.

In the macrophage phagosome, a process of maturation, during which sequential fusion with early endosomes, late endosomes and lysosomes, appears to be required for the acquisition of various proteolytic enzymes, and for the phagosome to perform degradative functions (Desjardins *et al.*, 1997) (Figure 4.1). The sequential delivery of proteases to the phagosome of J774 mouse macrophages emphasises their heterogenous distribution along the endocytic pathway (Garin *et al.*, 2001; Lennon-Duménil *et al.*, 2002a). Cathepsins B and Z appear to be amongst the first to be delivered to the phagosome. The activity of cathepsin B in the phagosome increases with time, suggesting that whilst cathepsin Z may be located in early endosomes, cathepsin B may be distributed throughout the endocytic pathway. Cathepsins L and D appear to be located in the late endosomes and lysosomal compartments. Finally cathepsin S seems mainly associated with late endosomes (Claus *et al.*, 1998; Lennon-Duménil *et al.*, 2002a), whereas, cathepsin H occurs primarily in the early endosome (Jahraus *et al.*, 1998). Apart from these studies very little work has focussed on the

distribution of cathepsins in macrophages. Whether these proteases are restricted to the endocytic compartments or whether they may occur in “secretory lysosomes” or other vesicles is unknown.

The strategy adopted in this study was first to establish the ultrastructural and immunofluorescent distribution of cathepsins in J774 mouse macrophages using single labelling, while optimising labelling and checking adequate preservation of ultrastructure and tissue immunogenicity. This was followed subsequently by double labelling to establish cathepsin colocalisations, once again, considering cathepsin H as an early endosome marker (Jahraus *et al.*, 1998) and cathepsin S as a late endosome marker (Claus *et al.*, 1998; Lennon-Duménil *et al.*, 2002a). Finally, LysoTracker was used to verify whether the cathepsins were associated with the (acidic) late endosomes, “lysosomes”, and the equivalent of the most acidic (or V-ATPase-positive) compartment seen in the Anes *et al.* (2006) study and whether a less acidic LAMP-1-positive compartment and a non-acidic, LAMP-1-negative compartment (possibly a LYAAT-positive compartment) could be identified. Further colocalisation studies were carried out with anti-LAMP-1 and anti-LAMP-2 to see whether any difference in cathepsin colocalisation in “lysosomal” subpopulations could be discerned.

For fluorescent labelling of J774 macrophages where preservation of ultrastructure is less crucial, PFA was used and the presence and preservation of cathepsins B, D, H, S and L antigenicity was first verified. Ultrastructural preservation is important for EM and a combination fixative (PFA and glutaraldehyde) was, therefore, used in preliminary immunogold labellings. Double labelling colocalisation studies were subsequently performed.

4.2.1 Reagents

Reagents for culture, fixation and embedding, immunolabelling of ultrathin sections and for fluorescent immunolabelling of J774 cells for cathepsins B, D, H, S and L were prepared according to Sections 2.2.1, 2.7.1.1, 2.7.3.1 and 2.8.1.1, respectively.

The anti-cathepsin antibodies used were as previously described (Section 3.7.1). Goat anti-rabbit IgG FITC, donkey anti-chicken IgG CY3 and rabbit anti-chicken IgG FITC secondary antibodies were employed.

4.2.2 Procedure

J774 cells were cultured, fixed and embedded in LR White resin according to the procedure in Sections 2.2.2 and 2.7.1.2. Protein A gold labelling on the ultrathin sections was performed with rabbit anti-cathepsin H [20 µg/ml], chicken anti-cathepsin S [20 µg/ml], chicken anti-cathepsin D [50 µg/ml], chicken anti-cathepsin B [10 µg/ml] and rabbit anti-cathepsin L [20 µg/ml] according to Section 2.7.3.2. Cathepsins in vesicle populations were judged to be membrane-bound if located around the vesicle periphery and luminal or “free” if observed within the vesicle itself.

Fluorescent immunolabelling was performed with rabbit anti-cathepsin H [100 µg/ml (epifluorescence) or 20 µg/ml (confocal)], chicken anti-cathepsin S [20 µg/ml], chicken anti-cathepsin D [100 µg/ml (epifluorescence) or 50 µg/ml (confocal)], chicken anti-cathepsin B [20 µg/ml], rabbit anti-cathepsin L [20 µg/ml], goat anti-rabbit IgG FITC [5 µg/ml or 2 µg/ml], donkey anti-chicken IgG CY3 [2 µg/ml] and rabbit anti-chicken IgG FITC [10 µg/ml] according to Section 2.8.1.2. Pre-immune controls were performed in all cases to check labelling specificity. Double labelling controls were also performed omitting or substituting antibodies with pre-immunes and changing the order of the labelling to check non-specificity of all components of the labelling system. As macrophages are fairly small and round and normal epifluorescence microscopy focal planes are fairly thick it may, therefore, be difficult to unequivocally determine colocalisation using conventional epifluorescence. Confocal microscopy was, therefore, also used where possible, as it allows for the viewing of thin “optical slices” to exclude apparent colocalisation due to superimposition of two differently labelled vesicles within the viewed focal plane. Labelling was, therefore, viewed using either an Olympus epifluorescent microscope and F-View CCD camera or a Zeiss 510 Meta confocal microscope and images analysed visually using ImageJ software. Images of colocalisation using colour (i.e. red and green images merged to form yellow) are highly influenced by display settings and intensity, and, therefore, colocalisation based on colour analysis alone is problematic and can lead to incorrect conclusions. Grey scale images (i.e. black and white) on the other hand, are not affected by display settings and should be assessed when visually judging the following colocalisation images, as the yellow colour (indicating the degree of colocalisation in the composite image) varies depending on settings and printer type. In confocal images, the number of colocalising vesicles in at least 3 representative cells was assessed manually, reported as a percentage and checked with reference to the epifluorescent image.

4.2.3 Results

No non-specific protein A gold- or fluorescent labelling was observed in controls and labelling was assumed to be specific (results not shown). Ultrastructural preservation was extremely variable as is evident in micrographs labelled for cathepsin H (Figure 4.4, C) and cathepsin B (Figure 4.7, C), where labelled vesicles (± 100 nm) are only slightly electron-dense and are not easily discerned (Figure 4.4, C) or preservation is moderately acceptable (Figure 4.7, C).

Early endosomes are usually fairly large (± 100 nm), quite electron-translucent vesicles with an associated tubular network (Ghosh *et al.*, 1994). Neither tubular network nor any vesicle definition is evident in the cathepsin H-labelled sections (Figure 4.4, C). The majority of labelled vesicles are possibly early endosomes, similar in size (± 100 nm) but more electron-dense or secretory vesicles i.e. small (± 20 nm) and electron-translucent containing procathepsin H (Figure 4.4, C), in approximately equal proportions as indicated by blots (Figure 3.11, A, lane 4). Labelling in the epifluorescent image (Figure 4.4, A) rather than the confocal image (Figure 4.4, B1 and B3) appears more distinct and with larger organelles [more like early endosomes (± 100 nm) than small (± 20 nm) secretory vesicles]. Labelling also appears membrane bound (Figure 4.4, C). Cathepsin H labelling, however, seemed variable but mainly spread throughout the cell (Figure 4.4, A and B).

Cathepsin S labelling was also performed with a peptide antibody (Figure 4.5, A, B and C) but appears to give denser, more definite labelling at the EM level, with labelling apparently located near or in tubulovesicular areas in the cell, possibly associated with the ER (Figure 4.5, C). The more electron-dense organelles are possibly late endosomes (± 50 nm) but the vesicles associated with the ER (± 20 nm) would be anticipated to contain newly synthesised precursor cathepsin S, which, according to western blots, should represent the content of the majority (approximately 90% pro-) of vesicles (Figure 3.13, A, lane 3).

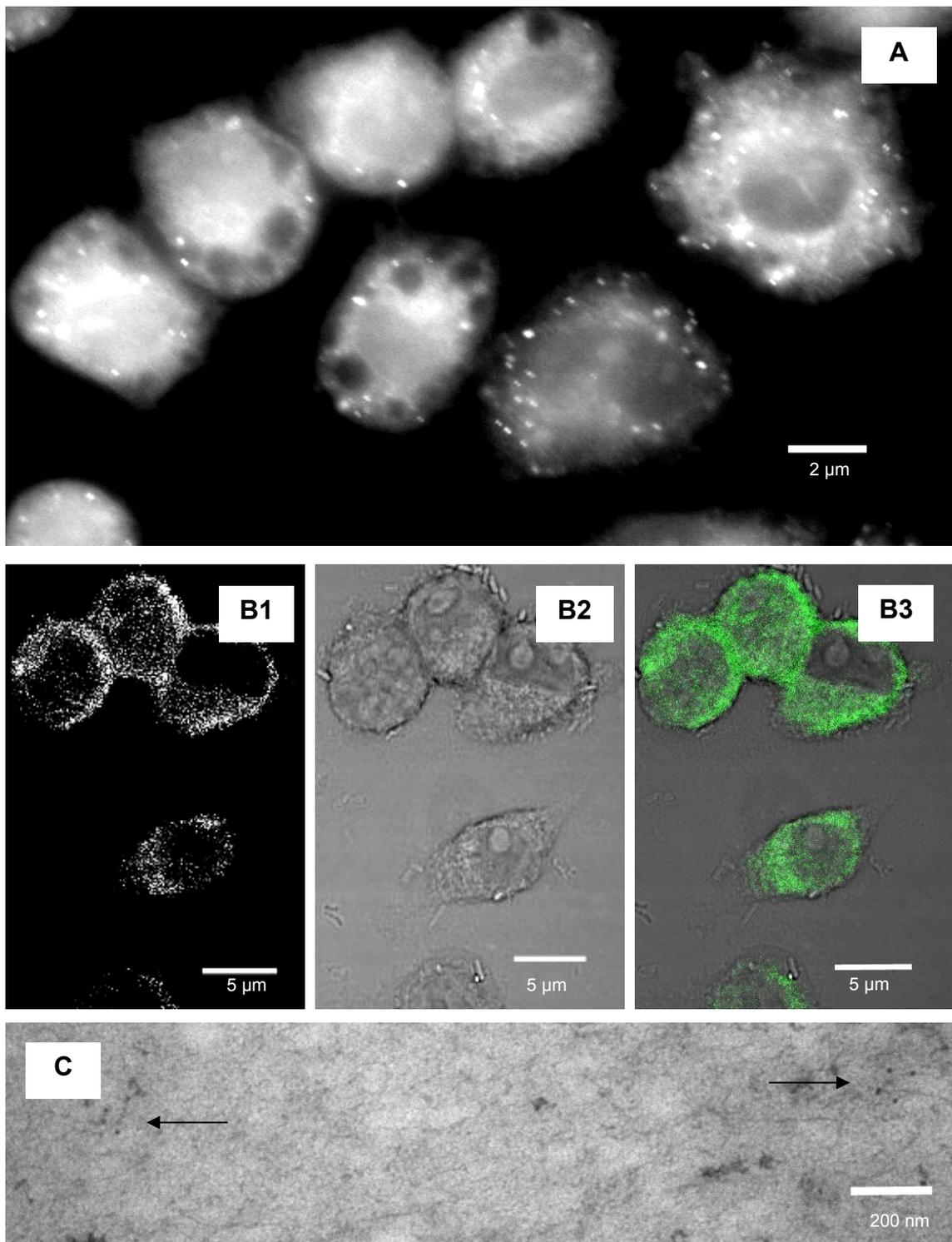


Figure 4.4 Fluorescent and protein A gold labelling of cathepsin H in J774 macrophages. Rabbit anti-cathepsin H [100 µg/ml (A) or 20 µg/ml (B1)] and goat anti-rabbit IgG FITC [5 µg/ml (A) or 2 µg/ml (B1)] applied to cells on coverslips, initially fixed with 3.7% PFA and permeabilised with saponin. Coverslips viewed with an Olympus epifluorescent microscope (A) or a Zeiss Meta 510 confocal microscope (B). FITC filter (A and B1), DIC image (B2), composite image (B3). Bars = 2 µm (A) or 5 µm (B) . Rabbit anti-cathepsin H [20 µg/ml (C)] and protein-A gold probe (10 nm) used on LR White sections viewed using a Philips CW120 Biotwin TEM (80-100 kV). Cathepsin H labelling seen in slightly electron-dense vesicles (arrows), some possibly membrane-associated. Bar = 200 nm.

Ultrastructural preservation and staining seems fairly good, but many vesicles seem swollen and not all membraneous structures are equally well preserved (Figure 4.5, C). Cathepsin S labelling seems either located within the vesicle (approximately 34%) and apparently soluble, or membrane-bound (approximately 66%) (Figure 4.5, C). Immunofluorescence labelling for cathepsin S (Figure 4.5, A and B) does not appear to be distributed as peripherally as the cathepsin D labelling (Figure 4.6, A and B) but seems a little more extensively spread throughout the cell than cathepsin H (Figure 4.4, A and B). Such a distribution of cathepsin S may concur with both a late endosomal distribution and the high perinuclear ER and Golgi-association indicated by the predominant levels of precursor enzyme (approximately 90%) reflected in blots (Figure 3.13, A, lane 3). From the size of vesicles present in images of cathepsin S labelling seen in immunofluorescence micrographs, vesicles seem to be largely secretory (± 20 nm), containing approximately 66% membrane-bound cathepsin S (precursor), and very few active cathepsin S containing-late endosomes (± 50 nm) (Figure 4.5, C and Table 4.3).

Immunofluorescence labelling of cathepsin D, on the other hand, shows labelling in vesicles that are larger than most other organelles (± 150 - 200 nm) except the early endosomes (± 100 nm) (Figure 4.6, A). These are seen in the cytoplasm and towards the cell periphery, with some polarised cathepsin D distribution (Figure 4.6, A and B). Cathepsin D is also seen in the pseudopodia of activated cells (Figure 4.6, B, cell on top left), suggesting possible secretion or involvement in invasion. Though cathepsin D is traditionally regarded as a “lysosomal marker”, it is usually associated with a digestive body often called an endosome-lysosome “hybrid organelle” (size ± 150 - 200 nm) (Griffiths, 1996a) (Table 4.1) like those in Figure 4.6, A, B and C.

Cathepsin D has also been suggested to occur in macrophage early endosomes in (Diment *et al.*, 1988). This may also account for a peripheral distribution of cathepsin D (Figure 4.6, A and B). If this is the case, however, cathepsin D would be anticipated to colocalise with cathepsin H (Jahraus *et al.*, 1998). On the other hand, most of the labelled vesicles should contain mature cathepsin D (western blots indicate approximately 80% mature enzyme, Figure 3.10, A, lane 4). This would mean that vesicles may also be late endosomal (± 50 nm) or hybrid endosome-lysosomal organelles or digestive bodies (± 150 - 200 nm) (Figure 4.6, A and B). From their size, however, the majority of mature cathepsin D-labelled organelles would seem to be hybrid or digestive bodies (± 150 - 200 nm). Cathepsin D also seems, to a

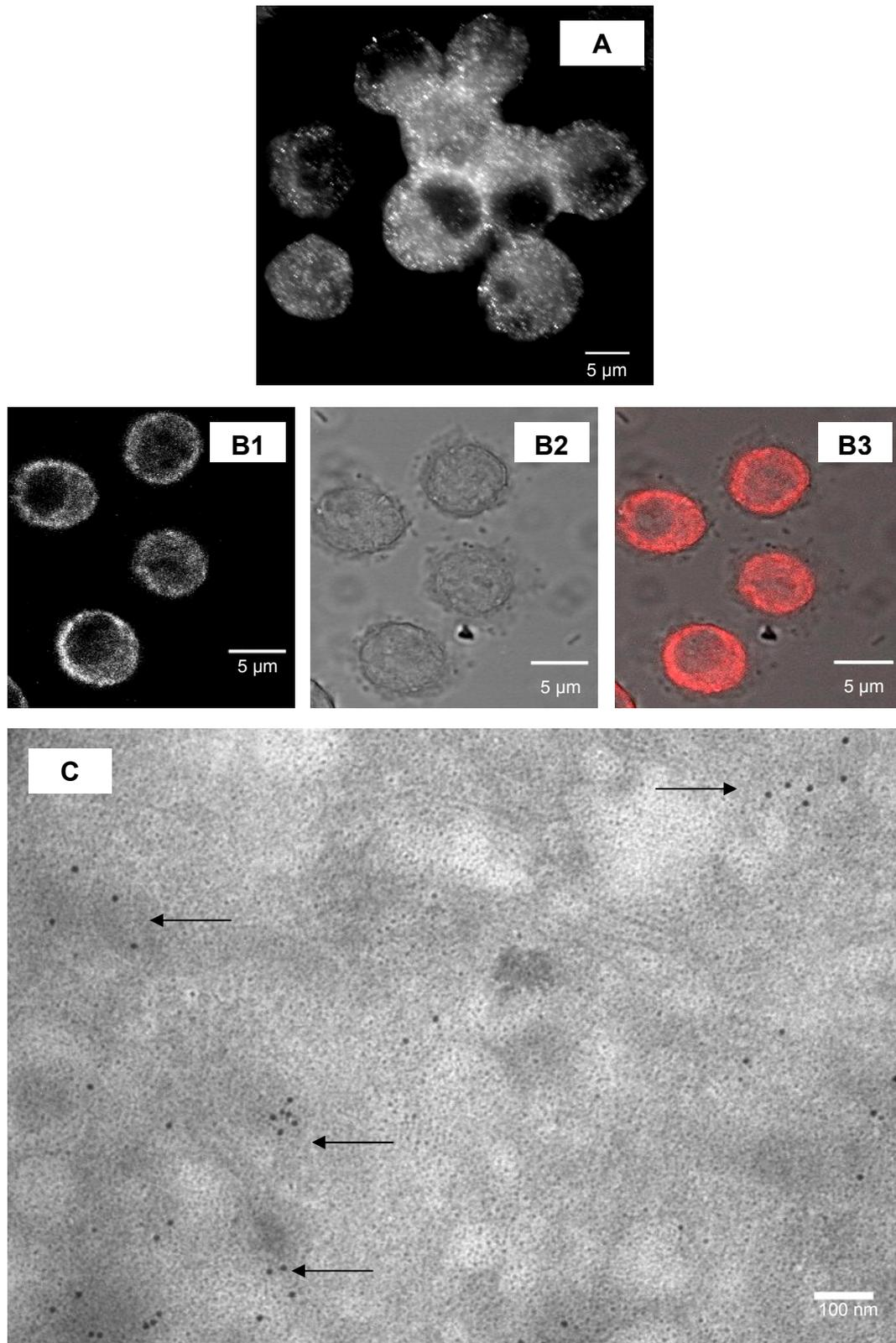


Figure 4.5 Fluorescent and protein A gold labelling of cathepsin S in J774 macrophages. Chicken anti-cathepsin S [20 µg/ml (A and B1)] and donkey anti-chicken IgG CY3 [2 µg/ml (A and B1)] applied to cells on coverslips, initially fixed with 3.7% PFA and permeabilised with saponin. Coverslips viewed with an Olympus epifluorescent microscope (A) or a Zeiss Meta 510 confocal microscope (B). CY3 filter (A and B1), DIC image (B2), composite image (B3). Bars = 5 µm. Chicken anti-cathepsin S [20 µg/ml (C)], a rabbit anti-chicken linker antibody [50 µg/ml (C)] and protein-A gold probe (10 nm) used on LR White sections viewed using a Philips CW120 Biotwin TEM (80-100 kV). Cathepsin S detected in tubulovesicular areas (arrows), the majority membrane-bound. Bar = 100 nm.

small extent, membrane-associated (Figures 4.6, C and Figure 4.10, C, 66% free and 34% membrane-bound) (Table 4.3), suggesting a presence in early endosomes (Diment *et al.*, 1988).

Cathepsin B on the other hand, appears to localise to electron-dense vesicles (± 50 and 100 nm, respectively) resembling late endosomes or “hybrid” organelles on the basis of size (usually containing processed cathepsins). Small vesicles (± 20 nm) close to membraneous systems resembling ER where precursor enzyme would occur were also observed (Figure 4.7, C). Such a distribution seems to fit with the 50:50 precursor:mature cathepsin B content of J774 cells evident in blots (Figure 3.9, A, lane 4). In Figure 4.7, C, once again, a variable ultrastructural preservation is evident, this time in a single section, with organelles and structures towards the left-hand-side of the micrograph becoming less well preserved. Labelling also seems to indicate a 60% membrane-association (possibly precursor enzyme) as gold labels seems to be located around the periphery of labelled vesicles (Figure 4.7, C). In approximately 40% of vesicles cathepsin B appeared lumenally distributed and soluble or “free” (Figure 4.7, C and other micrographs not shown) (Table 4.3).

Cathepsin L labelling with the anti-cathepsin L peptide antibody is sparse (Figure 4.8, A and B), with labelling being largely confined to small vesicles (± 20 nm) and membraneous ER-like structures positioned towards the perinuclear area of the cell and scattered sparsely through the cell (Figure 4.8, C). This labelling pattern and distribution was anticipated, since western blots indicated that J774 cells contain approximately 50% precursor and approximately 50% mature cathepsin L (Figure 3.12, A, lane 3) consistent with ER/Golgi vesicles containing precursor enzyme and larger vesicles (± 50 and 100 nm) possibly representing late endosomes and “hybrid” organelles, respectively, containing active enzyme (Figure 4.8, A, B and C). The majority of cathepsin L (70%) appears membrane-bound (Figure 4.8, C) (Table 4.3).

It should be noted that bacillus-like structures seen in many of the micrographs are artefacts introduced in the mounting of the labelled cells on coverslips (Figure 4.4, B2 and B3; 4.5, B2 and B3; 4.8, A2 and A3; 4.9, B3 and B4; 4.10, B3;

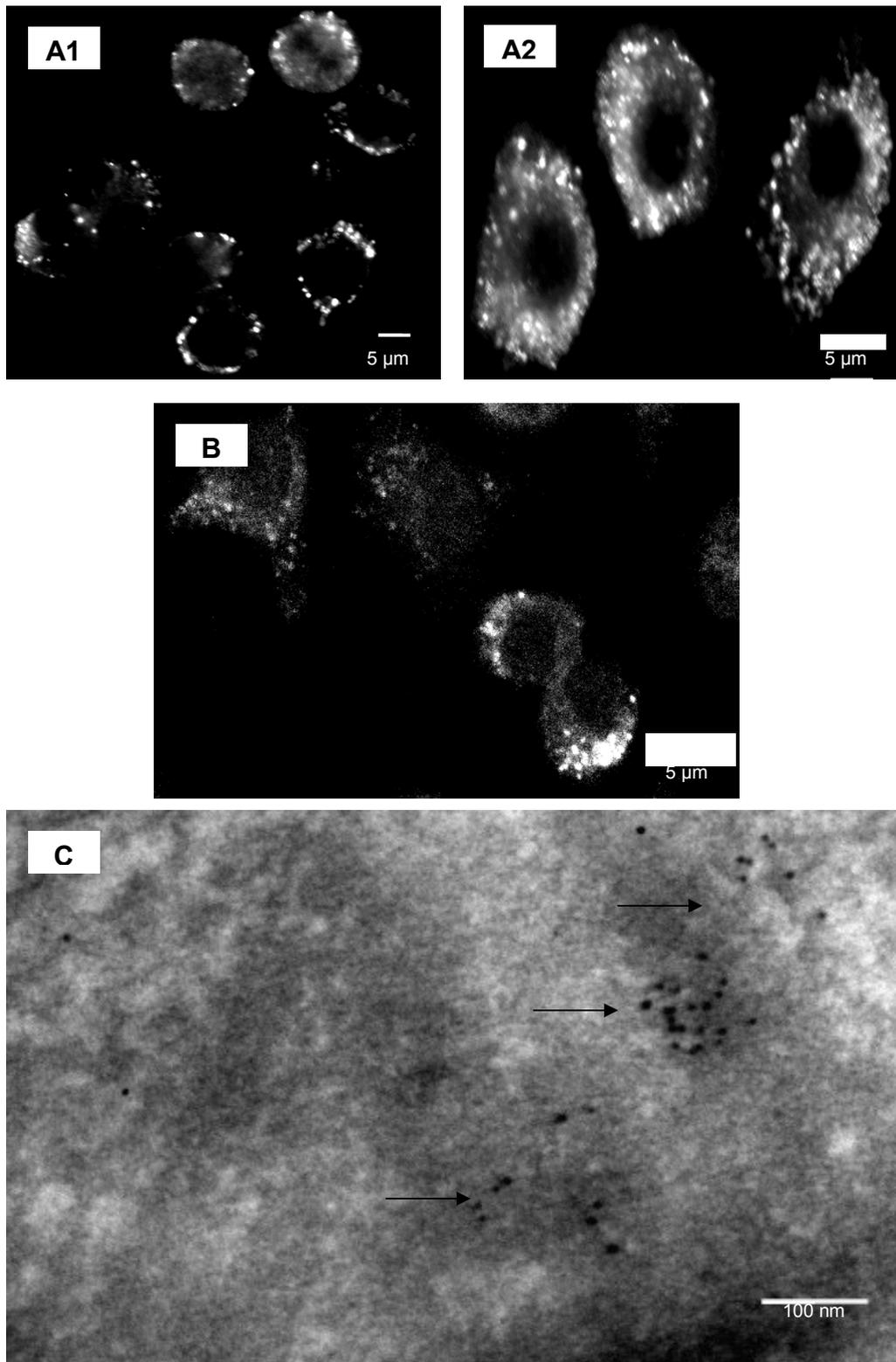


Figure 4.6 Fluorescent and protein A gold labelling of cathepsin D in J774 macrophages.

Chicken anti-cathepsin D [100 µg/ml (A1) or 200 µg/ml (A2 and B)] and donkey anti-chicken IgG CY3 [2 µg/ml (A1 and A2)] or rabbit anti-chicken FITC IgG [10 µg/ml (B)] applied to cells on coverslips, initially fixed with 3.7% PFA and permeabilised with saponin. Coverslips viewed with an Olympus epifluorescent microscope (A) or Zeiss Meta 510 confocal microscope (B). Bars = 5 µm.

Chicken anti-cathepsin D [10 µg/ml (C)], a rabbit anti-chicken linker antibody [50 µg/ml (C)] and protein-A gold probe (10 nm) were used on LR White sections which were viewed using a Philips CW120 Biotwin TEM (80-100 kV). Cathepsin D in electron-dense vesicles (arrows). Bar = 100 nm.

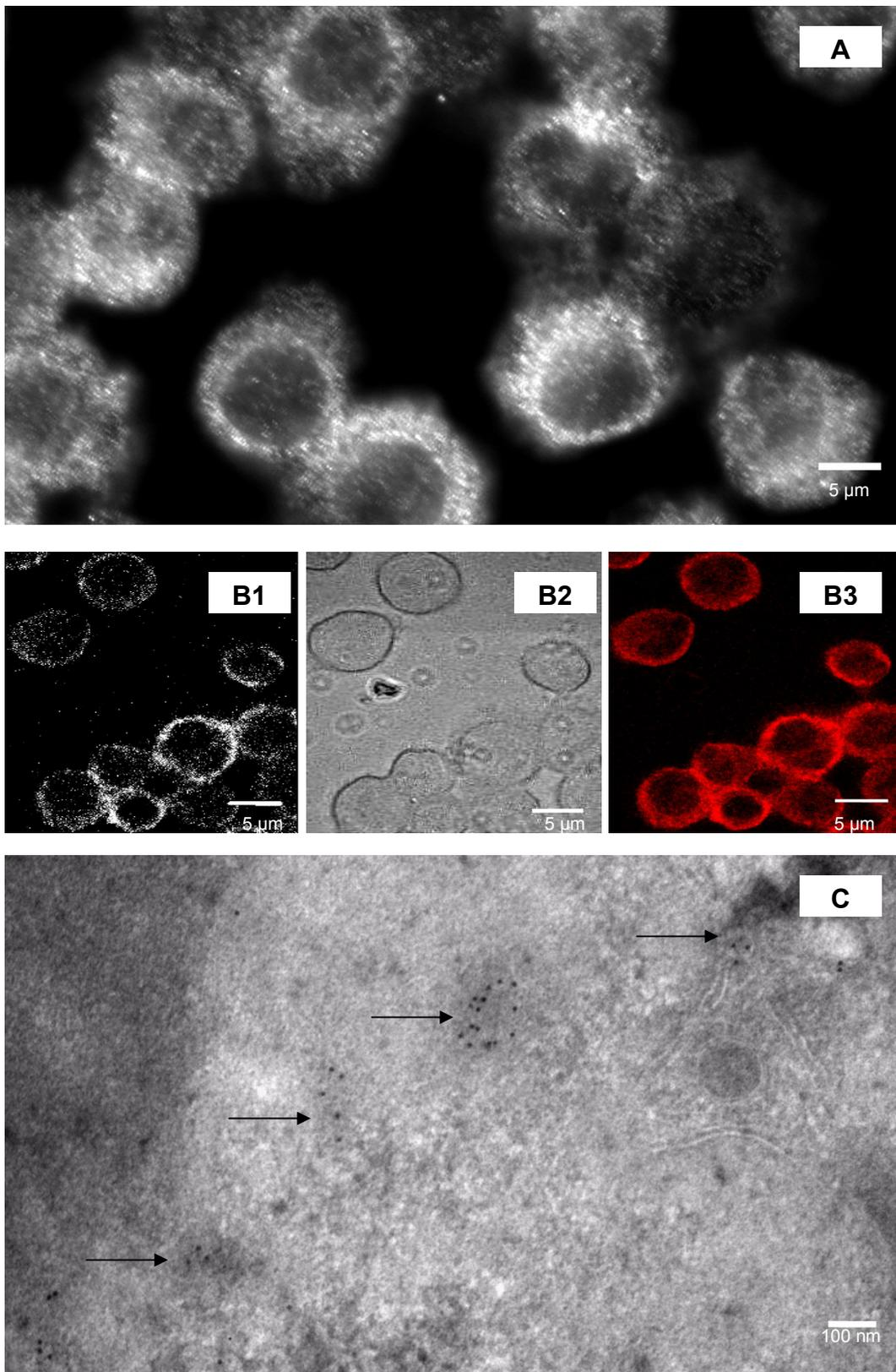


Figure 4.7 Fluorescent and protein A gold labelling of cathepsin B in J774 macrophages.

Chicken anti-human liver cathepsin B [20 µg/ml (A and B1)] and donkey anti-chicken IgG CY3 [2 µg/ml (A and B1)] applied to cells on coverslips, initially fixed with 3.7% PFA and permeabilised with saponin. Coverslips viewed with an Olympus epifluorescent microscope (A) or Zeiss Meta 510 confocal microscope (B). CY3 filter (A and B1), DIC image (B2), composite image (B3). Bars = 5 µm.

Chicken anti-human liver cathepsin B [10 µg/ml (C)], a rabbit anti-chicken linker antibody [50 µg/ml (C)] and protein-A gold probe (10 nm) used on LR White sections viewed using a Philips CW120 Biotwin TEM (80-100 kV). Cathepsin B in electron-dense vesicles, possibly membrane-bound (arrows) and close to membraneous systems. Bar = 100 nm.

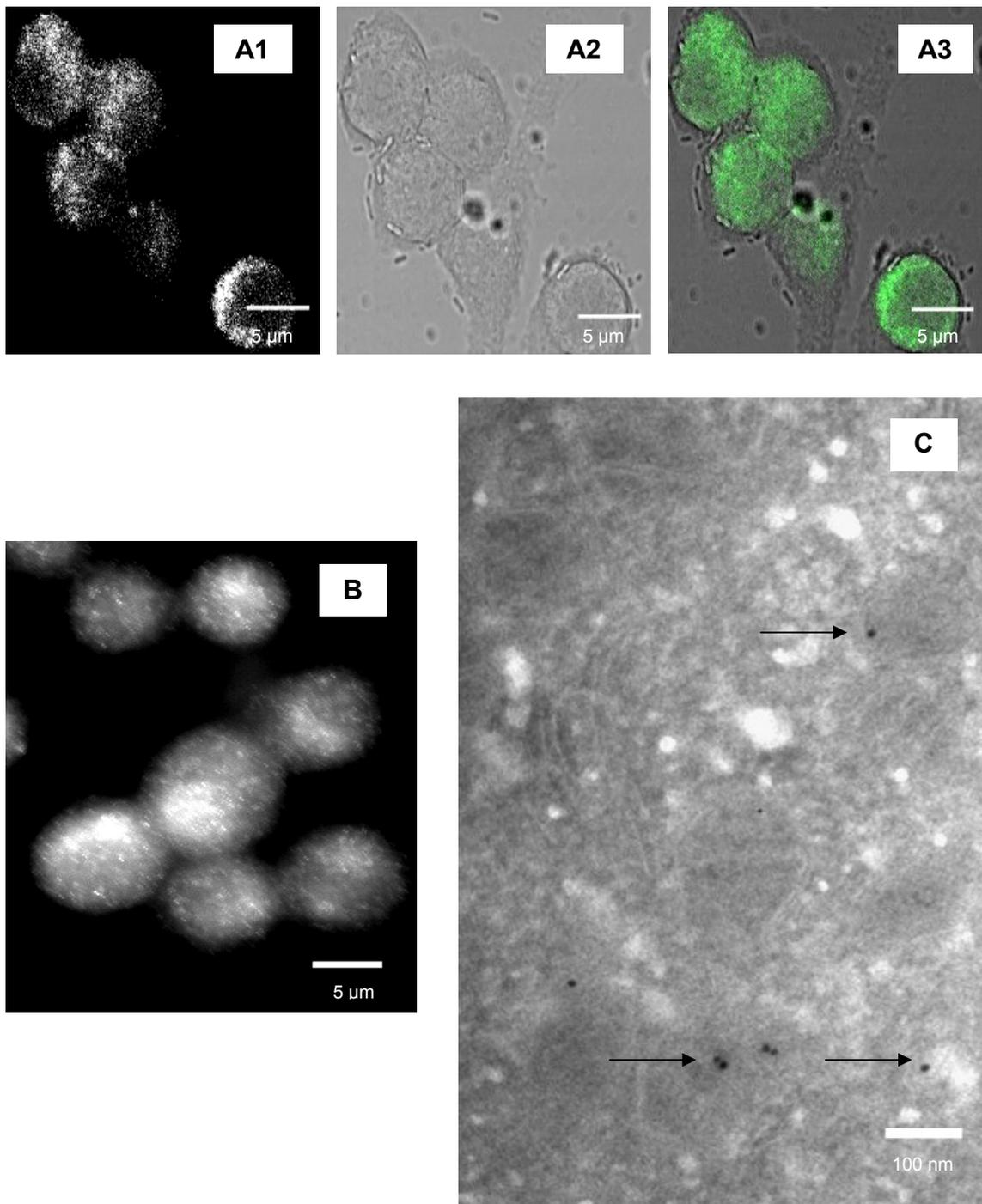


Figure 4.8 Fluorescent and protein A gold labelling of cathepsin L in J774 macrophages.

Rabbit anti-cathepsin L [20 $\mu\text{g/ml}$ (A1 and B)] and goat anti-rabbit IgG FITC [5 $\mu\text{g/ml}$ (A1 and B)] applied to cells on coverslips, initially fixed with 3.7% PFA and permeabilised with saponin. Coverslips viewed with an Olympus epifluorescent microscope (B) or a Zeiss Meta 510 confocal microscope (A). FITC filter (A1 and B), DIC image (A2), composite image (A3). Bars = 5 μm .

Rabbit anti-cathepsin L [20 $\mu\text{g/ml}$ (C)] and protein-A gold probe (10 nm) used on LR White sections viewed using a Philips CW120 Biotwin TEM (80-100 kV). Cathepsin L detected in small vesicles, possibly membrane-bound (arrows). Bar = 100 nm.

Summary

Table 4.3 Summary western blot data, apparent vesicle morphology and enzyme distribution.

	Precursor form (%)	Mature form (%)	Vesicle type	M (%)	F (%)
Cat H	50	50	S/LT	50	50
Cat S	90	10	>S/LE/Lys	66	34
Cat D	20	80	LE/Lys	34	66
Cat B	50	50	S/>LE	66	34
Cat L	50	50	>S/LE	66	34

Abbreviations: Cat, cathepsin; LT, large (± 100 nm) electron-translucent, early endosome-like; S, small (± 20 nm) secretory vesicle-like; LE, large (± 50 nm), electron-dense, late endosome-like; Lys, lysosome-like, hybrid, digestive organelles (± 150 - 200 nm); M, membrane-bound; F, free; >, mostly.

Results (Table 4.3) seem to indicate the presence of at least 4 vesicle types, small (± 20 nm) electron-translucent secretory-like (possibly containing membrane-bound, precursor cathepsins especially cathepsins H, S, B and L), early endosomal-type vesicles containing mature cathepsin H, large (± 100 nm). Cathepsins D, L, S and B appear to be present in late endosomes (± 50 nm) and large “hybrid” organelles (± 150 - 200 nm) contain cathepsins D, B and L. Vesicle types could not, at this stage, be accurately assigned, however, without at least probes indicating acidity (LysoTracker) or some ultrastructural detail.

4.3 Colocalisation of cathepsins in J774 macrophages

Cathepsin precursor forms should be found only in the ER, Golgi and any secretory vesicles either transporting precursor from the ER and Golgi to the late endosome for activation or being secreted from the cell (approximately 10% of traffic) (Pillay *et al.*, 2002).

The polyclonal cathepsin antisera used in the current study detect both the proforms (associated with ER, Golgi and non-acidic vesicular compartments) and the mature, active enzymes (late endosomes, lysosomes and other acidic vesicular compartments). Therefore, the presence and percentage of precursor or mature forms of the cathepsins, it was hoped, could possibly be predicted from western blot data and by morphological identification of the containing compartment or vesicle. This assignment, it was hoped, would subsequently be confirmed using labelling for LAMP-1 and -2 and the demonstration of a low pH, all usually associated with the classical late endosome and lysosome which should contain mature enzyme (Fukuda *et al.*, 1991).

Both double immunogold and fluorescent labelling were also performed to check that cathepsins H and S do not colocalise and to assess whether other cathepsins i.e. cathepsins B and L, colocalise with the markers for early endosomes (± 100 nm, cathepsin H), late endosomes (± 50 nm, cathepsin S) or “lysosomes”, hybrid organelles or digestive bodies (± 150 - 200 nm, cathepsin D) or if additional vesicle populations were present.

4.3.1 Reagents

Reagents for culture, fixation and embedding, immunolabelling of ultrathin sections and fluorescent immunolabelling of J774 cells for cathepsins B, D, H, S and L were prepared according to Sections 2.2.1, 2.7.1.1, 2.7.3.1 and 2.8.1.1, respectively.

The anti-cathepsin and secondary fluorescent antibodies used, were as previously described (Section 3.7.1 and 4.2.1).

4.3.2 Procedure

J774 cells were cultured, fixed and embedded in LR White resin according to the procedure in Sections 2.2.2 and 2.7.1.2. Double protein A gold labelling on the ultrathin sections was performed with chicken anti-cathepsin S [15 $\mu\text{g/ml}$] and rabbit anti-cathepsin H [50 $\mu\text{g/ml}$], chicken anti-cathepsin D [10 $\mu\text{g/ml}$] and chicken anti-cathepsin S [10 $\mu\text{g/ml}$], chicken anti-cathepsin B [10 $\mu\text{g/ml}$] and chicken anti-cathepsin D [15 $\mu\text{g/ml}$], chicken anti-cathepsin B [10 $\mu\text{g/ml}$] and rabbit anti-cathepsin L [20 $\mu\text{g/ml}$] according to Section 2.7.3.2. Fluorescent immunolabelling was performed with chicken anti-cathepsin S [15 $\mu\text{g/ml}$ or 50 $\mu\text{g/ml}$] and rabbit anti-cathepsin H [100 $\mu\text{g/ml}$ or 80 $\mu\text{g/ml}$], chicken anti-cathepsin D [200 $\mu\text{g/ml}$] and chicken anti-cathepsin S [20 $\mu\text{g/ml}$ or 50 $\mu\text{g/ml}$], chicken anti-cathepsin D [100 $\mu\text{g/ml}$ or 200 $\mu\text{g/ml}$] and chicken anti-cathepsin B [10 $\mu\text{g/ml}$ or 50 $\mu\text{g/ml}$], chicken anti-cathepsin D [200 $\mu\text{g/ml}$] and rabbit anti-cathepsin L [50 $\mu\text{g/ml}$], chicken anti-cathepsin B [15 $\mu\text{g/ml}$ or 50 $\mu\text{g/ml}$] and rabbit anti-cathepsin L [15 $\mu\text{g/ml}$ or 50 $\mu\text{g/ml}$], chicken anti-cathepsin S [50 $\mu\text{g/ml}$] and chicken anti-cathepsin B [50 $\mu\text{g/ml}$], chicken anti-cathepsin S [20 $\mu\text{g/ml}$ or 50 $\mu\text{g/ml}$] and rabbit anti-cathepsin L [20 $\mu\text{g/ml}$ or 50 $\mu\text{g/ml}$], donkey anti-chicken IgG CY3 [2 $\mu\text{g/ml}$ or 1 $\mu\text{g/ml}$], goat anti-rabbit IgG FITC [5 $\mu\text{g/ml}$ or 3 $\mu\text{g/ml}$ or 2 $\mu\text{g/ml}$], rabbit anti-chicken IgG FITC [10 $\mu\text{g/ml}$ or 6 $\mu\text{g/ml}$] according to Section 2.8.1.2. Labelling was viewed using either an Olympus epifluorescent microscope and F-View CCD camera or a Zeiss 510 Meta confocal microscope and images analysed using ImageJ software and manually as previously described (Sections 2.8.1.2 and 4.2.2).

As the polyclonal anti-mature cathepsin antisera used cannot distinguish between precursor and mature forms of the enzyme, cathepsins associated with membranous, ER/Golgi-like structures were assumed to be precursor and inactive. Those associated with vesicles may represent either mature active enzyme in acidic compartments or precursor in secretory vesicles in non-acidic vesicles. Due to generally poor ultrastructural preservation achieved, the knowledge that most of the cathepsin S and cathepsin D, would label mainly precursor or mature cathepsin, respectively, labelling for cathepsins S and B and cathepsins S and L were performed using only fluorescence microscopy.

When both antibodies used in the colocalisation experiment were from the same host, a fixation step between labelling fixation steps and the relevant controls were performed to eliminate any possible cross-reactivity between primary and secondary labelling systems (Section 2.7.1.2 and 2.8.1.2, respectively).

4.3.3 Results

Labelling showed no non-specificity (results not shown). Cathepsin H and cathepsin S labelling does not appear to colocalise to any extent (less than 20%, Figure 4.9, A, B and C), except in perinuclear areas where the synthesis and processing may occur concurrently (e.g. in the ER and Golgi) or where cells come into close contact (Figure 4.9, A and B). This seems to be most clearly demonstrated in epifluorescence labelling results (Figure 4.9, A). Confocal immunofluorescence labelling seems, however, to indicate that some peripheral polarised labelling colocalisation may also occur (Figure 4.9, B).

Protein A gold labelling confirms both cathepsin S and cathepsin H were separately located (Figure 4.9, C). Cathepsin S is associated with tubulovesicular areas (Figure 4.9, C) as was previously observed with the single labelling (Figure 4.5, C). Labelling for the potential early endosome marker (cathepsin H) was anticipated to be more peripherally located than labelling for the potential late endosome marker (cathepsin S), but in some places in the cell this seems to be the opposite (Figure 4.9, A and B). Western blots showed that approximately 50% cathepsin H and approximately 90% cathepsin S in the J774 cells are of the precursor form (Figure 3.11, A, lane 3 and Figure 3.13, A, lane 3, respectively). Labelling, however, indicates that neither enzyme colocalises to any extent, even if in their respective secretory (± 20 nm, precursor enzyme-containing) vesicle populations (Figure 4.9,

A, B and C). Though ultrastructural preservation is once again poor, larger slightly electron-dense vesicles possibly represent late endosomes (± 50 nm) and the balance of small electron-translucent (± 20 nm) or electron-dense (± 30 - 50 nm) vesicles possibly representing secretory vesicles or “secretory lysosomal” populations, respectively (Figure 4.9, C).

It is difficult to say whether confocal microscopy or conventional epifluorescence gives more labelling information, as different levels of antibody were used (Figure 4.9, A and B). Confocal labelling did reveal some peripheral colocalisation, however. The thinner “optical slice” being examined prevents such information from being obscured in conventional fluorescence microscopy (Figure 4.9, A - epifluorescence compared to Figure 4.9, B - confocal). From EM labelling results, however, it would seem that cathepsin H and cathepsin S labelling may only assist in assigning cathepsins to either the early or late endosomes or to secretory vesicles if fair ultrastructural detail is preserved (Figure 4.9, C). Once again vesicular structures seem more swollen than other membraneous organelles such as the ER (Figure 4.9, C).

Immunofluorescent labelling for cathepsin S and D seemed to indicate that these cathepsins are largely non-colocalised (approximately 25% colocalised) except in a few large structures which possibly represent hybrid endosome-lysosome organelles (± 150 - 200 nm) (Figure 4.10, A and B) and in perinuclear areas which may represent the areas of synthesis and processing, the ER and Golgi (Figure 4.10, A and B). Western blotting data indicate that cathepsin D is mainly mature (Figure 3.10, A, lane 4) and cathepsin S immature (Figure 3.13, A, lane 3). Since cathepsin D is considered mainly a marker for the “lysosome” (Connor, 2004) or digestive body of the cell, the number (usually relatively few) and size of colocalising vesicles, possibly confirms that such vesicles are what are known as “late endosome-lysosome hybrid organelles”. These organelles are especially obvious in confocal micrographs where an optical slice of approximately 1 - 2 μm is recorded (Figure 4.10, B) and seem to be most concentrated in regions of cell-cell contact (Figure 4.10, A). Protein A gold labelling seems to confirm a lysosome-like digestive body localisation as it reveals colocalisation of cathepsins S and D in large (± 150 - 200 nm) electron-dense, non-multivesicular vesicles (Figure 4.10, C, red arrows). Cathepsin S (Figure 4.10, C, black arrows) and cathepsin D (Figure 4.10, C, white arrows) are also seen located separately in small vesicles (± 20 nm) that are possibly secretory (containing precursor enzymes).

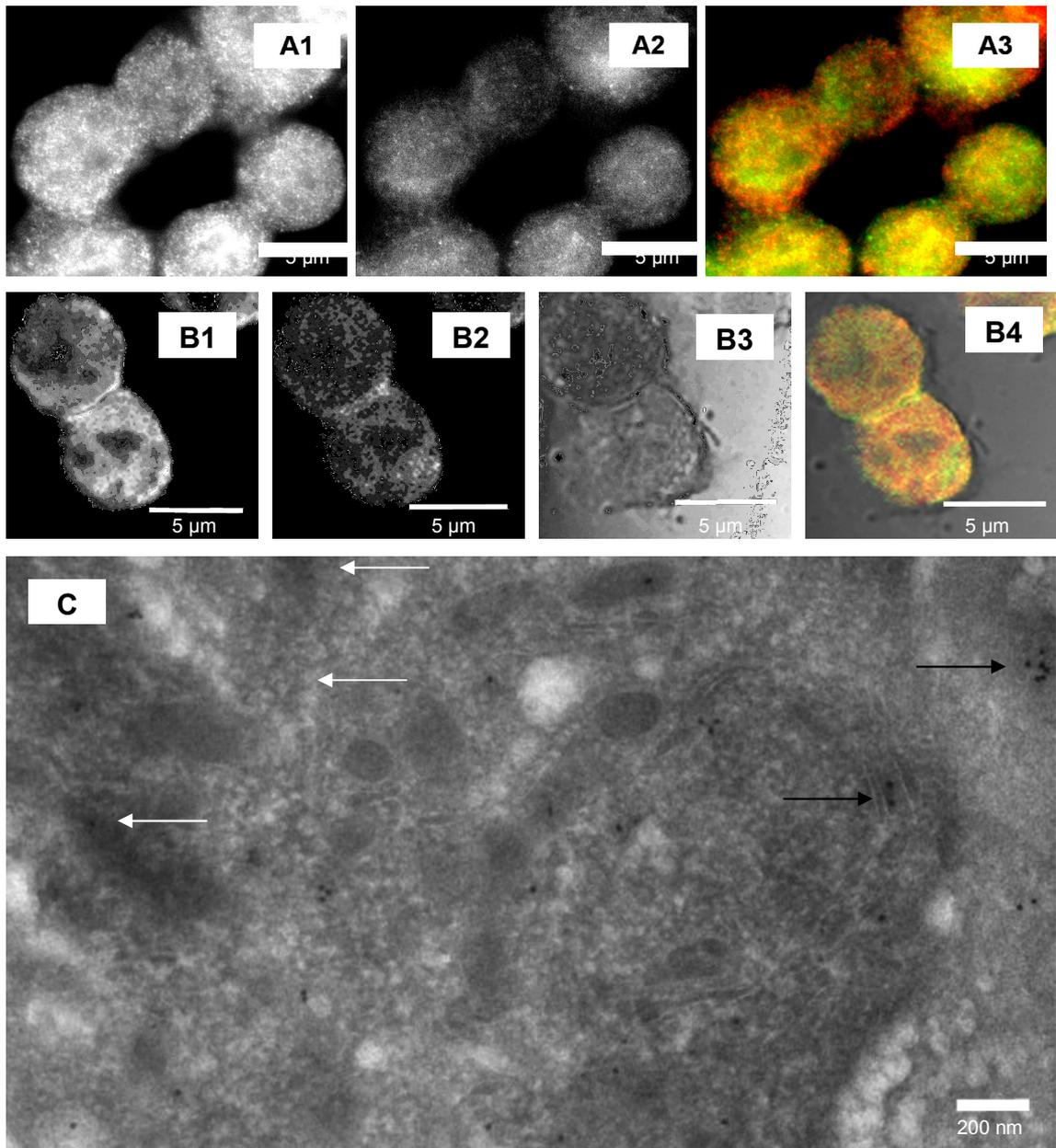


Figure 4.9 Fluorescent and protein A gold labelling of cathepsins S and H in J774 macrophages.

Chicken anti-cathepsin S [15 $\mu\text{g/ml}$ (A1)] or rabbit anti-cathepsin H [100 $\mu\text{g/ml}$ (B1)] and donkey anti-chicken IgG CY3 [2 $\mu\text{g/ml}$ (A1)] or goat anti-rabbit IgG FITC [2 $\mu\text{g/ml}$ (B1)], post-fixed (3.7% PFA) and probed with rabbit anti-cathepsin H [80 $\mu\text{g/ml}$ (A2)] or chicken anti-cathepsin S [50 $\mu\text{g/ml}$ (B2)] and either goat anti-rabbit FITC [2 $\mu\text{g/ml}$ (A2)] or donkey anti-chicken CY3 [2 $\mu\text{g/ml}$ (B2)], applied to cells on coverslips, initially fixed with 3.7% PFA and permeabilised with saponin. Coverslips viewed using an Olympus epifluorescent microscope (A) a Zeiss 510 Meta confocal microscope (B). CY3 filter (A1 and B2), FITC filter (A2 and B1), DIC image (B3), composite image (A3 and B4). Bars = 5 μm .

Rabbit anti-cathepsin H [18 $\mu\text{g/ml}$ (C)], chicken anti-cathepsin S [15 $\mu\text{g/ml}$ (C)], a rabbit anti-chicken linker antibody [50 $\mu\text{g/ml}$ (C)] and protein-A gold probe for cathepsin H (10 nm) and for cathepsin S (15 nm) used on LR White sections viewed using a Philips CW120 Biotwin TEM (80-100 kV). Cathepsin H (white arrows), cathepsin S (black arrows) did not appear to colocalise. Bar = 200 nm.

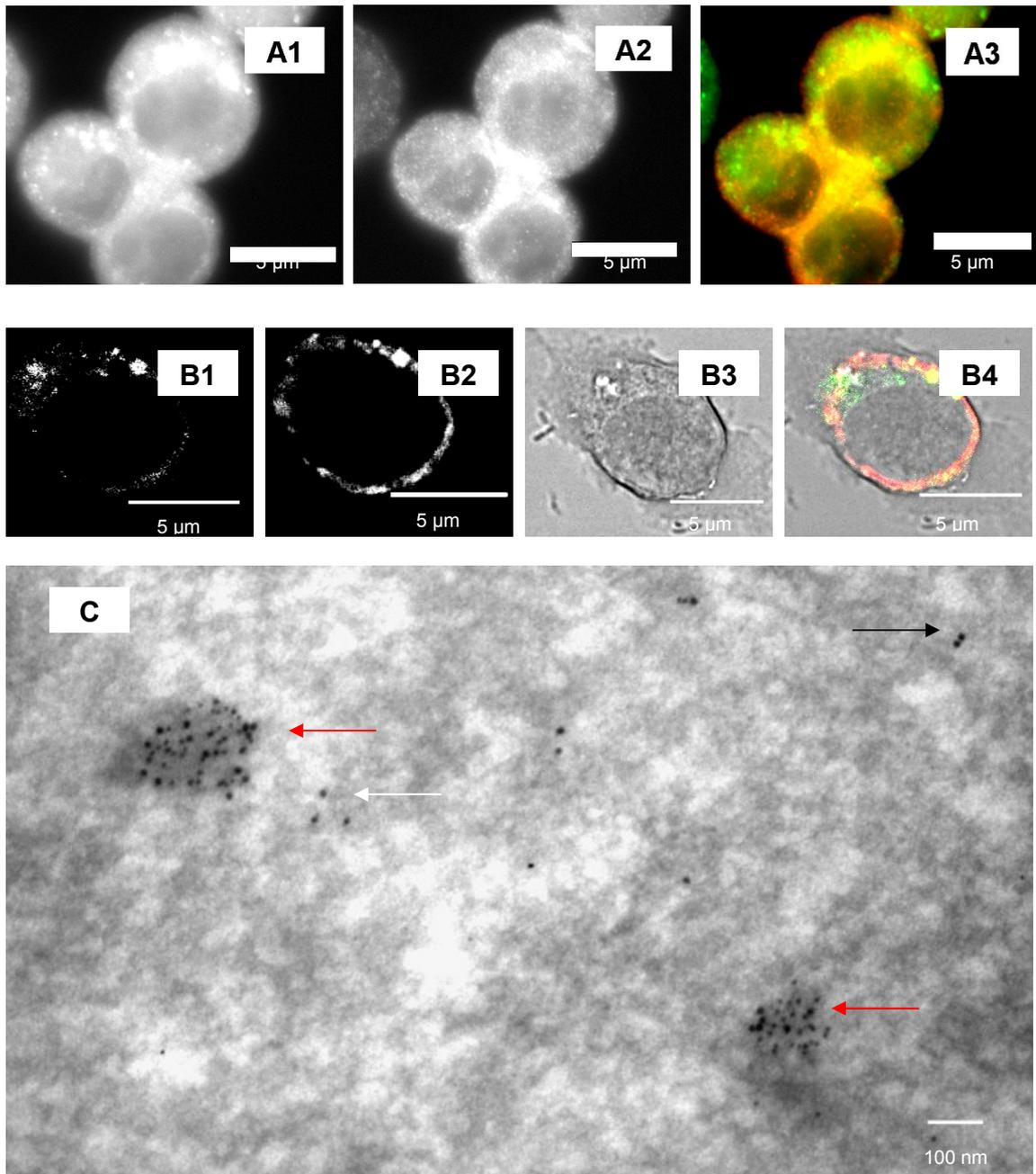


Figure 4.10 Fluorescent and protein A gold labelling of cathepsins D and S in J774 macrophages.

Chicken anti-cathepsin D [200 $\mu\text{g/ml}$ (A1 and B1)] and rabbit anti-chicken FITC [10 $\mu\text{g/ml}$ (A1 and B1)], post-fixed (3.7% PFA) and probed with chicken anti-cathepsin S [20 $\mu\text{g/ml}$ (A2) or 50 $\mu\text{g/ml}$ (B2)] and donkey anti-chicken IgG CY3 [2 $\mu\text{g/ml}$ (A2 and B2)], applied to cells on coverslips, initially fixed with 3.7% PFA, and permeabilised with saponin. Coverslips viewed using an Olympus epifluorescent microscope (A) or a Zeiss 510 Meta confocal microscope. FITC filter (A1 and B1), CY3 filter (A2 and B2), DIC image (B3), composite image (A3 and B4). Bars = 5 μm .

Chicken anti-cathepsin D [10 $\mu\text{g/ml}$ (C)], chicken anti-cathepsin S [10 $\mu\text{g/ml}$ (C)], a rabbit anti-chicken linker antibody [50 $\mu\text{g/ml}$ (C)] and protein-A gold probe for cathepsin D (10 nm) and for cathepsin S (15 nm) used on sections viewed using a Philips CW120 Biotwin TEM (80-100 kV). Cathepsin S and D colocalised in certain areas (red arrows). However, cathepsin S (black arrows) and cathepsin D (white arrows) still appeared separately. Bar = 100 nm.

Cathepsins B and D, like cathepsins S and D, also appear to colocalise (approximately 30%) in a few electron-dense, “lysosomal” vesicles possibly late endosomes (± 50 nm) (Figure 4.11, C, black arrows), though there are also vesicles in which either cathepsin B or cathepsin D are separately located (Fig 4.11, C, white arrows). Vesicular labelling for cathepsin B appears to be slightly more peripherally located than labelling for cathepsin D (Figure 4.11, B). Some of the peripheral vesicles not colocalised with cathepsin D may represent procathepsin B-labelled organelles, as indicated by blots (approximately 50% precursor and 50% mature, Figure 3.9, A, lane 4). Certain regions showing colocalisation between cathepsins B and D appear in peripheral invadopodia-like protrusions, suggesting possible secretion of electron-dense vesicular compartments such as “secretory lysosomes” (± 30 -50 nm) to assist invasion (Figure 4.11, C, black arrows, upper left-hand-side).

Fluorescent immunolabelling confirmed colocalisation between cathepsins B and D in a few vesicles towards the cell periphery (Figure 4.11, A and B). There also appear to be vesicular compartments that label only for cathepsin D or cathepsin B, with fewer labelling for cathepsin D than B (Figure 4.11, A, B and C). At least half of the non-colocalised cathepsin B-labelled organelles are small (± 20 nm) and electron-translucent and may contain newly synthesised precursor cathepsin B, in which case it is possible to speculate that they are secretory vesicles (Figure 4.11, C). The rest, according to western blots (Figure 3.9, A, lane 4), should contain mature active cathepsin B. As these do not colocalise with cathepsin D and their morphology is not definitive in electron micrographs (Figure 4.11, C), it is difficult to classify these vesicles without further markers or probes.

Cathepsins D and L colocalise in approximately 40% of labelled vesicle populations (Figure 4.12, A), cathepsin D appearing to be present in fairly large (± 150 -200 nm), vesicular compartments (Figure 4.12, A1) in non-activated macrophages (judged non-activated due to round morphology). In activated macrophages (judged activated due to elongated morphology), however, there is an almost total lack of colocalisation, approximately less than 20% indicating colocalising vesicles may have been secreted, and the remaining cathepsin L is possibly of the precursor form (Figure 4.12, B1), and remaining cathepsin D is active, occurring mainly in hybrid organelles. The activated cells mentioned above were not activated on purpose. During the culture process the addition of trypsin-EDTA appeared on

occasion to activate cells, resulting in the loss of the round morphology and formation of

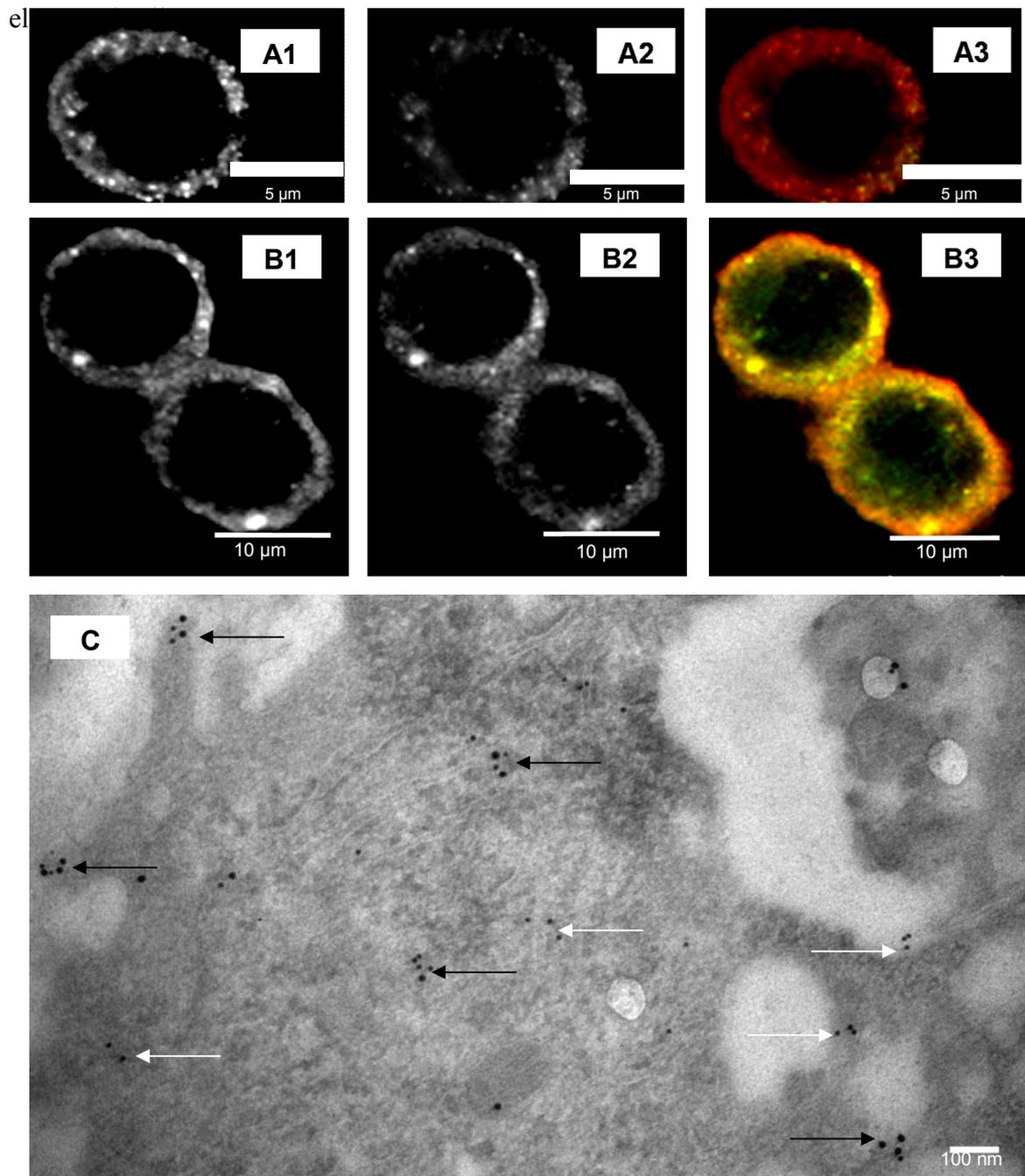


Figure 4.11 Fluorescent and protein A gold labelling of cathepsins D and B in J774 macrophages.

Chicken anti-cathepsin D [100 µg/ml (A2) or 200 µg/ml (B2)] and rabbit anti-chicken IgG FITC [10 µg/ml (A2 and B2)], post-fixed (3.7% PFA) and probed with chicken anti-cathepsin B [15 µg/ml (A1) or 50 µg/ml (B1)] and donkey anti-chicken IgG CY3 [2 µg/ml (A1 and B1)], applied to cells on coverslips, initially fixed with 3.7% PFA and permeabilised with saponin. Coverslips viewed using an Olympus epifluorescent microscope (A) or a Zeiss 510 Meta confocal microscope (B). CY3 filter (A1 and B1), FITC filter (A2 and B2), composite image (A3 and B3). Bars = 5 µm (A) or 10 µm (B).

Chicken anti-human liver cathepsin B [10 µg/ml (C)] and chicken anti-cathepsin D [15 µg/ml (C)] and a rabbit anti-chicken linker antibody [50 µg/ml (C)] and protein-A gold probe for cathepsin B (10 nm) and for cathepsin D (15 nm) used on LR White sections viewed using a Philips CW120 Biotwin TEM (80-100 kV). Cathepsin B and D in vesicles (black arrows) or only cathepsin B (10 nm) or cathepsin D (15 nm) (white arrows). Bar = 100 nm.

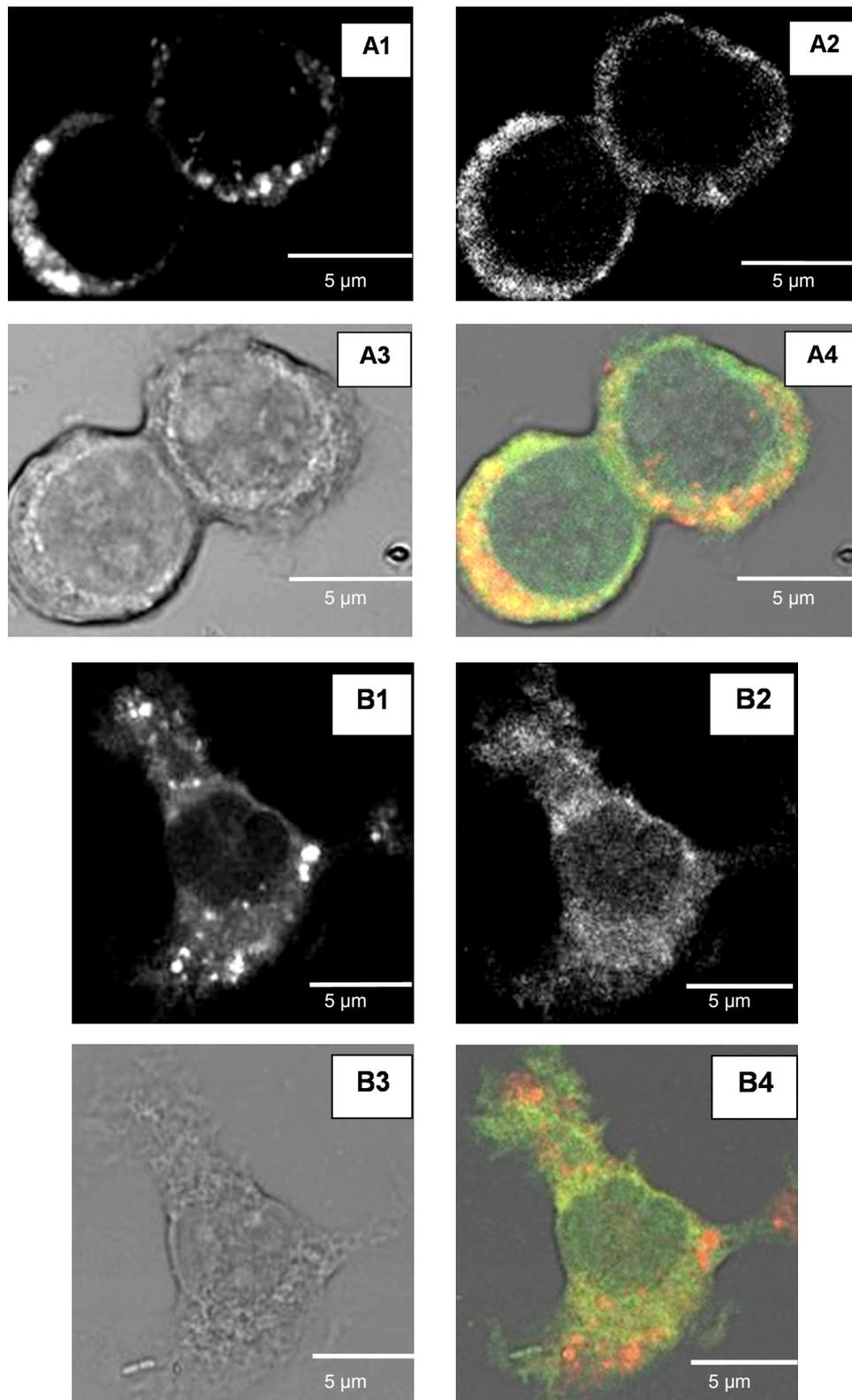


Figure 4.12 **Fluorescent labelling of cathepsins D and L in J774 macrophages.**

Chicken anti-cathepsin D [200 µg/ml (A1 and B1)] and donkey anti-chicken IgG CY3 [2 µg/ml (A1 and B1)], post-fixed (3.7% PFA), probed with rabbit anti-cathepsin L [50 µg/ml (A2 and B2)] and goat anti-rabbit IgG FITC [2 µg/ml (A2 and B2)], applied to cells on coverslips, initially fixed with 3.7% PFA and permeabilised with saponin. Coverslips viewed using a Zeiss 510 Meta confocal microscope. CY3 filter (A1 and B1), FITC filter (A2 and B2), DIC images (A3 and B3), composite images (A4 and B4). Bars = 5 µm.

Few compartments show colocalisation between cathepsins B and L, according to fluorescence microscopy (approximately 25% colocalisation) (Figure 4.13, A and B). Regions showing colocalisation often occur between cells in contact (Figure 4.13, B) or towards one cell edge (Figure 4.13, A). The latter observation seems confirmed by EM where cathepsin B and L colocalisation seemed to occur in relatively small vesicles (± 30 -50 nm) possibly “secretory lysosomes” mainly towards the cell periphery (Figure 4.13, C, red arrows). Cathepsin B (Figure 4.13, C, white arrows) and cathepsin L (Figure 4.13, C, black arrows) were also observed individually in small (± 20 nm) vesicles, reminiscent of secretory vesicles which may contain newly synthesised proforms of the proteases in different vesicle populations. Vesicular swelling and generally poor ultrastructure made EM confirmation of results less useful (Figure 4.13, C).

Labelling colocalisation for cathepsins S and B was difficult to interpret without EM clarification of the labelling pattern, however. It seems to indicate a large amount of colocalisation (approximately 70%) of which approximately 50% occurs in small vesicle (± 20 nm) populations reminiscent of secretory-type vesicles which usually contain newly synthesised procathepsins and colocalisation in very few ± 50 nm vesicles resembling late endosomes (Figure 4.14, A). This would seem to support blot data which indicates the major form of cathepsin S in J774 cells is the precursor (Figure 3.13, A, lane 3) and that this is also, to some extent true for cathepsin B (approximately 50% immature) (Figure 3.9, A, lane 4). Colocalisation would also seem to indicate that the enzymes are co-expressed and co-packaged (Figure 4.14, A3).

In labelling for cathepsins S and L only minor numbers of small (± 20 nm) vesicles show apparent colocalisation (approximately 25%) in non-activated cells (Figure 4.15, A). Cathepsin S appears to be distributed throughout the cells and especially peripherally, whereas, cathepsin L labelling is more centrally located (Figure 4.15, A2 and A3, respectively). Here, too, the compartments labelled seem small (± 20 nm) supporting blot predictions that most of the cathepsin S and approximately 50% of cathepsin L of J774 cells may be in the precursor form in secretory vesicles (Figure 3.13, A, lane 3 and Figure 3.12, A lane 3, respectively). In activated cells (elongated), however, (Figure 4.15, B) a higher percentage of colocalisation seems apparent (approximately 70%), indicating how cell activation may affect results.

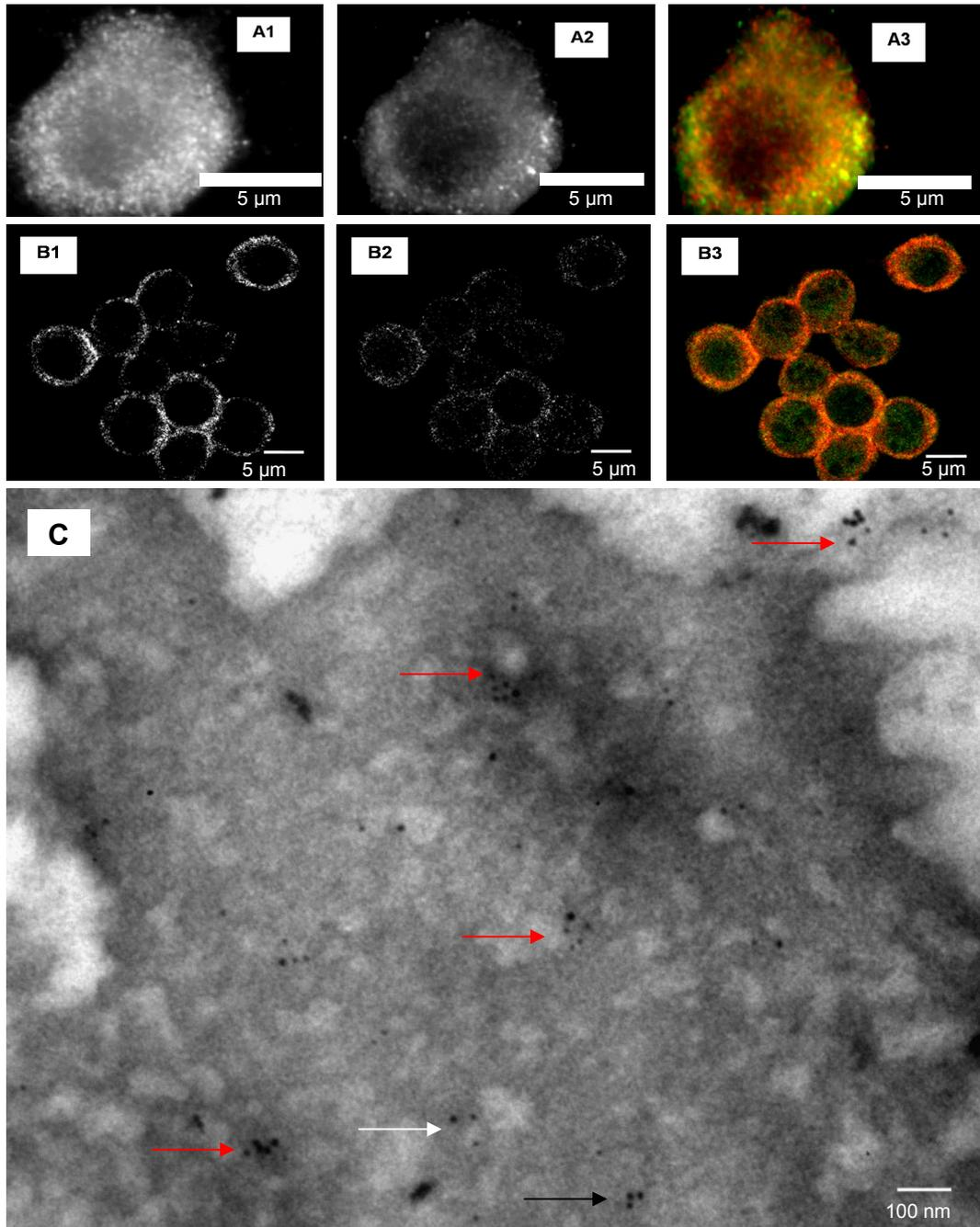


Figure 4.13 Fluorescent and protein A gold labelling of cathepsins B and L in J774 macrophages.

Chicken anti-cathepsin B [15 µg/ml (A1) or 50 µg/ml (B1)] and donkey anti-chicken IgG CY3 [2 µg/ml (A1) or 1 µg/ml (B1)], post-fixed (3.7% PFA), probed with rabbit anti-cathepsin L [15 µg/ml (A2) or 50 µg/ml (B2)] and goat anti-rabbit IgG FITC [5 µg/ml (A2) or 2 µg/ml (B2)], applied to cells on coverslips, initially fixed with 3.7% PFA and permeabilised with saponin. Coverslips viewed using an Olympus epifluorescent microscope (A) or a Zeiss 510 Meta confocal microscope (B). CY3 filter (A1 and B1), FITC filter (A2 and B2), composite images (A3 and B3). Bars = 5 µm.

Chicken anti-human liver cathepsin B [10 µg/ml (C)], rabbit anti-cathepsin L [20 µg/ml (C)], a rabbit anti-chicken linker antibody [50 µg/ml (C)] and protein-A gold probe for cathepsin B (10 nm) and for cathepsin L (15 nm) used on LR White sections viewed using a Philips CW120 Biotwin TEM (80-100 kV). Cathepsin B and L colocalised in certain vesicles (red arrows). Cathepsin B (white arrows) and cathepsin L (black arrows) still appeared separately. Bar = 100 nm.

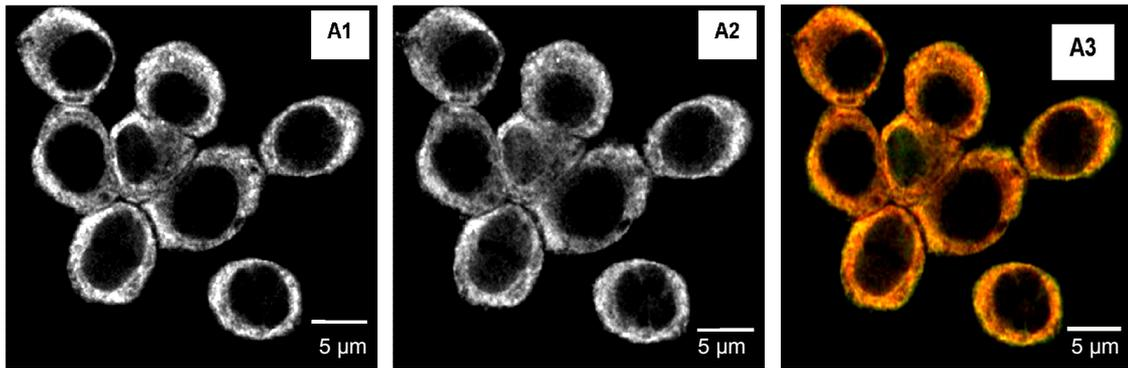


Figure 4.14 **Fluorescent labelling of cathepsins S and B in J774 macrophages.**

Chicken anti-cathepsin S [50 µg/ml (A1)] and donkey anti-chicken IgG CY3 [1 µg/ml (A1)], post-fixed (3.7% PFA), probed with chicken anti-cathepsin B [50 µg/ml (A2)] and rabbit anti-chicken IgG FITC [10 µg/ml (A2)], applied to cells on coverslips, initially fixed with 3.7% PFA and permeabilised with saponin. Coverslips viewed using a Zeiss 510 Meta confocal microscope. FITC filter (A1), CY3 filter (A2), composite image (A3). Bars = 5 µm.

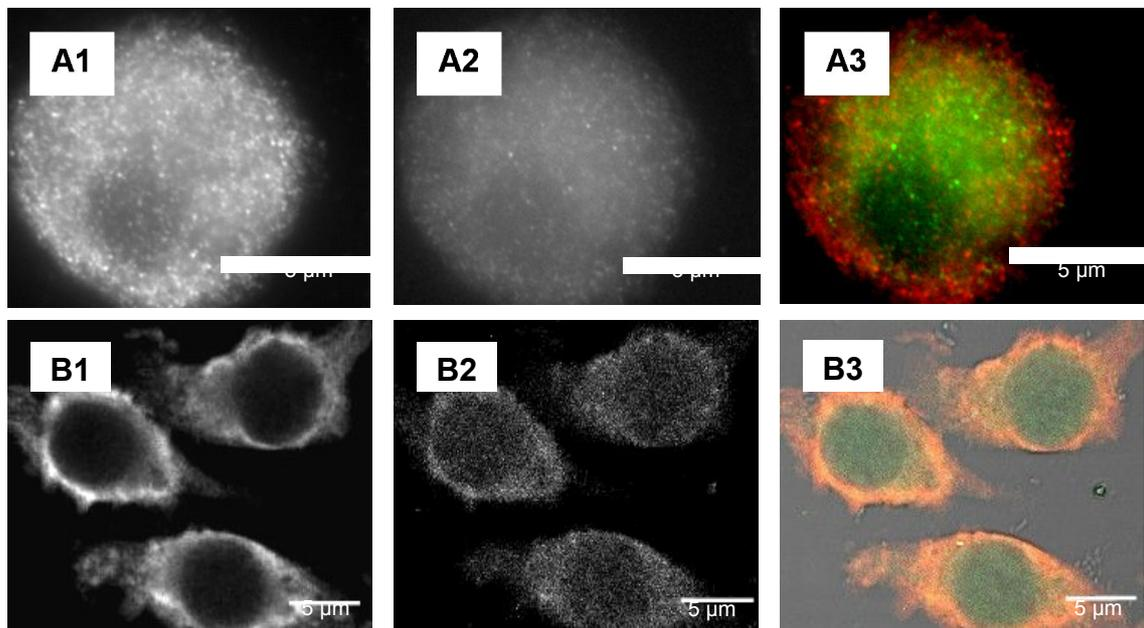


Figure 4.15 **Fluorescent labelling of cathepsins S and L in J774 macrophages.**

Chicken anti-cathepsin S [20 µg/ml (A1)] or 50 µg/ml (B1)] and donkey anti-chicken IgG CY3 [2 µg/ml (A1) or 1 µg/ml (B1)], post-fixed (3.7% PFA), probed with rabbit anti-cathepsin L [20 µg/ml (A2) or 50 µg/ml (B2)] and goat anti-rabbit IgG FITC [5 µg/ml (A2) or 2 µg/ml (B2)], applied to cells on coverslips, initially fixed with 3.7% PFA and permeabilised with saponin. Coverslips viewed using an Olympus epifluorescent microscope (A) or a Zeiss 510 Meta confocal microscope (B). CY3 filter (A1 and B1), FITC filter (A2 and B2), composite images (A3 and B3). Bars = 5 µm.

Summary

In summary, the data represented in Table 4.4 seem to indicate the possible presence of at least 2 major vesicle populations labelled for cathepsin H (vesicle 1A and B). One population appears secretory, containing either membrane-bound or free procathepsin H (± 20 nm, vesicle 1B). The other population is possibly an early endosomal population containing active cathepsin H (Claus *et al.*, 1998) (± 100 nm, vesicle 1A). Without labelling for other cathepsins to check colocalisation with cathepsin H and further markers or probes, it is difficult to know whether cathepsin H would be a good marker for an early endosomal population (provisional early endosomal vesicle 1A and a secretory vesicle population 1B).

Precursor cathepsins B and S could be mainly colocalised and membrane-bound (Table 4.4). The mature cathepsin S (approximately 10%) may be largely colocalised with mature cathepsin B in late endosomes (± 50 nm) and there seem to be relatively few late endosomes. Colocalisation would best be checked at the EM level and with labelling for precursor and mature cathepsins and a marker, such as the 215 kDa MPR, for the late endosome (provisionally classified in this study as a late endosome, vesicle 2).

There seems more active cathepsin B (approximately 40% more) than active cathepsin S [the total active cathepsin S appears to be approximately 10%, whereas, cathepsin B is approximately 50%, Table 4.4]. It is highly likely that the 30% of active cathepsin B and 40% of mature cathepsin L colocalise with mature cathepsin D, generally found in classical “lysosomal” or “hybrid” organelles, [i.e. most acidic and cathepsin D labelling (de Duve, 1983)] or in an acidic, digestive organelle other than the late endosome (if cathepsin S is a marker for the late endosome) (Table 4.4) (provisional hybrid, digestive vesicle 3, distinct from the late endosome).

If secretory vesicles were included, 4 vesicle types (an early endosomal-, late endosomal-, a digestive and secretory vesicle type) are evident by this stage. These vesicle populations could be assigned with more certainty to known vesicle population groups if antisera recognising precursor and mature cathepsins and hence the enzymes in late endosomes/lysosomes and precursor enzymes of secretory vesicles could be identified. It also seemed necessary, at this stage, to include a second marker for the late endosome or lysosomal population. Without the availability of antisera against the precursor enzyme, or

LYAAT and V-ATPase antibodies (to differentiate early endosomes from the Hck/LYAAT vesicle), LysoTracker seemed the obvious choice as a marker for acidic compartments including late endosomes, classical lysosomes and possibly other vesicles such as the V-ATPase-rich compartment described by Anes *et al.* (2006). LAMP-1 and -2 also seemed appropriate for identifying both the classical late endosomes and lysosomes (Fukuda *et al.*, 1991).

4.4 Localisation of cathepsins in LAMP-1 and LAMP-2 positive compartments

Several highly N-glycosylated proteins are present in “lysosomal” membranes and are known as LAMP-1, LAMP-2 and LAMP-3 (Eskelinen *et al.*, 2003). LAMP-1 and LAMP-2 are evolutionarily related and share great structural similarity (Fukuda *et al.*, 1991), however, they appear to be differentially regulated. LAMP-1 appears to be constitutively expressed (Amos *et al.*, 1990), whereas, LAMP-2 expression varies with cell type and with the developmental stage of the cell (Hattem *et al.*, 1995; Hua *et al.*, 1998).

At steady state, most LAMPs are localised to the limiting membranes of both classical late endosomes and lysosomes (Fukuda *et al.*, 1991) and have, therefore, been used as markers for these compartments in many studies. Small amounts have, however, been detected in classical early endosomal membranes, the plasma membrane as well as in the limiting membrane of autophagic vacuoles (Eskelinen *et al.*, 2002; Eskelinen *et al.*, 2003). LAMP surface expression appears to occur in certain cell types including cytotoxic T lymphocytes and highly metastatic tumour cells as well as under certain conditions such as the activation of platelets and blood monocytes (Kannan *et al.*, 1996; Eskelinen *et al.*, 2003). In contrast to LAMP-1 and -2, LAMP-3 appears to be predominantly located in multivesicular late endosomes and is associated with the internal membranes of these compartments which are rich in lysobisphosphatidic acid (Kobayashi *et al.*, 2000). Interestingly, LAMP-3 appears to be shared by both endocytic compartments as well as specialised secretory organelles. These include the Weibel-Palade bodies of endothelial cells (Kobayashi *et al.*, 2000), azurophil granules of neutrophils (Dahlgren *et al.*, 1995) and the α -granules of platelets (Eskelinen *et al.*, 2003). Unexpectedly, LAMP-1 and LAMP-2 are not located in the azurophil granules of neutrophils but appear to be present in peroxidase-negative specific granules and secretory vesicles (Dahlgren *et al.*, 1995).

The functional significance of LAMPs has been unknown for many years. It was originally thought that they served only as structural elements for lysosomal membranes (Furuta *et al.*, 1999; Furuta *et al.*, 2001). LAMPs have high carbohydrate content and it was thought that these complex carbohydrates maintained the stability of the 'lysosomal' membrane by protecting them from various hydrolytic enzymes (Fukuda *et al.*, 1991). Recent studies, however, have demonstrated a number of specific functions for LAMPs. Mice deficient in LAMP-1 appear to be viable and fertile, and the various properties of lysosomes such as the processing of enzymes, enzyme activity, pH as well as morphology and subcellular distribution remain normal. An up-regulation of LAMP-2 was observed in certain tissues and it appears that increased levels of LAMP-2 are required to compensate for the lack of LAMP-1 (Andrejewski *et al.*, 1999). LAMP-2 deficient mice, however, show severe symptoms. Approximately 50% of the mice die 20-40 days post partum and are smaller in size. There is also significant accumulation of autophagic vacuoles in their liver, muscle and heart (Tanaka *et al.*, 2000). LAMP-2 deficiency is also the main defect in Danon disease, which is characterised by fatal cardiomyopathy, mental retardation and mild skeletal myopathy with an accumulation of autophagic vacuoles in both the skeletal and cardiac muscle. It has been suggested that LAMP-2 deficiency results in impaired recycling of the 46 kDa MPR and the subsequent mistargeting of specific lysosomal enzymes. The accumulation of autophagic vacuoles is, therefore, due to impaired lysosomal degradation (Eskelinen *et al.*, 2002).

LAMP-3 is a tetraspanin and has been shown to act as a "molecular facilitator" by enhancing the formation and stability of signaling complexes. It also appears to be involved in cell activation and mediator release (Mahmudi-Azer *et al.*, 2002). Recently, it has been demonstrated that LAMP-3 appears to act as a cell surface binding partner for TIMP-1. In MCF10A human breast epithelial cells, TIMP-1 associates with integrin $\beta 1$ in a LAMP-3-dependent manner, regulating signaling pathways involved in cell survival and polarisation (Jung *et al.*, 2006). This is extremely interesting as TIMPs have long been known to be involved in signaling but the mechanism has always been unclear.

LAMP-1, LAMP-2 and LysoTracker were used in the current study as markers for classical late endosomal and lysosomal compartments, as they have both been identified in classical late endosomes and lysosomes of various cell types including macrophages (Desjardins *et al.*, 1994a; Jahraus *et al.*, 1998 Eskelinen *et al.*, 2002; Sun-Wada *et al.*, 2003; Anes *et al.*,

Rat anti-mouse LAMP-1 (1D4B) and rat anti-mouse LAMP-2 (ABL-93) were obtained from the Developmental Studies Hybridoma Bank (University of Iowa, Iowa City, Iowa, USA) and goat anti-rat IgG-alkaline phosphatase conjugate was from Sigma.

The anti-cathepsin and secondary fluorescent antibodies used, were as previously described (Section 3.7.1 and 4.2.1). Goat anti-rat IgG FITC and goat anti-rabbit IgG TRITC were also used.

4.4.2 Procedure

Serum-containing and serum-free J774 mouse macrophage homogenates and supernatants were prepared (Section 3.6.2), separated on a 12.5% (v/v) Laemmli gel (Section 2.3.1.2), transferred to nitrocellulose and probed with rat anti-LAMP-1 [1:800], rat anti-LAMP-2 [1:1000] and goat anti-rat IgG-alkaline phosphatase [1:30 000] according to Section 2.6.2.2.

J774 cells were cultured (Section 2.2.2) and fluorescent immunolabelling performed with rat anti-mouse LAMP-1 [1:300 or 1:800 or 1:900], rat anti-mouse LAMP-2 [1:900 or 1:1200], chicken anti-cathepsin D [100 µg/ml or 200 µg/ml], chicken anti-cathepsin B [50 µg/ml], rabbit anti-cathepsin H [100 µg/ml], chicken anti-cathepsin S [100 µg/ml] and rabbit anti-cathepsin L [20 µg/ml]. Goat anti-rat IgG FITC [3 µg/ml or 2µg/ml or 1 µg/ml], donkey anti-chicken IgG CY3 [1.5 µg/ml or 2 µg/ml], goat anti-rabbit IgG TRITC [18 µg/ml or 11 µg/ml] were used as detection antibodies according to Section 2.8.1.2. In some instances, only the Olympus epifluorescent microscope was used for viewing immunolabellings as the Zeiss 510 Meta confocal was only on loan for 3 months and soon became unavailable. Images were analysed using ImageJ software. The percentage colocalisation was determined as described in Section 4.2.2. As the polyclonal anti-mature cathepsin antisera used cannot distinguish between precursor and mature forms of the enzyme, cathepsins associated with LAMPs-positive and/or acidic organelles will assumed to be mature and active.

4.4.3 Results

The commercial LAMP-1 and LAMP-2 antibodies characterised using crude J774 mouse macrophage homogenates revealed bands of approximately 109 kDa and 113 kDa corresponding to LAMP-1 and LAMP-2, respectively (Figure 4.16, lanes 2 and 4, Figure 4.17, lanes 2 and 4), confirming the specificity and suitability of these antisera for immunolabelling studies on the J774 cell line.

initially be released as precursors and subsequently as active enzymes after a slow acidifying or maturation process. Whether there are two enzyme processing sites, a late endosome and another acidic organelle (i.e. LAMPs-positive, acidic, MPR-negative and containing mature lysosomal enzymes) (Table 4.1) or whether the late endosome “matures” into such an organelle is unknown. The latter scenario seems a possibility from the current cathepsin S-labelling results. Cathepsin S, however, seems located mainly in secretory and late endosomal vesicle populations.

Mature cathepsin D, present in 80% of vesicles, on the other hand, colocalised in a 50:50 ratio with LAMP-1 and LAMP-2 (Figure 4.21, A and C, respectively, i.e. within 50% of all mature cathepsin D-containing vesicles, possibly $\pm 30-50$ nm, “secretory lysosomes”, ± 50 nm late endosomes and $\pm 150-200$ nm hybrid organelles). LAMP-1 and -2 may colocalise with each other within the same 50% of active cathepsin D-labelled vesicles of all vesicle populations or may colocalise minimally at 20% (i.e. 2 x 30% of mature cathepsin D-labelled vesicles associated with one label and 20% associated with both labels, contributing to a total of 80% active enzyme) or some proportion between these two extremes i.e. 20-50% colocalisation between LAMP-1 and -2. With good EM ultrastructure and triple labelling for cathepsin D (precursor and mature), LAMP-1 and -2 it may be possible to identify the different LAMP labelling populations.

Activation (elongated cell morphology) seemed to increase the level of colocalisation of cathepsin D with LAMP-1 to almost 100% of the ± 50 nm late endosome-like vesicles containing the mature cathepsin (Figure 4.21, B) (LAMP-2 colocalisation could not be assessed as a similarly activated cell could not be found and triple labelling was not performed). The increase in association with LAMP-1 (up to approximately 100%) upon activation (Figure 4.21, B) illustrates how dynamic and variable localisations may be with activation.

Colocalisation seems to occur mainly in specific areas of the cell and such organelles seem to be relatively large (± 50 nm) and greater than 100 nm ($\pm 150-200$ nm) (Figure 4.21, A and B). These are possibly late endosomes and “hybrid” organelles or digestive bodies, therefore, agreeing with previous Summary observations (Summary end of Section 4.3 and Table 4.4).

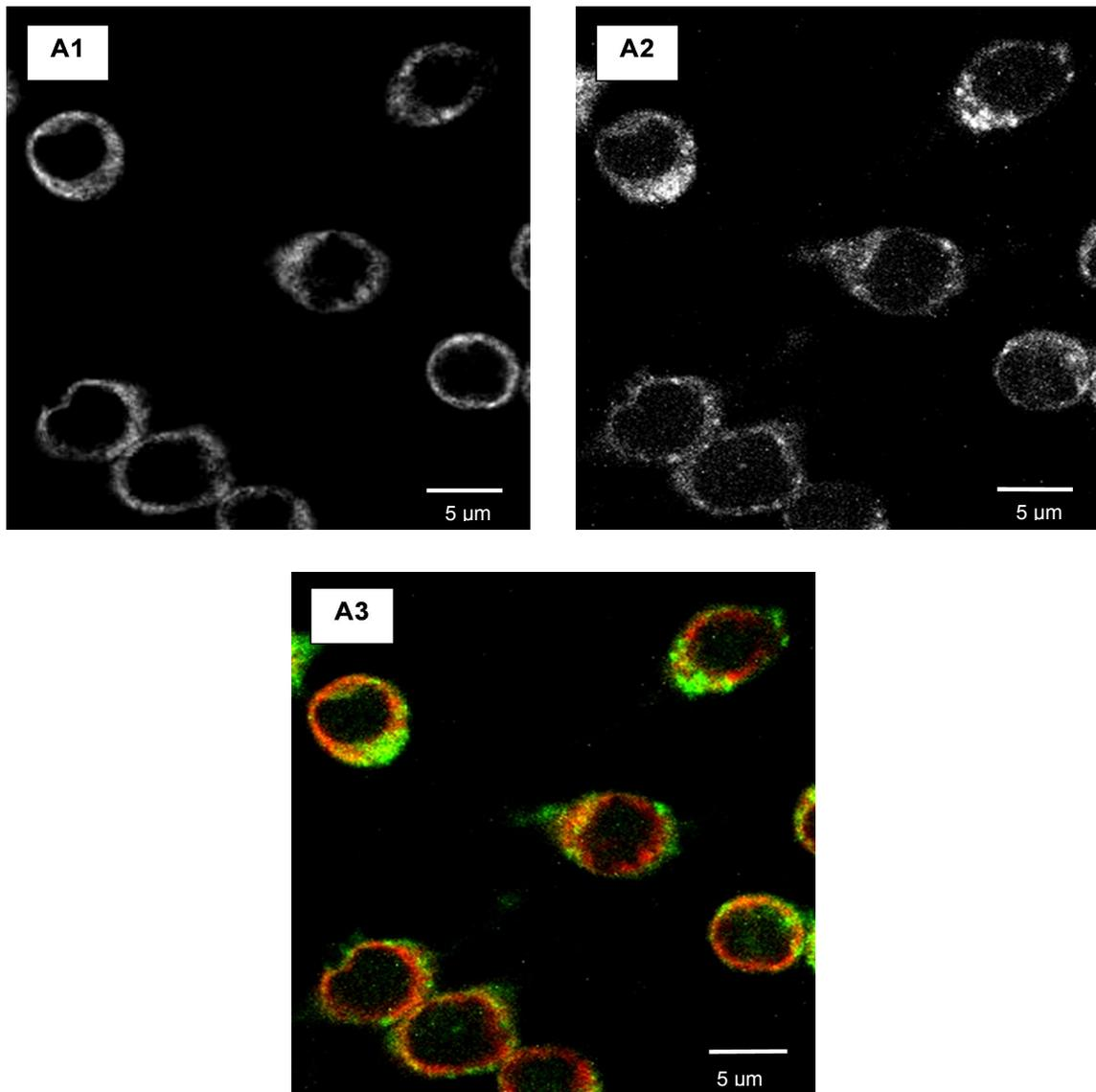


Figure 4.20 Fluorescent labelling of LAMP-1 and cathepsin S in J774 macrophages.
Chicken anti-cathepsin S [50 µg/ml (A1)] and donkey anti-chicken CY3 [2 µg/ml (A1)], post-fixed (3.7% PFA), probed with rat anti-mouse LAMP-1 [1:900 (A2)] and goat anti-rat FITC [2 µg/ml (A2)] applied to cells on coverslips, initially fixed with 3.7% PFA and permeabilised with saponin. Coverslips viewed using a Zeiss 510 Meta confocal microscope. CY3 filter (A1), FITC filter (A2), composite image (A3). Bars = 5 µm.

recycling endosome localisation of TIMP-2 needs confirmation with labelling of non-permeabilised cells and labelling for MT1-MMP and proMMP-2, respectively.

- Boyum, A. (1976) Isolation of lymphocytes, granulocytes and macrophages. *Scand. J. Immunol.* (Supp. 5) **5**, 9-15.
- Brew, K., Dinakarbandian, D. and H. Nagase. (2000) Tissue inhibitors of matrix metalloproteinases: evolution, structure and function. *Biochim. Biophys. Acta* **1477**, 267-283.
- Bright, N. A., Reaves, B. J., Mullock, B. M. and J. P. Luzio. (1997) Dense core lysosomes fuse with late endosomes and are re-formed from the resultant hybrid organelles. *J. Cell Sci.* **110**, 2027-2040.
- Brown, W. J., Goodhouse, J. and M. G. Farquhar. (1986) Mannose-6-phosphate receptors for lysosomal enzymes cycle between the Golgi complex and endosomes. *J. Cell Biol.* **103**, 1235-1247.
- Bühling, F., Waldburg, N., Resenauer, A., Heimburg, A., Golpon, H. and T. Welte. (2004) Lysosomal cysteine proteases in the lung: role in protein processing and immunoregulation. *Eur. Respir. J.* **23**, 620-628.
- Busiek, D. F., Ross, F. P., McDonnell, S., Murphy, G., Matrisian, L. M. and H. G. Welgus. (1992) The matrix metalloproteinase matrilysin (PUMP) is expressed on developing human mononuclear phagocytes. *J. Biol. Chem.* **267**, 9087-9092.
- Butor, C., Griffiths, G., Aronson, N. N. and A. Vark. (1995) Co-localization of hydrolytic enzymes with widely disparate pH optima: implications for the regulation of lysosomal pH. *J. Cell Sci.* **108**, 2213-2219.
- Campaine, A., Schein, J. D., Tabb, J. S., Mohan, P. S. and R. A. Nixon. (1995) Limited proteolytic processing of the mature form of cathepsin D in human and mouse brain: post-mortem stability of enzyme structure and activity. *Neurochem. Int.* **27**, 385-396.
- Campbell, E. J., Cury, J. D., Lazarus, C. J. and H. G. Welgus. (1987) Monocyte procollagenase and tissue inhibitor of metalloproteinases. *J. Biol. Chem.* **262**, 15862-15868.
- Campbell, E. J., Silverman, E. K. and M. A. Campbell. (1989) Elastase and cathepsin G of human monocytes quantification of cellular content, release in response to stimuli, and heterogeneity in elastase-mediated proteolytic activity. *J. Immunol.* **143**, 2961-2968.
- Campbell, E. J., Cury, J. D., Shapiro, S. D., Goldberg, G. I. and H. G. Welgus. (1991) Neutral proteinases of human mononuclear phagocytes. Cellular differentiation markedly alters cell phenotype for serine proteinases, metalloproteinases and tissue inhibitor of metalloproteinases. *J. Immunol.* **146**, 1286-1293.
- Candiano, G., Porotto, M., Lanciotti, M. and G. M. Ghiggeri. (1996) Negative staining of proteins in polyacrylamide gels with methyl trichloroacetate. *Anal. Biochem.* **243**, 245-248.

- Elliott, E., Dennison, C., Fortgens, P. H. and J. Travis. (1995) Paraformaldehyde fixation of neutrophils for immunolabeling of granule antigens in cryoultrasections. *J. Histochem. Cytochem.* **43**, 1019-1025.
- Ellouz, F., Adam, A., Ciorbaru, R. and E. Lederer. (1974) Minimal structural requirements for adjuvant activity of bacterial peptidoglycan derivatives. *Biochem. Biophys. Res. Commun.* **59**, 1317-1325.
- Emonard, H., Bellon, G., Troeberg, L., Berton, A., Robinet, A., Henriet, P., Marbaix, E., Kirkegaard, K., Pathy, L., Eekhout, Y., Nagase, H., Hornebeck, W. and P. J. Courtoy. (2004) Low density lipoprotein receptor-related protein mediates endocytic clearance of pro-MMP-2-TIMP-2 complex through a thrombospondin-independent mechanism. *J. Biol. Chem.* **279**, 54944-54951.
- Eskelinen, E-L., Illert, A. L., Tanaka, Y., Schwarzmann, G., Blanz, J., von Figura, K. and P. Saftig. (2002) Role of LAMP-2 in lysosome biogenesis and autophagy. *Mol. Biol. Cell* **13**, 3355-3368.
- Eskelinen, E-L., Tanaka, Y. and P. Saftig. (2003) At the acidic edge: emerging functions for lysosomal membrane proteins. *Trends Cell Biol.* **13**, 137-145.
- Ey, P. L., Prowse, S. J. and C. R. Jenkin. (1978) Isolation of pure IgG1, IgG2a, IgG2b immunoglobulins from mouse serum using protein A-Sepharose. *Biochemistry* **15**, 429-436.
- Falcon-Perez, J. M., Nazarian, R., Sabatti, C., and E. C. Dell'Angelica. (2005) Distribution and dynamics of Lamp1-containing endocytic organelles in fibroblasts deficient in BLOC-3. *J. Cell Sci.* **118**, 5243-5255.
- Faurschou, M. and N. Borregaard. (2003) Neutrophil granules and secretory vesicles in inflammation. *Microb. Infect.* **5**, 1317-1327.
- Fernandez-Patron, C., Hardy, E., Sosa, A., Seoane, J. and L. Castellanos. (1995a) Double staining of Coomassie-Blue-stained polyacrylamide gels by imidazole-sodium dodecyl sulfate-zinc reverse staining: sensitive detection of Coomassie Blue-undetected proteins. *Anal. Biochem.* **224**, 263-269.
- Fernandez-Patron, C., Calero, M., Collazo, P. R., Garcia, J. R., Madrazo, J., Musacchio, A., Soriano, F., Estrada, R., Frank, R., Castellanos-Serra, L. R. and E. Mendez. (1995b) Protein reverse staining: high efficiency microanalysis of unmodified proteins detected on electrophoresis gels. *Anal. Biochem.* **224**, 203-211.
- Ferrari-Lacraz, S., Nicod, L. P., Chicheportiche, R., Welgus, H. G. and J-M, Dayer. (2001) Human lung tissue macrophages, but not alveolar macrophages, express matrix metalloproteinases after direct contact with activated T lymphocytes. *Am. J. Respir. Cell Mol. Biol.* **24**, 442-451.

Wubbolts, R., Fernandez-Borja, M., Oomen, L., Verwoerd, D., Janssen, H., Calafat, J., Tulp, A., Dusseljee, S. and J. Neefjes. (1996) Direct vesicular transport of MHC class II molecules from lysosomal structures to the cell surface. *J. Cell Biol.* **135**, 611-622.

Xie, B., Dong, Z. and I. J. Fidler. (1994) Regulatory mechanisms for the expression of type IV collagenases/gelatinases in murine macrophages. *J. Immunol.* **152**, 3637-3644.

Zeng, G. and A. J. Millis. (1994) Expression of 72-kDa gelatinase and TIMP-2 in early and late passage human fibroblasts. *Exp. Cell Res.* **213**, 148-155.

Zheng, T., Zhu, Z., Wang, Z., Homer, R. J., Ma, B., Riese, R. J. Jr., Chapman, H. A. Jr., Shapiro, S. D. and J. A. Elias. (2000) Inducible targeting of IL-13 to the adult lung causes matrix metalloproteinase- and cathepsin-dependent emphysema. *J. Clin. Invest.* **106**, 1081-1093.

Zor, T. and Z. Selinger. (1996) Linearisation of the Bradford protein assay increases its sensitivity: theoretical and experimental studies. *Anal. Biochem.* **236**, 302-308.

Zuo, F., Kaminski, N., Eugui, E., Allard, J., Yakhini, Z., Ben-Dor, A., Lollini, L., Morris, D., Kim, Y., DeLustro, B., Sheppard, D., Pardo, A., Selman, M. and R. Heller. (2002) Gene expression analysis reveals matrilysin as a key regulator of pulmonary fibrosis in mice and humans. *Proc. Natl. Acad. Sci. USA* **99**, 6292-6297.

PUBLICATIONS